UiA University of Agder

Master

Case Study of Alternatives to Grid Expansion

Reducing Grid Connection Requirements for Large Scale EV Charging Stations through Photovoltaic and Energy Storage Integration

JON ERIK NESSE
KRISTIAN BROHAUG

SUPERVISOR
João Leal, University of Agder
Kristine Lehrmann Solvang, Å Energi
Per Oddvar Osland, Glitre Nett
Stine Myhre, Institute for Energy Technology

University of Agder, 2024
Faculty of Engineering and Science
Department of Engineering and Sciences

Obligatorisk gruppeerklæring

Den enkelte student er selv ansvarlig for å sette seg inn i hva som er lovlige hjelpemidler, retningslinjer for bruk av disse og regler om kildebruk. Erklæringen skal bevisstgjøre studentene på deres ansvar og hvilke konsekvenser fusk kan medføre. Manglende erklæring fritar ikke studentene fra sitt ansvar.

I henhold til universitetets retningslinjer for bruk av kunstig intelligens (KI) i forbindelse med korrekturlesing [1][24.05.2024], har ChatGPT blitt benyttet i denne oppgaven for språklig veiledning og forbedring av språket. ChatGPT har blitt brukt til å innhente synonymforslag, utføre oversettelser og gi språklige tilbakemeldinger. Det er viktig å presisere at ChatGPT ikke har blitt brukt til å generere originalt innhold, formulere ideer eller påvirke de vesentlige delene av forskningen.

1.	Vi erklærer herved at vår besvarelse er vårt eget arbeid, og at vi ikke har brukt andre kilder eller har mottatt annen hjelp enn det som er nevnt i besvarelsen.	Ja
2.	**Vi erklærer videre at denne besvarelsen:** • Ikke har vært brukt til annen eksamen ved annen avdeling/universitet/høgskole innenlands eller utenlands. • Ikke refererer til andres arbeid uten at det er oppgitt. • Ikke refererer til eget tidligere arbeid uten at det er oppgitt. • Har alle referansene oppgitt i litteraturlisten. • Ikke er en kopi, duplikat eller avskrift av andres arbeid eller besvarelse.	Ja
3.	Vi er kjent med at brudd på ovennevnte er å betrakte som fusk og kan medføre annullering av eksamen og utestengelse fra universiteter og høgskoler i Norge, jf. Universitets- og høgskoleloven §§4-7 og 4-8 og Forskrift om eksamen §§ 31.	Ja
4.	Vi er kjent med at alle innleverte oppgaver kan bli plagiatkontrollert.	Ja
5.	Vi er kjent med at Universitetet i Agder vil behandle alle saker hvor det forligger mistanke om fusk etter høgskolens retningslinjer for behandling av saker om fusk.	Ja
6.	Vi har satt oss inn i regler og retningslinjer i bruk av kilder og referanser på biblioteket sine nettsider.	Ja

Publiseringsavtale

Fullmakt til elektronisk publisering av oppgaven Forfatter(ne) har opphavsrett til oppgaven. Det betyr blant annet enerett til å gjøre verket tilgjengelig for allmennheten (Åndsverkloven. §2).
Oppgaver som er unntatt offentlighet eller taushetsbelagt/konfidensiell vil ikke bli publisert.

Vi gir herved Universitetet i Agder en vederlagsfri rett til å gjøre oppgaven tilgjengelig for elektronisk publisering:	Ja
Er oppgaven båndlagt (konfidensiell)?	Nei
Er oppgaven unntatt offentlighet?	Nei

Acknowledgements

This is the final work which is meant to represent 30 study credits in the course ENE500, but also marks the end of a two-year Master's program in Renewable energy. The study was undertaken at the University of Agder, Campus Grimstad.

First, we want to take this opportunity to thank our supervisors in Glitre Nett and the Institute for Energy Technology (IFE), Per Oddvar Osland and Stine Myhre. They have consistently supported us with weekly meetings and given us feedback several times of the week, technical and academic responses. Without your help, this thesis not have been possible. Thereafter, we want to show Kristine Lehrmann Solvang from Å Energy our gratitude. She has supported us on the economic input data of the technologies. Additionally, we appreciate your quick response on Microsoft Teams. Nevertheless, Joao Leal, our supervisor from the Univerity of Agder. We are grateful for the help you gave us in the beginning of the project to get us started. Additionally, your door was always open if we needed you.

In the end, we thank our wives, who have helped us through long days. Their understanding and support were critical to finish this project. Additionally, we would like to give a special thanks to our friends and fellow students Mathias M. Hagane and Eskil Furuset for both academic and social discussions throughout the spring. After 5 years at university, we look forward to starting in the industry and hope we can use the knowledge we have learned in study for future work. Thanks to all the teachers who have helped to get us through this study.

Kristiansand, June 2024

Abbreviations: A Guide

Abbreviation	Meaning
AM	Air Mass
BESS	Battery Energy Storage System
CAPEX	Capital Expenditure
DHI	Direct Horizontal Irradiance
DNI	Direct Normal Irradiance
DOC	Depth of Charge
ESS	Energy Storage System
EV	Electrical Vehicle
GLPK	GNU Linear Programming Kit
GHI	Global Horizontal Irradiance
HESS	Hydrogen Energy Storage System
IES	Integrated Energy System
IFE	Institute of Energy Technology
LCOS	Levelized cost of storage
LP	Linear Programming
MILP	Mixed Integer Linear Programming
NREL	National Renewable Energy Laboratory
NVE	The Norwegian Water Resources and Energy Directorate
OPEX	Operating Expense
P2P	Power-to-Power
PEM	Proton-exchange membrane
PNNL	Pacific Northwest National Laboratory
PV	Photovoltaic
SOC	State of Charge
TMY	Typical Meteorological Year
VBiPV	Vertical Bifacial Photovoltaic

Abstract

The increasing share of electric vehicles requires more charging stations, which in turn demands more available grid capacity. In many situations, this necessitates an expansion in the regional and transmission grid, which is both expensive and time consuming. This thesis explores the possibility that an integrated energy system consisting of PV, battery energy storage systems, and hydrogen energy storage systems can reduce the investment costs for grid connection at new large-scale charging stations (1-10 MW). Additionally, the load pattern and the correlation between load and traffic patterns were examined. The thesis looks at four different locations near the main highway in Agder County, where the proportion of seasonal tourists is high. An optimization model developed by S. Myhre was used as a comparison tool to identify the most cost-effective solution for grid connection. This model aims to find the most optimal solution for grid connection based on minimizing investment costs, the model considers both grid reinforcement and alternatives technologies such as solar power and energy storage.
The following cases were simulated:

- The lowest investment cost for grid connection, considering today's (2024) cost of grid connection and alternative technologies.
- The lowest investment cost for grid connection in a future cost situation, evaluated from a long-term perspective that takes into account technological developments and cost reductions for alternative technologies.
- How much investment costs need to fall for the various elements in Integrated Energy System (IES) for the technologies to have a lower investment cost than traditional grid expansion.
- What is the lowest investment cost for the combination of grid connection when the model is forced to limit grid expansion.
- What is the best investment for grid connection considering the lifetime of the grid and alternative technologies, when the model is forced to limit grid expansion.

The load at the charging stations near the main thoroughfare in Agder County has high activity during the holiday seasons of Christmas, Easter, and the summer holiday. Additionally, the charging stations typically have peak load demand in the middle of the day during the high season, while during the rest of the year the peak load demand is usually after working hours. It was also observed that the load and traffic patterns correlated better at locations where the proportion of commuters is lower.

The results show that in the current cost scenario, the alternative technologies are not more profitable than grid expansion. However, by 2030, the cost of PV could fall enough to have a lower investment cost than traditional expansion, but will lead to weaker supply security. By 2050, the cost of batteries with a C-rate of 0.5 (indicating they can fully discharge in 2 hours) could potentially decrease significantly, thereby helping to reduce some of the reliance on grid connections. Batteries with lower C-rates and hydrogen energy storage systems, will not be profitable by 2050. If one wishes to replace grid capacity with alternative technologies the

total investment cost will grow exponentially with grid capacity reduction. A small reduction in grid capacity will have a small increase in investment cost, while a large reduction in grid capacity will lead to a significantly higher investment cost. Over a 30-year perspective, it will still be profitable to invest in solar cell production, when one can sell the excess energy.

The authors recommend replacing the current optimization solver with a commercial product that is faster and can handle more complex models. This provides an opportunity to expand the model to include a more complete grid tariff, include more technologies, rebuild the model to consider the total investment, a stochastic analysis of load and demand analysis and/or use traffic patterns as the basis for the estimation.

Sammendrag

Den økende andelen av elbiler krever flere ladestasjoner, noe som igjen krever ny ledig nettkapasitet. I mange sitasjoner krever dette en utbedring i det overliggende nett, som både er dyrt og tidkrevende. Denne oppgaven ser på muligheten for at et integrert energisystem bestående av PV, batterilagrings- og hydrogen-basert lagringssystemer kan redusere investeringskostnadene til netttilknytning hos nye storskala ladestasjoner. I tillegg ble lastuttaksmønstret og sammenhengen mellom lastuttak og lademønster undersøkt. Studien ser på fire ulike lokasjoner nær hovedfartsåren i Agder Fylke, der andelen av sesong turister er høy. En optimaliseringsmodell utviklet av S. Myhre ble brukt som et sammenligningsverktøy for å identifisere den mest kostnadseffektive løsningen for nettilkobling. Modellen har som mål å finne den mest optimale løsningen for nettilkobling basert på å minimere investeringskostnadene. Modellen vurderer både tradisjonel nettytbyglese og alternative teknologier som solkraft og energilagring.
Følgene caser ble simulert:

- Den rimligste investeringskostnaden for nettilkobling, tatt i betraktning de nåværende kostnadene for nettilkobling og alternative teknologier.
- Den rimeligste investeringskostnaden for nettilkobling i en fremtidig kostnadssituasjon, vurdert i et langsiktig perspektiv som tar hensyn til teknologiutvikling og kostnadsreduksjon.
- Hvor mye må investeringskostnadene falle for de ulike elementene i IES for at teknologiene skal ha lavere investeringskostnad enn tradisjonell nettutbygging
- Hva er den rimeligste investeringskostnaden for kombinasjonen av netttilknyttning når modellen tvinges til å begrense nettutbyggingen
- Hva er den beste investeringen for netttilknyttning over 30år når modellen tvinges til å begrense nettutbyggingen

Lastuttaket hos ladestasjonene nær hovedfartsåren i Agder Fylke har en tydelig høyaktivitetsperiode i ferieperiodene jul, påske og fellesferien. I tillegg vil de typisk ha toppforbruket midt på dagen i høysesongen, mens ellers i året vil toppforbruket være typisk etter arbeidtid. Det ble også observert at lastuttaket og trafikkmønsterer korrelerte bedre ved lokasjonene der andelen pendlere er lavere.

Resultatene viser at ved dagens kostnadsscenario er ikke alternativene mer lønnsomt enn nettutbygging. Men i 2030 kan kostnaden på PV falle nok til at det får en lavere investeringskostnad enn tradisjonell utbygging, men dette vil føre til en svaker forsyningssikkerhet. Innen 2050 kan kostnaden for batterier med en C-rate på 0,5 (som indikerer at de kan utlades helt på 2 timer) potensielt reduseres betydelig, og dermed bidra til å redusere noe av avhengigheten av nettilkoblinger. Hvis man ønsker å erstatte nettkapasitet med alternative teknologier, vil den totale investeringskostnaden øke eksponentielt med reduksjon i nettkapasiteten. En liten reduksjon i nettkapatieten ha en liten økning i investeringskostnaden, mens en stor reduksjon i nettkapastieten vil føre til en vesentlig høyere kostnad investeringskostnad. Over et 30 års perspektiv vil det uansett lønne seg å investere i solceller produksjon,

når man kan selge overskuddsenergien.

Forfatterne anbefaler å estatte den nåværende optimaliseringsløseren med et kommersielt produkt som er raskere og kan takle større modeller. Dette gir en mulighet til utvide modelen for å inkludere en mer kompleks versjon av nettariffen av netttariff, inkludere flere teknologier, ombygge modellen til å se på den totale den totale investeringen, og/eller bruke trafikkmønsteret som grunnlag for estimeringen.

Contents

List of Figures

List of Tables

Chapter 1

Introduction

Electrical energy is an essential part of Norwegian society, and over the last ten years, stable access to electricity has been taken for granted [2]. The Norwegian grid was mainly built between 1945 and 1960s [3], and its primary objective is to ensure stable supply of electrical energy to the customers. The Norwegian power system was mainly constructed to have a direct flow from large-scale power stations to the consumers. However, as more distributed generation, flexible solutions, prosumers, and increased control of the system, the system becomes more complex with automated solutions and bi-directional power flow.

In Norway the public grid companies are responsible for the electrical grid [2]. Due to the electrical grid system is a monopoly, the grid companies are obligated to connect the consumption to the grid, but also give gird capacity to customers which will supply the grid with electrical energy. One of the most important tasks for a grid company is to ensure robust and reliable security of supply. Supply security is defined as the ability to continuously deliver sufficient energy to all customers reliably and stably [4]. A part of supply security is operational security, where the grid company has a duty to ensure that each customer has sufficient capacity to meet its demand [4].

The available capacity in the Norwegian power grid is restricted, where Norwegian Water Resources and Energy Directorate estimates grid reinforcement may take up to ten years [5] [6]. In addition, a combination of new industry and the electrification of Norwegian transportation will decrease available capacity [7]. A high demand for capacity can result in a long waiting time to build the grid connection with the requested capacity. In several cases, the regional- and/or transmission grids must be reinforced in addition to the local upgrades to the distribution grid. This will take time and is expensive [8]. The grid companies are required by law to connect the customers to the grid with their capacity demands [6]. If possible, the customer can get a conditional grid connection, where the customer could get a temporary lower capacity or disconnected entirely for a period. This option can give more customers faster access to the grid and possibly a lower cost [6].

The limited access to available capacity can delay electrification, which is an important part of the green shift. As of today's date, 15% of the global carbon emission is linked to the transport sector. The Norwegian government has set a goal for 2025, all sales of new passenger cars should be zero-emission [9]. Additionally, in 2030, it is tough requirements for commercial transport. A larger part of the sector is forced to switch to green energy as fuel. That will result in a larger capacity demand for electrical energy [9]. According to a report conducted by Norwegian Water Resources and Energy Directorate (NVE) [5], Norway's capacity must increase to 2200 MW to meet the capacity requirement of the transport sector in 2030. Charging stations will be a significant proportion of the grid capacity requirement, and the total requirement will be 700 MW. Due to the aggregation factor of 60%, the actual requirement is 420 MW. In addition, the industry and other elements in society will also

require more grid capacity [5].

1.1 Motivation

This thesis is written for Glitre Nett in relation to their project Data Arena. Data Arena is a website for customers that wishes to connect the grid or expand their grid connection capacity. The website shows an overview of the available grid capacity and gives a cost estimate for grid connection requests. The goal of Data Arena is to inform its customers about the limitations of grid expansion and let the customer make an informed decision to choose the best solutions [10]. Additionally, the project aims to optimize decisions made when building new grid connection by including alternative technologies. The Data Arena project includes more goals, which can be read about on the DataArena project page. As alternatives to grid expansion is not currently included in Data Arena, this thesis will focus on the cost-effectiveness of alternative technologies.

1.2 Problem

To answer whether alternative technologies can replace grid expansion, an optimization model designed by S. Myhre [11] was used as a tool to minimize the total system cost for grid connection. A simulation of four locations was conducted, where grid capacity requested are related to EV charging stations. This thesis aims to answer the following research questions:

- Are PV applications, battery energy storage systems (BESS) and/or hydrogen energy storage systems (HESS) economically competitive alternatives to traditional grid expansion for large scale EV charging stations?
- How will technology cost development affect the competitiveness of alternatives to traditional grid expansion for large scale EV charging stations?
- If traditional grid expansion is the most cost-effective solution for new grid connections in large scale EV charging stations, how much of a cost reduction does PV applications, BESS and HESS need to be economically competitive? And what are the effects on the grid structure?
- Can PV applications and energy storage systems (ESS) increase the capacity of EV charging stations without building additional grid capacity? How will this influence the total investment cost?
- Is there a correlation between traffic patterns and the load of EV charging stations?

In this thesis photovoltaic (PV) is used as an umbrella term for solar power production.

1.3 Scope

This thesis investigates the high-voltage grid connection of four EV charging stations close to the main thoroughfare in for summer tourists in Agder County, Norway. Each of the locations have existing load profiles and requests for more grid capacity. The capacity requests range between 1 MW and 10 MW.

Further, the thesis studied an integrated energy system, consisting of different types technologies being PV systems, Battery Energy Storage Systems (BESS) with 2h, 4h and 6h time rates and Hydrogen Energy Storage Systems with 10h, 20h and 100h time rates. The

PV systems in question is roof PV, land PV and vertical bifacial PV (VBiPV). Technologies related to other forms of energy storage and power production is not considered. Each of the technologies have its own inverter calculated into its costs, which gives each of the technologies its own inverter efficiency. Inverter technologies and solutions are not investigated.

The elements is connected to an internal grid, together with the load. Figure 1.1 illustrates the integrated energy system (IES), where the internal grid is defined on the right side of the measuring point, while the left side is the public grid system. The customer owns the internal grid. The task ignores legal feasibility and regulations. Additionally, the grid tariff was simplified to only consist of electricity tax and energy terms.

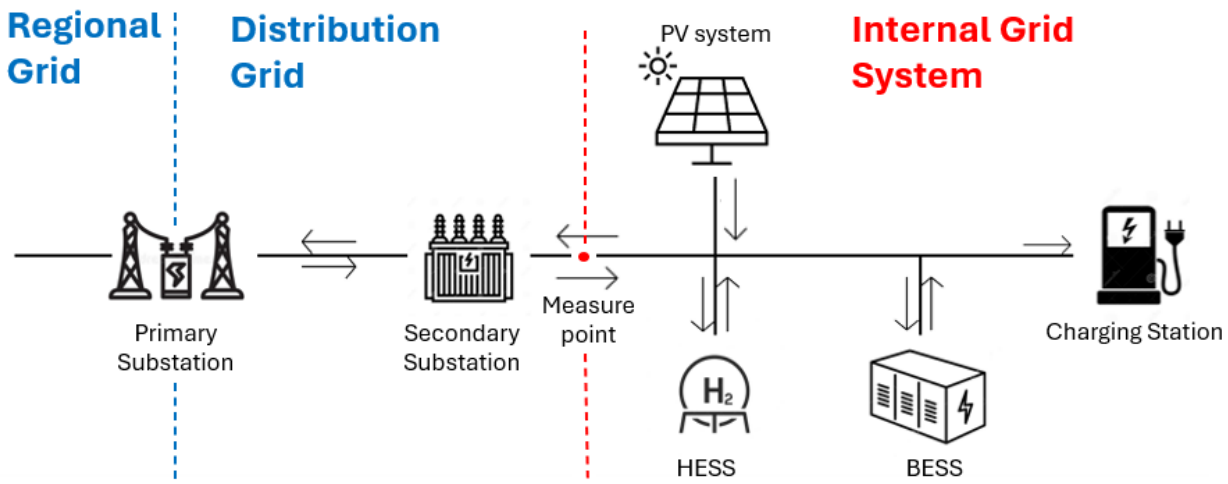

Figure 1.1: Illustration of IES

1.4 Structure of the Thesis

The thesis is structured in 10 chapter

- **CHAPTER 2 Literature Review:** A Presentation of relevant research with the purpose of reducing the capacity requirements for the grid
- **CHAPTER 3 Theory:** A Explanation of fundamental theories related to electrical grid, PV systems, BESS, HESS, correlation and linear optimizing.
- **CHAPTER 4 Cost Review:** A literature review of the investment costs associated with the simulated technologies, as well as a review of the costs associated with grid tariffs in Agder County
- **CHAPTER 5 Model:** A presentation of the model that was used to simulate the result.
- **CHAPTER 6 Model Input Data Collection Approach:** A review of the used data inputs to the model and the method of how the inputs were determined.
- **CHAPTER 7 Location and Case Description:** A presentation of the analysed and simulated locations. Additionally, an overview of the simulated cases, including different scenarios for grid capacity and technology costs.
- **CHAPTER 8 Results and Discussion:** A presentation and discussion of the simulated cases and the different cost scenarios. Additionally, an analysis of the locations and information about the correlation between load and traffic is displayed and discussed.
- **CHAPTER 9 Conclusion:** A Summary of the key findings from the study
- **CHAPTER 10 Further Work:** An overview of the authors' suggestions for future work

1.5 Grammatical Guidance

For grammatical guidance, the AI-based writing assistant Grammarly [12] and the AI-based language model ChatGPT (OpenAI) [13] have been used in this thesis. This has been done in accordance with UiA's regulations on the use of AI for proofreading [1]. The authors confirm that AI has been used solely in an attempt to improve the quality of the language and the flow of the text. Additionally, the authors confirm that no academic content has been generated by artificial intelligence in this report.

Chapter 2

Literature Review

In the literature, there are several articles about the simulation of different PV systems. Additionally, there are several commercial tools to simulate traditional PV systems. An article written by Nesse and Brohaug [14] in the Univerity of Agder's course ENE 503 builds a python model to estimate production from a vertical bifacial PV (VBiPV) application. In this article the model was compared against data from Over Easy's PV system and concluded the model gave an accurate estimation of the production of VBiPV systems [14]. Where Over Easy is a Norwegian company that builds VBiPV mounting systems for flat roofs. The result of the simulation shows that VBiPV systems have a higher specific yield for a location in Agder compared to traditional flat-roof PV systems. The production profiles of VBiPV typically have morning and evening peaks and the authors claim that a typical production pattern matches the energy demand better than a traditional system. In addition, due to the wide daily production profile, a VBiPV system requires less grid capacity [14].

Another article, written by Jouttijärvi [15], tested the matching of production profiles of vertical and conventional PV systems. A simulation was built in Matlab based on PVlib, which is a library developed for PV calculations and simulations. The production profiles were simulated in a system consisting of grid and customers. The simulated results show that a combination of vertical and commercial PV will give a more stable production [15]. Nevertheless, a VBiPV system will match the demand better than a traditional PV system and produce more energy per installed power. The article concluded that a VBiPV system will increase the grid's PV hosting capacity significantly and a 30-70 ratio between monofacial and VBiPV is optimal [16].

There exists also a litterature which looks at a reduction in production peak, which will be important in the future. Since the integration of non-regulated energy sources will result in production peaks on the grid. A master thesis written by Gabrielsen investigates the option of using dynamic throttling of a wind turbine farm as an alternative to grid expansion [17]. The thesis argues that increasing the production capacity (more wind turbines), while throttling the power output, will increase total profits of wind farms. In the case studied, the wind farm could increase its capacity from 60 MW to 81 MW. Due to the power production throttling in the case described in the thesis the revenue from electricity sales decreases with 0.24 %. However, the CAPEX decreases such that revenue in relation to investment cost increases with 1 %, which makes up for the loss from power throttling [17]. Johansen [18] claims that dynamic throttling for PV systems can save millions of NOK in grid expansion, but results in a reduction of income for the customer. As of March 2024, this is not a viable solution due to regulative restrictions/issues and technical challenges. Nevertheless, dynamic throttling of PV applications can be an important part of the grid in the future [18].

In the literature, it is been carried out several investigations of using batteries in the grid as an alternative to grid reinforcing and expansion. Brubæk's master thesis [19] investigated

the option of using batteries as an alternative to grid reinforcement. The main focus was on cabin customers in the distribution grid, where batteries can supply power to the customers in the hours of high consumption, compared to the capacity of the grid. To investigate if battery could reinforce the grid, a technical simulation model was built in Python. The model's main focus is on short-time energy storage and voltage regulation, which are typical tasks for a battery system [19]. The result shows that batteries are as good a technical solution as grid reinforcement, but the cost of the battery is higher than reinforcing the grid. The annual battery cost was 77 % higher than the annual grid reinforcement cost [19].

Another master thesis, written by Spjotvolf et al. [20], investigates battery storage systems as an alternative to traditional grid expansion in the distribution grid. Both technical and economic perspectives were investigated and simulated in MATLAB. The conclusion was that the battery system is a better technical solution than traditional grid expansion, but the cost associated with battery systems is too high compared to grid expansion [20].

Other alternatives to reduce the grid expansion are flexibility and peak shaving. Several studies look at solutions for scenarios where peak load is high compared to average load [21] [22]. In a study conducted by Rasoulinezhad et al. [21], the authors investigate a BESS control system which adjusts the loads in a microgrid to reduce peak demand. The model utilized electric vehicles, in addition to BESS, to regulate the load [21]. Another article by Ramadan [22] utilized electric vehicles for peak shaving. A MATLAB model was developed to optimize the charging/discharging process. The simulation flattened the consumption and reduced the capacity requirement [22]. Additionally, in 2017, NVE conducted a mapping of the potential use of electric car batteries as grid-connected batteries [23]. They claimed that 10-50% of the peaks could be reduced by electric cars in 2030.

An extensively reviewed system that has been predicted to reduce grid expansion is the microgrid. A master thesis conducted by Hellesø [24] developed a method to identify potential areas for microgrids in the distribution grid in Mid-Norway [24]. The model uses Power Netbas to find locations with low grid voltages. Necessary data was imported to a MATLAB script which estimates five different microgrid solutions. These solutions were cost-benefit analysed. The thesis tested its method on two different locations. Where Hellesø concluded that in scenarios with:

- Low power consumption
- Low grid voltage, where grid expansion is required
- Substation at the end of a radial grid
- Radial grid with long high-voltage lines for radial extension

With these conditions microgrids can be more economically advantageous [24].

Utsira is a Norwegian island with a microgrid system. The island has 200 people and it is supplied with a subsea cable. A study from 2010 carried out by Ulleberg et al. [25] investigated the option for a microgrid on the island. The system was simulated and consisted of a 600 kW wind turbine, 10 kW PEM fuel cell, 55 kW hydrogen engine, 55 kWh BESS (for short-term storage) and a 50 kW electrolyser. The article concluded that wind energy and storage systems can supply the island for 2-3 days. A larger system will increase the operation time, but also increase the cost of the system. The article argues that the surplus electric energy could be used more effectively than power-to-power (P2P), where the excess electric energy production could be used to fuel hydrogen vehicles. When the report was carried out, only 20 % of energy from the turbines was used on the island. To produce hydrogen for

vehicles and use electrical energy to heat households will increase the self-consumption ratio.

A master thesis carried out by Utvik [26] presents a new systematic method to plan a microgrid. By implementing an algorithm and digital tool the planning process of a microgrid will become faster. In the thesis, Matlab was utilized to calculate the electrical energy balance model, DYNKO to find the most cost-effective result and NETBAS for the electrical load flow analysis. The method starts with a preliminary analysis of the electric load and production. The annual and short-time electrical energy balance is analysed. If it is within the criteria, it will perform load flow analysis, short circuit analysis, reliability analysis, and risk analysis. If these are within the constraints, an economic analysis will give the most cost-effective result. The method was used to find the most economical and socially beneficial solution for Utsira that also addresses the environmental aspect. The method gave 3 options and all of them included subsea cable. Two of them included wind turbines, 3 MW and 5MW. A combination of subsea cable and 3 MW wind power will give the most economical and socially beneficial solution solution according to the method developed by Utvik.

A bachelor thesis carried out by Berge et al. [27] investigates different combinations of Rye microgrids. The location is on an island, where the grid cost is high. In the thesis, the microgrid consists of only a single consumer and a 225 kW wind turbine. A simulation was carried out to try to increase a higher self-supply rate by combining other types of generators and storage systems. The result shows a combination of wind turbine and PV application will give the best economical result. A combination including a storage system will be less economically viable. Especially hydrogen, which had the lowest cost-effectiveness over 30 years. However, the economic analysis claims a microgrid will be an unsuitable alternative to other possibilities, such as grid expansion. From a self-supply perspective, a storage system will be essential to reach a high ratio. The goal set in the thesis is 95% and a combination of wind and PV will give a ratio close to 60%. The same relationship will also apply to a combination of a wind turbine and a 330 kWh battery system. Increasing the battery capacity times will give a self-supply ratio of 95 %, but it is an economically unfavourable solution. The advantage of hydrogen, is a high self-supply ratio. A case where a hydrogen storage system supplies the microgrid with 10,9% will give a rate of 95%.

An article carried out by Živkovic et al. [28] investigated the option to build wind farms in the Kopaonik region in Serbia. It is a long distance from the closest energy sources and there are high transport losses in the grid. A farm will increase the power quality at the location and reduce losses due to transportation. The region's main customer is Kopanik Skicenter. A such solution will reduce the load of the grid. The excess energy can be supplied to the grid [28].

There are limited numbers of articles that investigate a combination of PV applications and charging stations. An article by Fachrizal et al. [29] looks at the option to combine the charging of cars and PV systems at workplaces. The traditional charging system starts when the car is connected, whereas this project simulates a case where the charging system is optimised to use most of the locally produced electric energy. One of the conclusions is the optimisation will give a better match-ratio between the PV system and car charging. Which will also reduce the cost of grid connection when the peak load is lower [29].

A study from the Netherlands conducted by Mouli et al. [30] investigated the option of using PV systems to reduce stress on the grid system. A 10kWp PV system with optimal tilt was designed for the roof of a working place. The result indicated that oversizing of the PV system on 30% is the optimal size for reducing the stress on the grid [30]. Additionally, a 10kWh BESS could reduce the grid energy exchange by 25% [30], but such a BESS will never replace the grid connection. Different charging profiles with different peak loads were

evaluated. Due to the PV system's production profile being simplified as a Gaussian distribution, a charging strategy which follows Gaussian distribution was considered the best approach in this case. The optimal peak was determined to be 5kW and 4kW for this PV system [30].

As far as the authors know, there is only one article that looks at a combined system of PV systems and charging stations in Norway. That is a master thesis conducted by Nes [31]. The article analyzed profile matching of PV systems and charging stations. The thesis concluded a low-power chargers have a better matching ratio than high-power chargers related to PV production profile [31].

Chapter 3

Theory

This chapter provides an overview of the theoretical background to ensure the reader has a better understanding of the concepts in this thesis. The chapter covers the Norwegian electrical system, PV production, battery (BESS) and hydrogen energy storage system (HESS). Additionally, an overview of solar data, correlation and linear optimizing is presented.

3.1 Norwegian Grid System

The Norwegian electrical power grid consists of cables, lines, transformers and generators, and extends across national borders. The lines and cables transport electrical energy from the power station to the consumers and can be described by three levels: transmission, regional and distribution [32]. The transmission grid is the highest level of the grid system, which operates between 300 kV and 420 kV. In Norway, this part is Statnett's responsibility. The transmission lines distribute the energy over long distances and to other countries. The regional grid is the medium level and operates between 66 kV and 132 kV. The transmission grid supplies the regional grid, which supplies distribution grids in the region. The regional grid is typically owned by the largest grid companies, such as Glitre Nett. In addition to supplying distribution grids, the largest electrical energy consumers are connected to this part of the grid. Most of the consumers on the Norwegian grid system are connected to the distribution grid. The different grid levels have different voltage levels, and to interconnect them, transformer stations are used. To transform the voltage up or down between the transmission and regional grid, a transformer station is utilized, while between the regional and distribution grid, a substation is utilized. In addition, the voltage levels can vary in the distribution grid. Typically, the voltage level in distribution is described as low voltage and high voltage, where low voltage is under 1000 V-AC and high voltage is over 1000 V-AC. Transformers are also utilized in this context, as voltage regulators between voltage levels [32]. Figure 3.1 illustrates the power system, where the hydropower plant is connected to the transmission grid and further to the consumer through different levels of the grid.

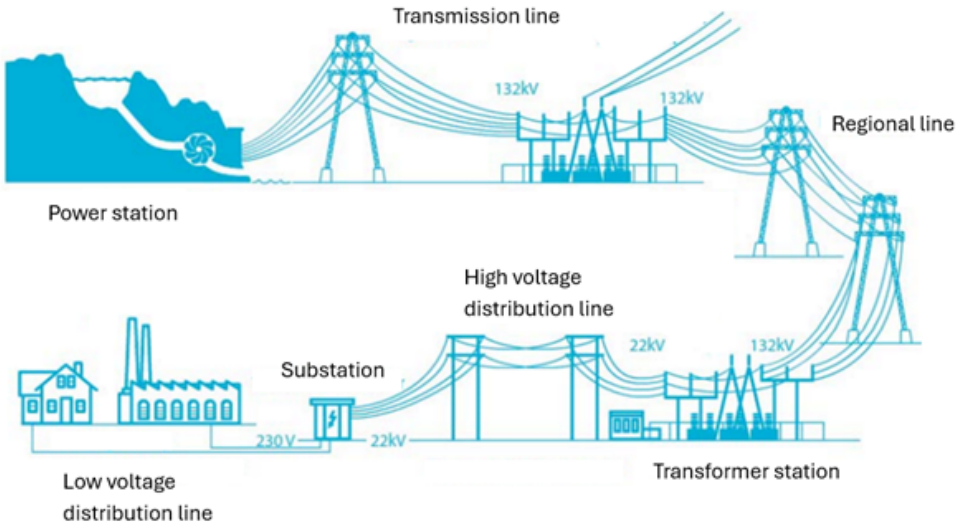

Figure 3.1: Illustration of the traditional Norwegian power system [33]

3.2 The Development of Electrical Energy Prices

The Norwegian grid system is connected to neighbouring countries, meaning electricity prices are influenced by events and actions abroad. In Europe, countries that use coal and gas as energy sources, which causes fossil fuel prices to be an important factor in the energy price [7]. In Norway, approximately all production of electrical energy comes from renewable energy sources, where many power plants are seemingly regulatable. This results in the price of electricity being strongly correlated with the weather. Additionally, prices are also determined by demand, which is in large part influenced by temperature [7].

Norwegian Water Resources and Energy Directorate (NVE) [7] predicts that electricity prices will continue to increase in Norway, but after a few years, the price will start to decrease again. An estimate conducted by NVE [7] claims the average price of electrical energy will be around 80 Norwegian Øre in 2030, while in 2040, the price will be around 49 Norwegian Øre. This trend is due to the increasing costs associated with carbon emission allowance and fossil fuels in Europe, which are expected to rise towards 2030. Additionally, Norwegian electrical energy consumption is predicted to increase considerably throughout 2030. However, it is not until 2030 that more production capacity is available. A large portion of these new energy sources will be non-regulatable, resulting in larger price variations during the day in the future [7].

3.3 Solar Energy Production and Technologies

3.3.1 Diffuse, Direct and Global Irradiation

The irradiation can be described in different ways, in this thesis irradiation and radiation will specifically reference electromagnetic radiation. The irradiation into a plane can be explained by the two components Direct Normal Irradiance (DNI) which is the irradiation directly from the sun; and Diffuse Horizontal Irradiance (DHI) which is radiation scattered in the atmosphere [34]. Global Horizontal Irradiance (GHI) is the sum of DNI and DHI. Equation 3.1 shows the formula for calculating GHI. Figure 3.2 illustrates the difference between DHI and DNI [34].

$$GHI = DHI + DNI \cdot cos(\theta_z) \tag{3.1}$$

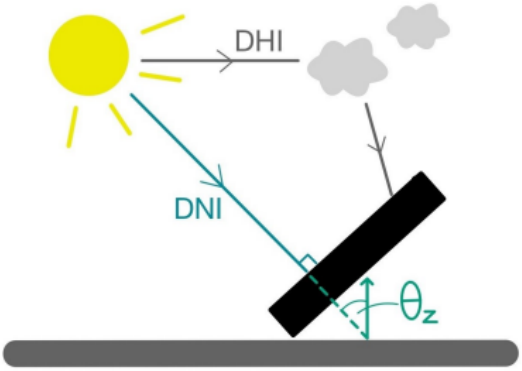

Figure 3.2: Illustration of irradiation of a PV system

3.3.2 Albedo and Reflection

When radiation hits a material, some part of the radiation will be reflected [34]. That is true for all materials, except for black bodies. These materials will absorb all radiation, but it is not relevant for PV applications. A measure of a material reflection properties is albedo (α). Albedo is a factor from 0 to 1, where 1 is 100 % reflection. A mathematical description of albedo is shown in Equation 3.2 [34].

$$\alpha = \frac{I_{reflected}}{I_{GHI}} \tag{3.2}$$

where $I_{reflected}$ is the reflected irradiation and I_{GHI} is the global irradiation onto the material. In the winter season, the snow results in a higher-ground reflection. Table 3.1 describes some typical albedo factors.

Table 3.1: Albedo factor varies from different materials [34]

Material	**Albedo**
Snow	0.5 - 0.9
grass	0.25
concrete	0.25 - 0.3

3.3.3 Sun's Position

The sun's position is an important factor for the irradiation of a location. As shown in Figure 3.3, the position of the sun can be described with an azimuth angle (γ_s) and an altitude angle (α_s) [34]. When the azimuth angle is low, the radiation will travel a further distance through the atmosphere. In Norway the sun's position vary greatly with the seasons, where in the winter the sun azimuth angle is lower than during the summer. This gives a clear radiation difference between the seasons. When irradiation travels in the atmosphere intensity losses occur, this loss is called Air Mass (AM). Higher AM means higher losses in irradiation intensity [34]. Equation 3.3 shows the equation that describes the air mass.

$$AM = \frac{1}{sin(\gamma_s)} \tag{3.3}$$

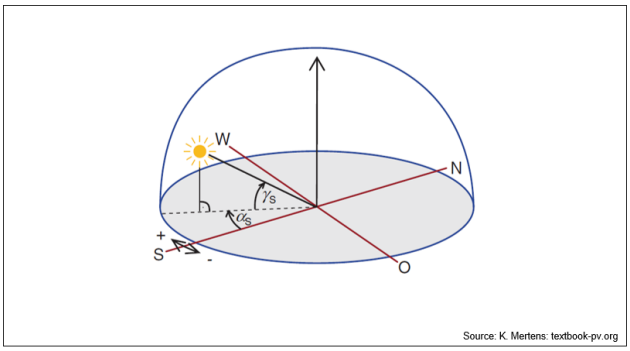

Figure 3.3: the azimuth angle (γ_s) and the altitude angle (α_s) describe the sun's position on the sky [34]

3.3.4 PV Modules

A PV module consists of several PV cells. The cells are often connected in series. Each cell produces a small amount of electrical energy, but in combination, results in a higher output. Typically, the larger the module, the more cells it contains. It is the number of cells that mainly determines the module's output production. While there are different types of PV technology designs, the most common is the mono-facial PV module. In the last few years, bifacial PV modules have been more popular. This technology can absorb energy from both sides of the panel, some can potentially generate more energy.

In the last couple of years, vertical bifacial PV modules (VBiPV) have been a technology with increasing focus. These modules are similar to the commercial bifacial systems, but are installed vertically [15]. Typically, the modules are installed facing east-west direction. In contrast to the traditional production profile, in which the peak production will be in the mid-day, the VBiPV technology will give a production profile with peaks in the morning and evening [15]. A system with a tilt angle which is optimized to produce the most energy, such as a traditionally bifacial application, will have a higher annual energy yield. Figure 3.4 illustrate a traditional land-installed PV application (a) and a VBiPV application (b).

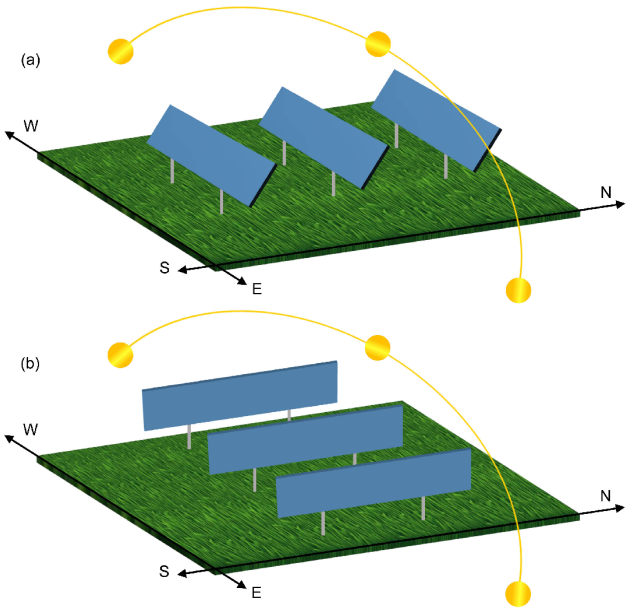

Figure 3.4: A traditional PV application has optimal tilt and faces south (a), while a VBiPV has 90-degree tilt and faces normally east-west (b) [35]

3.3.5 PV System

There exist several types of installations of PV systems, but two of the most common types are flat-roof installations and land installations [34]. Normally, these two types will have different connections. A flat-roof installation is often connected directly to the consumer, while land installations are connected directly to the grid.; The reason is the electric power production capacity of the PV system compared to the capacity of the grid. Land installations are much larger than flat-roof installations and need their own connection point [34].

A PV system consists often of one or more inverters and a smart energy meter [34]. Typically, PV modules are connected in series, called strings. These strings are further connected to inverters or generator connection boxes, depending on the system. the inverter's task is to convert the DC energy generated by PV cells to AC energy, which can be consumed or exported. Small-scale PV systems often use string inverters. In such a system, one or several strings are connected to an inverter and which supplies the electrical energy to the public grid. At a large-scale PV system, a central inverter can be used. In contrast to small-scale PV systems, which consist of several small inverters, large-scale PV systems only has one big capacity inverter. All strings are connected together in a connection box, which sends the DC energy to the central inverter. This inverter converts the electrical energy to AC, and supplies the public grid. The advantages of a central inverter are cost, lifetime and efficiency. Conversely, it is more vulnerable to shade. The string inverter is more robust to local shading, but it is linked higher cost [34].

Figure 3.5 illustrates a typical PV system [34]. The PV modules are connected in series and further connected to an inverter. The inverter converts the DC energy to AC energy and supplies the public grid. Between the inverter and the grid, it is a smart meter, which measures the electrical energy [34].

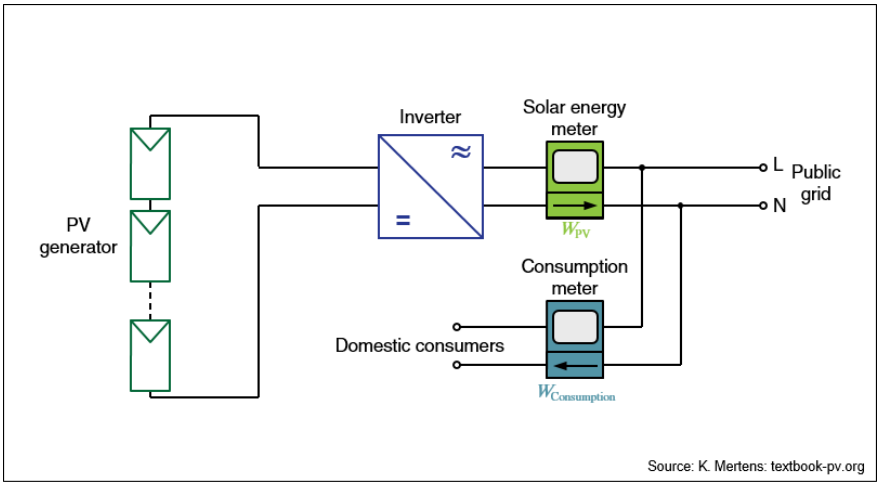

Figure 3.5: An example of a PV system [34]

3.4 Battery Energy Storage System

Battery is an electrochemical device that transforms electrical energy into chemical, and then back to electrical energy. This method allows for efficient storage of electrical energy. Often, the term Battery Energy Storage System (BESS) is used as the term for battery systems integrated into the electrical grid.

A battery is an electrochemical device that transforms electrical energy into chemical energy, and then back into electrical energy. This method allows for efficient storage of electrical

energy. Often, the term Battery Energy Storage System (BESS) is used to refer to battery systems integrated into the electrical grid.
In large-scale systems, e.g. electrical grid, the cost of BESS is typically too high to use as a long-term ESS. Due to the battery's properties, BESS is a good short-term ESS [36]. BESS can be used to stabilise the frequency and as a voltage regulator, which is a critical task in both on- and off-grid systems. The integration of renewable electrical energy sources, like PV modules and wind turbines, has resulted in this task being even more important than before. In such production technologies, the production can change rapidly, which will influence the grid and in the worst case, give the grid problems like surges [36].

3.4.1 Battery Characteristics

A well-used description of the battery's ability to store energy is Coulombic-efficiency. It is defined by how much electrical energy a battery can give in ratio to how much electrical energy the battery can take. The formula for Coulombic efficiency is given as Equation 3.4

$$\eta = \frac{i_d}{i_c} \tag{3.4}$$

where i_d is the discharge energy and i_c is the charge energy [37]. One of the strengths of the battery is the high round-trip efficiency. Battery can give close to 100 % of the energy used back to the system after storage [37]

Another well-used description of the properties of batteries is C-rate and E-rate. These values describe the charge and discharge rate. A battery with 1 C can charge with maximum power for 1 hour, while a battery with 0.5 C will charge for 2 hours and reach maximum capacity. Similarly, the E-rate will describe the same for the battery discharge property.

$$C\ rate = \frac{P_c}{E_{ss}} \tag{3.5}$$

where P_c is the charging power and E_ss is the capacity of the storage system.

Another important factor for the battery is the State of Charge (SOC) and Depth of Discharge (DOD). Even though a battery has a specific capacity, normally, a battery can not use its whole capacity. The lowest available capacity is described with the term DOD, while SOC is the current level of charge.

3.5 Hydrogen Energy Storage System

In comparison to BESS, hydrogen can also be used to store energy [38]. For long-term storage, hydrogen energy storage systems (HESS) often have lower lifetime costs than BESS, which is frequently used as an argument for HESS. In the future, where a larger part of the energy mix comes from non-regulatable weather dependent energy sources, more long-term storage will be required. Hydrogen is a environmental friendly method of storing energy. Hydrogen has a high energy density, around 33.3 kWh/kg, compared to e.g. gasoline which is around 11.9 kWh/kg. On the other hand, the mass density of hydrogen is low, around 0.089 kg/L, compared to gasoline has a mass density of around 0.72 kg/L [38].

Figure 3.6 illustrates a HESS. The illustrated system is connected to the grid with electrical cables. Electrical energy is supplied to the electrolyzer from the electrical grid. The electrolyzer converts electrical energy to chemical energy by splitting water molecules. Additionally, oxygen gas is a bi-product of this process. The hydrogen can be stored in a

high-pressure tank. When there is a demand for energy, the fuel cell can convert the chemical energy back to electrical energy. The hydrogen is forced from the tank to the fuel cell, where it reacts with oxygen gas to form water. Additionally, electric energy is released and can be supplied to the grid.

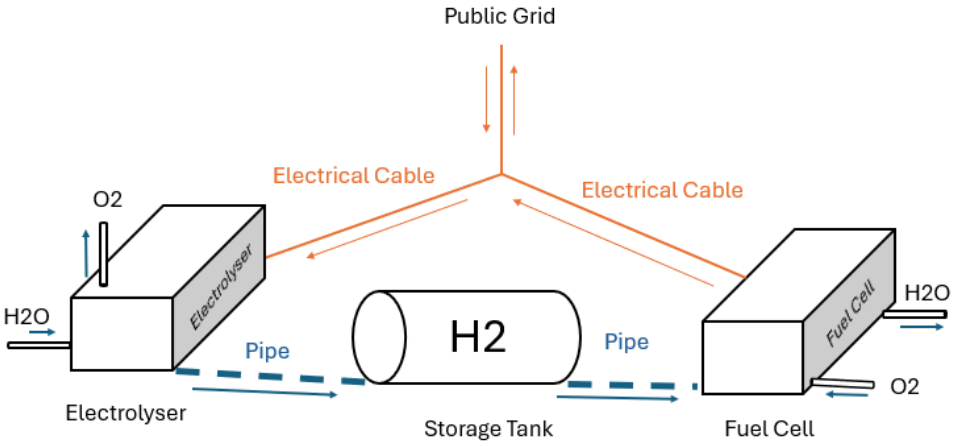

Figure 3.6: Illustration of a Hydrogen energy storage system

A disadvantage of HESS is the efficiency, where the efficiency is low in comparison with batteries [38]. Table 3.2 shows the typical efficiencies of varies electrolyser and fuel cell technology.

Table 3.2: Efficiency of electrolyzer and fuel cell [39] [40]

Technology	**The Current Efficiency**
PEM Electolyzer	56-60 %
PEM Fuel Cell	53-58 %

3.6 Optimization Algorithm

Optimization involves finding the best solution to a problem or a set of problems within certain constraints. Which is done by maximizing or minimizing the value of an objective function, subjected to the given constraints [41]. Algorithms are a common tool to optimise a problem. Linear programming (LP) problems are well-known, and there are several methods and algorithms to solve such problems. The methods utilized in this thesis are the simplex method; Branch and Bound method; and Cutting-plane method [41] [42] [43]. The linear solver employed to minimize the objective function 5.1 in this thesis is GNU Linear Programming Kit (GLPK). GLPK operates with a combination of the aforementioned methods [43].

A LP problem can be described as

$$\begin{aligned} max(c^T x) \\ Ax \leq b \\ x \geq 0 \end{aligned} \tag{3.6}$$

where the $C^T x$ the objective function subjected to maximization, $Ax \leq b$ represents the linear constraints and $x \geq 0$ limits the variable to be non-negative [41].

3.6.1 Simplex Algorithm

In 1947, Dantzig designed an optimization algorithm to solve LP problems, which is named the Simplex algorithm [41]. This algorithm is commonly used for optimizing economic models, but also for other types of problems. The primal simplex algorithm, can be geometrically illustrated as a irregular polygon, as shown in Figure 3.7 [41]. The algorithm starts in a corner, normally at the origin, and tries to move towards the solution sequentially in the direction of neighbouring corners. Each step will either increase or reduce the value of the object function, which leads to the optimal result over several iterations. When the solution cannot find a direction, the solution is optimal [41].

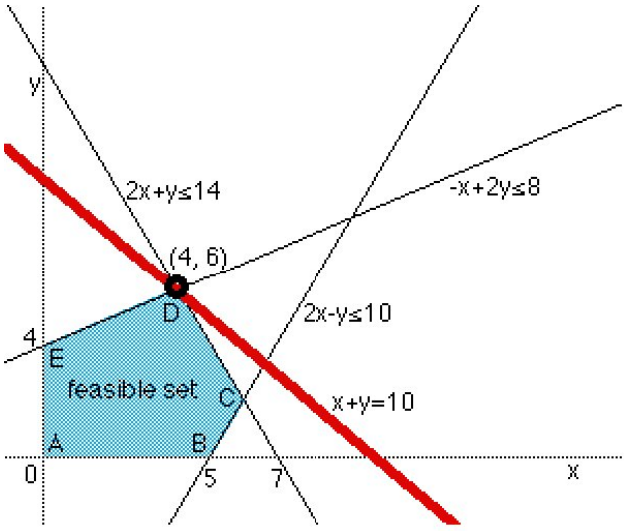

Figure 3.7: A illustration of the Simplex algorithm [41]

Dual Simplex is a algorithm derived from Simplex, where dual Simplex inverts the objective function for solving [41]. As shown in Equation 3.6, Simplex maximizes the objective function, while Dual Simplex minimizes the inverted objective function. Equation 3.7 describes the dual programming problem [41].

$$\begin{aligned} min(b^T y) \\ A^T y \geq c \\ y \geq 0 \end{aligned} \tag{3.7}$$

3.6.2 Branch and Bound

Branch and Bound is a popular algorithm in LP. The algorithm starts with defining a solution space [42]. Thereafter, the solution spaced is branched into sub-problems. For each sub-problem, upper and lower bounds are set. Each branch is evaluated by its bounds and is discarded if the solution is worse than optimal solution already found. This process continues until an accepted solution is found or there is no better solution [42]. Figure 3.8 illustrate Branch-and-Bound.

A further development of Branch and Bound is a combinatorial optimization algorithm called Branch and Cut, which includes an additional algorithm called cutting planes. Cutting planes is used to tighten LP relaxations and speed up the time consuming Branch and Bound algorithm.

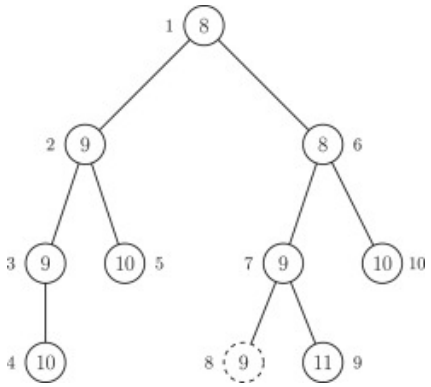

Figure 3.8: A illustration of Branch and Bound Method [42]

3.6.3 GNU Linear Programming Kit

As mentioned, in section 3.6, the used linear solver is the open-source GLPK. GNU is the name of the developers of the solver, and also a recursive acronym. The solver is designed to optimize LP, integer LP (ILP) and mixed integer LP (MILP) problems [43].

First, GLPK starts to solve the problem as a linear problem with Simplex. The solver evaluates the problem based on its characteristics whether it should use primal or dual Simplex. If the problem only contains integers, GLPK will use the result from Simplex as the final result. If the problem contains mixed integers, the solver will continue solving with Branch and Cut and use the result from Simplex as the upper bound (for maximizing) and the lower bound (for minimizing) for the objective function. The solver starts the branch and cuts the solution space. This process continues iteratively until the optimal solution is found.

3.7 Correlation

Correlation is a statistical tool, which can be used to describe the dependencies between two or more variables [44]. The result is represented by a value between -1 and 1. Factor 1 represents a perfect positive correlation, which means one variable increases, and the other variable increases in a consistent pattern. At factor -1, it is a perfect negative correlation, which means if one variable increases, the other variable decreases in a consistent pattern. If the correlation factor is 0, there is no correlation and there exists no dependency between the datasets [44].

Various methods exist, but Pearson and Spearman are two of the most common methods [44]. Pearson correlation describes the linear relationship between two continuous variables. Equation 3.8 displays the formula for Pearson correlation factor r_P [44].

$$r_P = \frac{\sum(x_i - \bar{x})(y_i - \bar{y})}{\sqrt{\sum(x_i - \bar{x})^2 \sum(y_i - \bar{y})^2}} \tag{3.8}$$

where x_i and y_i is the values in variables X and Y, while $\bar{x}$ and $\bar{y}$ is the mean value of the variables.

Another method, Spearman correlation, is a measure of monotonic dependencies between two variables [44]. In contrast to Pearson correlation, this method includes non-linear relationships in addition to linear ones. One of the strengths of Spearman correlation is that it ranks the data points rather than using their actual values. That is a contrast to the Pearson

correlation, which results the Spearman correlation having better performance with datasets containing outliers. Equation 3.9 displays the formula for Spearman correlation factor r_S [44].

$$r_S = 1 - \frac{6 \sum d_i^2}{n(n^2 - 1)} \tag{3.9}$$

where d is the difference between the ranks of the variables and n is the number of observations.

Chapter 4

Cost Review

This chapter reviews the cost estimations of various technologies as conducted in the literature, including predictions of cost developments.

4.1 PV Cost

The Norwegian Water Resources and Energy Directorate (NVE) has estimated the cost of the most common energy sources [45][46]. For flat-roof PV systems, the estimation was carried out by the consulting company Multiconsult and the industry association Solklyngen. NVE [45] claims that most of the flat-roof installed PV applications are west-east oriented with a 10-degree tilt and the specific yield is 750 hours. According to NVE [45], such a system has a cost of around 7200 NOK/kW, with an operational cost of 0.5 %. Due to the low number of land-installed PV applications in Norway, there is not sufficient data for accurate pricing. Therefore, NVE bases the numbers on the concession estimate [45]. For such a system, NVE [46] claims the cost is approximately 6700 NOK/kW, and the operational cost is around 2 % of the investment.

According to an article by IFE [47], the price of flat-roof installation was estimated to be 9 500 NOK/kW in 2018 but it could vary between 7 500 NOK/kW and 12 000 NOK/kW. The article claims the cost will drop in the future. In 2030, IFE has estimated the cost will be 5 500 NOK/kW, with a variation between 4 100 NOK/kW and 7 000 NOK/kW. According to the cost development in 2050, the cost will be 4 100 NOK/kW, with a variation between 3 000 NOK/kW and 5 200 NOK/kW. Additionally, the article estimated the cost of land-installed application is around 6 000 NOK/kW, and will be dropped in 2030 to 3 000 NOK/kW. For both technologies, the operation cost is around 0,5 % of the investment cost [47]. A Report by NREL [48] estimated a higher cost of PV farms compared to IFE. NREL's report claims the current cost is 1370$/kW. Furthermore, the report claims cost will be reduced to 60% of the current price in 2030, with a low-cost scenario reduction of 46% and high-cost scenario reduction of 80%. In 2050, the cost will be reduced to 46 % of the current cost, with a low and high-cost scenario by 38 % and 60% according to NREL.

A Dutch report written by Scharf et al. [49] conducted a study comparing Vertical Bifacial PV (VBiPV) and traditionally land-installed PV systems. According to the report, there is a higher cost associated with the VBiPV system, while the technology has other benefits, such as allowing the ground to be used for agriculture. However, the article describes the cost of several AgriPV systems. An 850 kWp system has an average cost of 572 €/kW, while a smaller system, 345.8 kW, has an average cost of 688 €/kW [49].

Å Energi has a database consisting of bids on solar parks and price estimates of PV applications. The price estimates are carried out by different consulting companies. A combination

of previous bids and estimates has given an price estimation of each PV appliction technology. For a flat-roof-installed system, the cost is estimated to be around 7000-8000 NOK/kW. In this estimate, the cost can vary significantly from roof to roof. For a land-installed system, the cost is associated with 6000-7000 NOK/kW, while for Agri-PV and vertical bifacial PV systems facing east-west, the cost is around 8300 NOK/kW. For VBiPV, the basis for cost estimation is weak because it is underdeveloped and not widely commercially available.

4.2 Energy Storage System Cost

Several articles have investigated the cost of energy storage methods. Biannually, NREL [50] publishes a report on the development of battery prices. This report compiles prices from multiple battery producers to determine the expected cost and performance. The values in Table 4.1 display the typical cost to a grid-connected battery system in relation to the C-rate, where higher C-rate yields a higher price. In addition, the report describes a typical round-trip efficiency is around 85% and the expected lifetime is around 15 years [50]. Battery energy storage systems (BESS) prices are predicted to decrease in the coming years. By 2030, the cost is estimated to decrease by between 16% and 40%, and by 2050, the reduction is projected to be between 28% and 67% [50].

Table 4.1: Price for 2021 [51]

C-rate	**Price**
1/2	537 $/kWh
1/4	446 $/kWh
1/6	386 $/kWh

Another article discusses the levelized cost of storage (LCOS) for a hydrogen system. The article is written by Leon et al. [52] and describes the cost of a proton exchange membrane (PEM) power-to-power hydrogen system. Due to the PEM technology's properties, it is the most suitable for storing excess energy. The capital expenditure (CAPEX) for the electrolyser and fuel cell was 650 €/kWh and 1700 €/kW, while the operating expense (OPEX) was 4% and 5% respectively, of the CAPEX. The system utilizes a salt cavern as a storage tank, and the cost is 0.9 €/kg of hydrogen, and OPEX is around 2% of CAPEX. The authors claim the storage method is much cheaper than compressed gas tanks [52].

According to the technical-economic report carried out by the Pacific Northwest National Laboratory (PNNL) [53], the cost of a 100 MW 10-hour hydrogen storage system is 312 $/kWh. The report, "Grid Energy Storage Technology Cost and Performance Assessment (2020)" [53], is a report that is published biannually and discusses the prices of different elements in a hydrogen system. The total price of a PEM electrolyser was 1 672 $/kW, while the PEM fuel cell is 1 397 $/kW. The storage capacity is around 9 $/kWh. This report predicts that the cost of the storage system will decrease [53]. A moderate estimate of the price in 2030 suggests the cost will be 161 $/kWh, while the low and high case is 144 $/kWh and 182 $/kWh [53]. A newer issue (2022) of the technical-economic report by PNNL updates the cost values for the hydrogen storage system [54]. The system cost is estimated to be around 295 $/kWh for a 10-hour system and 126 $/kWh for a 24-hour system [54]. The report also describes the cost per storage capacity as being approximately independent of the power capacity. The most important factor for the cost per kWh is the storage capacity [54]. In an internal project carried out by Myrhe, the cost of hydrogen was selected to be 279 $/kWh [11].

4.3 Economic Model for Grid Expansion

A master thesis written by Roestad and Alfsvåg [8] discusses the cost of grid connection. This study is the basis of Data Arena's economic model for grid expansion. It is a case study, where 4 different cases were investigated. Each case represents a different electrical grid connection and capacity requirement. Roestad and Alfsvåg built, in their report, an economic model to calculate the cost of the grid upgrade. The input of the model is the size of the main components. Equation 4.1 explains the mathematical model of the cost.

$$K(x_1, x_2, x_3) = k_0 + ax_1 + k_1 I_T + F(x_2) I_N + bx_3 \tag{4.1}$$

where k_0 represents the constant cost of the fixed startup costs for electrical grid expansion. a is a determined cost constant for each kilometer of cable/line and x_1 is the length needed for the expansion. $k_1 I_T$ term represents the cost of the switching field, where k_1 is the cost of the switching field and I_T is a binary variable that determines whether the circuit breaker needs to be expanded. $F(x_2)$ is the function of distribution substation cost. In contrast to the other terms, the cost linked to the capacity of the substation is a step function. Comparatively to the switching field term, the substation term also has a binary variable that determines whether the circuit breaker needs to be upgraded, represented by I_N. The last term in the model, bx_3 represents the cost of the transformer substation. b is the cost of the transformer substation per MW and x_3 is the capacity requirement.

The two first terms in the model, displayed in Equation 4.1, can determined by the function $f(x_1)$, shown in Equation 4.2.

$$f(x_1) = 783436x_1 + 149625 \tag{4.2}$$

Where x_1 is the length in km that is needed for the grid expansion. Equation 4.3 shows the step function of the distribution substation's cost. The function has a limit on the size and the system must have a capacity between 1 MW and 10 MW.

$$F(x_2) = \begin{cases} 407,184 \text{ NOK} & \text{when } 1 \text{ MW} \leq x_2 \leq 1.6 \text{ MW} \\ 642,791 \text{ NOK} & \text{when } 1.6 \text{ MW} < x_2 \leq 3.2 \text{ MW} \\ 878,398 \text{ NOK} & \text{when } 3.2 \text{ MW} < x_2 \leq 4.8 \text{ MW} \\ 1,266,879 \text{ NOK} & \text{when } 4.8 \text{ MW} < x_2 \leq 6.4 \text{ MW} \\ 1,502,486 \text{ NOK} & \text{when } 6.4 \text{ MW} < x_2 \leq 8 \text{ MW} \\ 1,738,093 \text{ NOK} & \text{when } 8 \text{ MW} < x_2 \leq 9.6 \text{ MW} \\ 2,126,574 \text{ NOK} & \text{when } 9.6 \text{ MW} < x_2 \leq 10 \text{ MW} \end{cases} \tag{4.3}$$

Where x_2 is the capacity of the substation in MW. Equation 4.4 shows a function that represents the last term in Equation 4.1. In comparison to Equation 4.3, the function's capacity is limited to between 1 MW to 10 MW.

$$f(x_3) = 5\,000\,000x_3, \quad \text{when } 1 \text{ MW} \leq x_3 \leq 10 \text{ MW} \tag{4.4}$$

Where x_3 is the capacity requirement of the transformer substation.

The thesis also describes the cost sensitivity for each component in the electrical grid expansion. The transformer substation has the highest cost sensitivity and will have the highest influence on the total cost.

4.4 Grid Tariff

All customers who desire electrical energy from the public grid are required to pay a grid tariff, which applies to both the production and consumption of energy. For electrical energy consumption from the public grid, the tariff consists of three terms: a fixed term, a power term and an energy term [55]. The fixed term is the annual fixed cost all customers must pay for the connection. The energy term relates to the cost customers must pay for the amount of energy they import from the public grid. Additionally, there is a power term. The customer must pay for the highest peak consumption each month. This cost rate varies depending on the season, with different rates for summer and winter. In addition to the grid tariff, customers are obligated to pay Enova support. Compared to power term, this cost rate varies depending on season. Table 4.2 shows the grid tariff values for a large-scale customer. As shown, the tariff depends on low voltage connection and high voltage connection [55].

Table 4.2: Electricity Grid Fees for Low and High Voltage, including Enova Support

	Low Voltage	**High Voltage**	**Unit**
Fixed Term	500.00	1,000.00	NOK/month
Energy Term (all year)	0.0790	0.0660	NOK/kWh
Power Term Winter	96.00	84.00	NOK/kW/month
Power Term Summer	32.00	28.00	NOK/kW/month
Electricity Tax Winter	0.1644	0.1644	NOK/kWh
Electricity Tax Summer	0.0951	0.0951	NOK/kWh

There is also a grid tariff for electricity production that should be exported to the public grid [56]. This tariff consists of a fixed term and an energy term. Table 4.3 describes the cost rate for the different terms. As shown in the table, the cost rate depends on production capacity. For production stations larger than 1 MW, energy terms must be calculated individually [56].

Table 4.3: The cost rate for grid tariff terms in 2024 [56]

Production capacity	**Fixed term**	**Energy term**
$<$ 1 MW	0.0149 NOK/kW	-0.0320 NOK/kWh
$>$ 1 MW	0.0149 NOK/kW	calculated individually

Chapter 5

Model

To simulate the cases, an internal model designed by S. Myhre [11] was used as a tool in this thesis to simulate the most cost-efficient grid connection. Figure 5.1 illustrates how the model works. Locations data was used to simulate the local PV production profile and the requirements of grid expansion. The local PV production profile is not produced by the optimization model, but stem from another tool created by the authors for an earlier project [14]. Thereafter, the cost of grid expansion, energy storage system (ESS) and energy production technologies was included in the model as input values. A solver uses all these inputs to estimate the most cost-effective grid connection, whether it is a traditional grid expansion or an integrated energy system (IES)

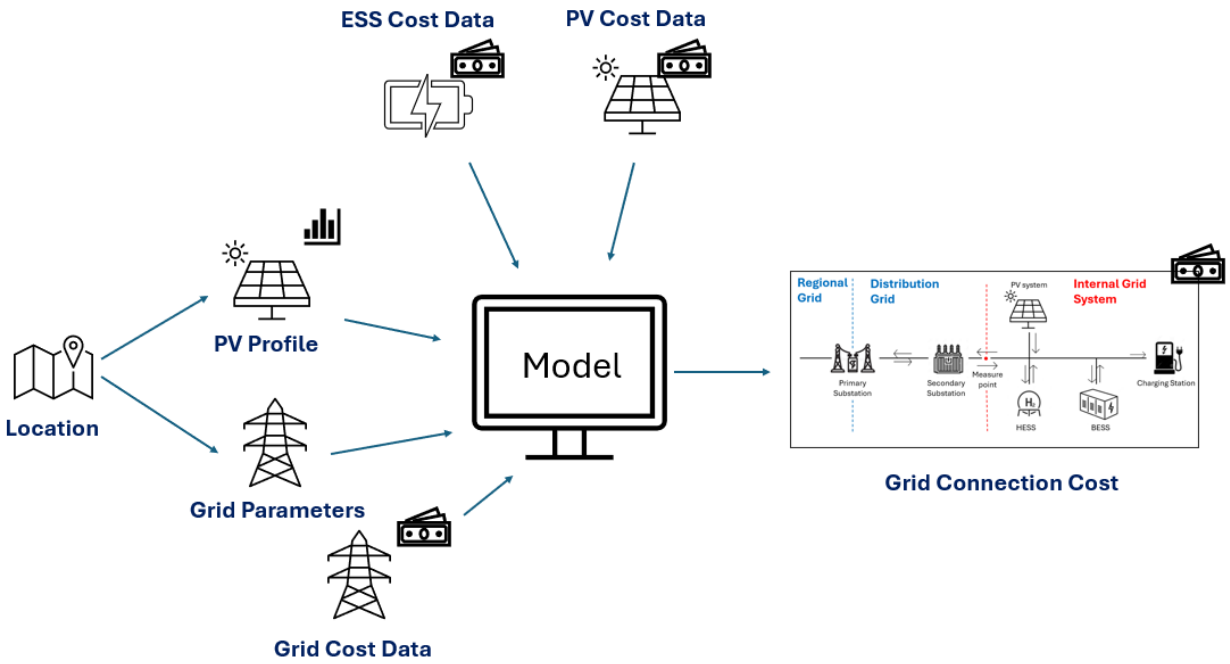

Figure 5.1: Illustration of the model's inputs and output, where grid parameters and PV profile are location dependent. Cost data is not.

5.1 Optimization Model

The model utilizes the mathematical optimization technique Mixed Integer Linear Programming (MILP) to minimize the objective function, which is described in section 5.3.1. MILPs variables can either be integers or non-integers and the different algorithms it employs is described in section 3.6. The objective function and its constrains was structured in python using the library *Pyomo.environ*, and the MILP solver applied was *glpk*.

Table 5.1: Overview of the optimization model input

Input	Unit	Notation	Explanation
Bus	String	-	A parameter to separate the different busses in the model
$Type$	String	-	A parameter to separate the different type of busses: Generator, Storage, Demand, Grid, Transformer and Substation. Where generator can be any type of electrical power production, but in this case it is only PV. Storage, on the other hand, is an umbrella term for ESS and can be BESS or HESS.
$LifeTime$	years	-	The lifetime of installed technology or grid given in years
$Length$	km	$C_{line,x}$	The length of the grid lines given in km.
$Directed$	Bool	-	$Directed$ is a variable indicating if the grid lines send electrical power one-directional or bi-directional. Where 1 is one-directional and 0 is bi-directional.
$FixedCapCost$	NOK	$CAPEX_{fixed}$	The fixed capital cost of investing in grid lines or substation.
$VariableCapCost$	NOK/km NOK/kW NOK/kWh	$CAPEX_{var}$	The variable capital cost for the different inputs of the model. NOK/km for grid lines; NOK/kW for substation, transformer, and generator; and NOK/kWh for storage.
$FixedOMCost$	NOK/kW NOK/kWh	$OPEX_{fixed}$	The fixed operational and maintenance cost per installed capacity. NOK/kW for generator and NOK/kWh for storage.
$InstalledCap$	kW kWh	$P_{install,x}$	InstalledCap is the already installed capacity of grid or grid alternative technology. kW for grid lines, generator, transformer and substation; and kWh for storage.
$maxDemand$	kW	$P_{load,max}$	$MaxDemand$ is the peak electrical power demand of the integrated energy system.
$MaxInstalledCap$	kW kWh	$P_{max,x}$	The maximum allowed capacity of generators(kW) and storage (kWh)
$Loss$	$x \in (0,1)$	$P_{line,loss}$	$Loss$ is the electrical power losses of the different components of the integrated energy system and the grid.
Eff	$x \in (0,1)$	η_G	Eff stands for efficiency, and is the efficiency of the generators.
$StorEff$	$x \in (0,1)$	η_{SS}	Storage efficiency is the efficiency of storage in the ESS. A value of less than 1 means that the storage will loose charge over time.
$DisEff$	$x \in (0,1)$	η_{dis}	$DisEff$ is how efficiently the ESS can discharge.
$ChaEff$	$x \in (0,1)$	η_c	$ChaEff$ is how efficiently the ESS can charge
SOC_Min	$x \in (0,1)$	SOC_{min}	SOC_Min is the minimum state of charge in the ESS.
SOC_Max	$x \in (0,1)$	SOC_{max}	$SOC_Max$is the maximum state of charge in the ESS.
$Crate$	$x \in (0,1)$	C_{rate}	The $Crate$ or C-rate is the rate of charge in a ESS. Higher C-rate makes the ESS charge and discharge faster. A C-rate of 1 makes the ESS fully charge/discharge in one hour.
$GenAvailability$	$x \in (0,1)$	P_G	$Genavailability$ is the electrical power production profile of the generators.
$Demand$	$x \in (0,1)$	P_{load}	$Demand$ is the load profile of a given location.
$GridSpotPrice$	$x \in (-\infty, \infty)$	G_{spot}	The price of electricity at a given hour.
$Operationalhour$	$x \in (0, 8759)$	t	Hours in a year, hourly time step used for the model.

5.2 Model Input

The model depends on economic and performance parameters. Key values of cost and operation of the selected PV-technologies, storage systems and grid connection was saved in a xlsx-file. The model imports these parameters into Python for further processing. Additionally, normalized load and production profiles are also inputs to the model. The model does not generate the load and production profiles, and therefore, this is an input parameter. Moreover, the electrical energy price was imported as a parameter. A full overview of the inputs of the model is described in table 5.1.

5.3 Objective function

In linear programming (LP), the objective function is a mathematical expressions that represents a quantity to be maximized or minimized. The model has two different objective functions that can be used to simulate two different outcomes. One simulates the most cost-effective investment cost, while the other simulates the most cost-effective result over a period. The model can use both objective functions, but they cannot run simultaneously. Which objective function should be used must be determined before the model is run, depending on which results are desired. Both objective functions are a combination of decision variables that describes the total cost of connecting a load to the grid and IES. The decision variables and the objective function is described in the functions in the two subsection below

5.3.1 Investment Cost Objective Function

The objective function was split into five different equations for improved clarity on each of the terms. The objective function is given in equation 5.1

$$obj = obj_{gen} + obj_{stor} + obj_{line} + obj_{rg} + obj_{st} \tag{5.1}$$

where each of the terms of the objective function is obj_x and the complete objective function is obj.

The first term deals with the cost of PV and is given in equation 5.2.

$$obj_{gen} = \sum_{g \in Generators} (C_{gen,g}\, P_{inv,g}) \tag{5.2}$$

where $C_{gen,g}$ represents the variable investment cost per capacity PV installed, given in NOK/kW, and $P_{inv,g}$ represents the invested capacity, given in kW.

The second term of the objective function deals with the cost of ESS and is given in equation 5.3.

$$obj_{stor} = \sum_{b \in Storages} (C_{stor,b}\, P_{inv,b}) \tag{5.3}$$

where $C_{stor,g}$ represents the variable investment cost per capacity ESS installed, given in NOK/kWh, and $P_{inv,b}$ represents the invested capacity, given in kWh.
The third term of the objective function deals with the cost of the cable lines and is given in equation 5.4.

$$obj_{line} = \sum_{l \in Lines} (C_{line,l}\, L_l + C^{fixed}_{line,l}) \tag{5.4}$$

where $C_{line,l}$ is the variable investment cost per km cable line invested in, given in NOK/km, L_l is the length of the cable line, given in km, and $C^{fixed}_{line,l}$ is the fixed capital cost, given in NOK.

The fourth term of the objective function deals with the cost of the regional grid expansion and is given in equation 5.5.

$$obj_{rg} = \sum_{t \in RegionalGrid} (C_{rg,t}\ P_{rg,t}) \tag{5.5}$$

where $C_{rg,t}$ is the variable capital cost per kW installed regional grid expansion, given in NOK/kW, and $P_{rg,t}$ is the capacity of the invested regional grid expansion, given in kW.

The final term in the objective function deals with the cost of substations and is given in equation 5.6.

$$obj_{st} = \sum_{s \in Substations} (C_{st,s}\ P_{inv,s} + C^{fixed}_{st,s}) \tag{5.6}$$

where $C_{st,s}$ represent the variable capital cost per kW installed substation, given in NOK/kW, $P_{inv,s}$ represents the capacity of the invested substation, given in kW, and $C^{fixed}_{st,s}$ represents the fixed capital investment of the substation, given in NOK.

5.3.2 Lifespan Objective Function

To simulate the total cost over a period, the reinvestment cost, income of selling electricity and cost of buying electricity are included. the objective function of total cost is displayed in 5.7.

$$obj_n = obj_{gen,n} + obj_{stor,n} + obj_{line} + obj_{rg} + obj_{st} + obj_{buy\&sell} + obj_{sell,Tariff} + obj_{buy,Tariff} \tag{5.7}$$

where $obj_{gen,n}$ represents the part of the objective function for investment cost for generators, including reinvestment over the simulated lifespan, $obj_{stor,n}$ represents the part of the objective function for investment cost for ESS, including reinvestment over the simulated lifespan, $obj_{buy\&sell}$ represents the cost of buying and selling electrical energy, $obj_{sell,Tariff}$ represents the tariff and tax of the energy sold to the grid, and $obj_{buy,Tariff}$ represents the load tariff.

The first term represents the investment cost of generators including reinvestment. The investment starts in year 0 with a reinvestment every 30 years, discounted to the year of investment. The term is displayed in 5.8.

$$obj_{gen,n} = \sum_{g \in Generators} \left(C_{gen,g}\ P_{inv,g} + C_{gen,g}\ P_{inv,g} \sum_{lt_g=1}^{LT_g} \frac{1}{(1+r)^{(30\ lf_g)}} \right) \tag{5.8}$$

where lf_g is the number of 30-year periods within the lifespan of the total project and r is the rate. The model use 5% as rate value if non other value is defined.

In comparison to the lifespan term of the generators, the storage energy system also included a reinvestment, but every 15 years

$$obj_{stor,n} = \sum_{b \in Storages} \left(C_{stor,b}\ P_{inv,b} + C_{stor,b}\ P_{inv,b} \sum_{lt_{stor}=1}^{LT_{stor}} \frac{1}{(1+r)^{(15\ lf_{stor})}} \right) \tag{5.9}$$

where lf_{stor} is the number of 15-year periods within the project's lifespan.

The terms related to the grid (obj_{line}, obj_{rg} and obj_{st}) are the same as used in the original objective function displayed in Section 5.3.1 as Equation 5.4, 5.5 and 5.6. A reinvestment term must be included for a simulation longer than 60 years, which is the determined lifespan of the grid system.

The next term represents the cost of buying and income of selling electricity. The term is shown in Equation 5.10. The buying and selling of electricity from the IES was summed for a year and the sum was discounted for n year through an annuity factor.

$$obj_{buy\&sell} = \left(\sum_{t=1}^{8760} (C_{buy} - R_{sold}) \right) A_n^{-1} \tag{5.10}$$

where C_{buy} is the cost of buying and R_{sold} is the economical selling of the electricity out of the IES. A_n^{-1} is the inverted annuity factor. Equation 5.11 shows the equation of the present value of an ordinary annuity over n years.

$$A_n^{-1} = \frac{(1+r)^n - 1}{r(1+r)^n} \tag{5.11}$$

where r is the rate. The model use 5% as rate value if non other value is defined.

The penultimate term is the term that represents the grid tariff for power production. The grid tariff's cost rate of the amount of energy was multiplied by the exported energy out of the IES at the time and summed up for the year. The Equation 5.12 displays the term.

$$obj_{sell,Tariff} = \left(\sum_{t=1}^{8760} (T_P E_{sold}) \right) A_n^{-1} \tag{5.12}$$

where T_P is the cost rate of energy terms in the production tariff and E_{sold} is the amount of sold electricity for the actual hour

The final term for lifespan simulation is grid tariff related to the load. The tariff's cost rate and the electricity tax were multiplied by the amount of energy that was imported from the public grid and into the IES. That was summed for one year and the sum was discounted for n year through an annuity factor.

$$obj_{buy,Tariff} = \left(\sum_{t=1}^{8760} ((T_L + T_E) E_{buy}) \right) A_n^{-1} \tag{5.13}$$

where T_L is the cost rate of energy terms in the load tariff and T_E is the cost rate of electricity tax and E_buy is the amount of energy imported from the public grid to the IES

5.4 Investment Cost Calculation

To calculate the cost, the fixed cost dependent on decision variables was summed. This includes capital investment cost per decision variable and operational cost per decision variable. The decision variables vary from element to element. Equation 5.14 illustrates the investment cost for each technology.

$$C_{n,x} = CAPEX + OPEX_{fixed} \tag{5.14}$$

Where $CAPEX$ represents the fixed capital investment, while $OPEX_{fixed}$ is the fixed sum of the present values of the operational costs. $C_{n,x}$ represents the fixed cost per decision variables, where n represents the technology.

5.5 The Algorithms Constrains

To ensure the simulation is within physical limitations, the model have some constraints for the algorithms. The flow balance should be maintained at all times and the max capacity of the energy sources, lines/cables, transformer, substation and storage system should not be exceeded.

5.5.1 Power Flow Balance

The power flow balance represents the relationship between storage flow, power production, and load consumption. This should always be balanced according to the laws of energy conservation. The model ensures balance with the help of a constraint shown in Equation 5.15. The sum of production from each generator and the net sum of charging/discharging from each storage system should be in balance with load consumption and grid buy/sell flow. Additionally, the model accounts for losses in the grid system.

$$\sum_{i=G_1}^{G_n} P_{G_i}[t] \pm \sum_{i=SS_1}^{SS_n} P_{SS_i}[t] \mp P_{line,loss}[t] - P_{load}[t] - P_{export}[t] + (1 - \eta_{grid_loss}) P_{import}[t] = 0 \tag{5.15}$$

where P_{G_i} is the power production of generator i and P_{SS_i} is the power charging/discharging of the storage system i, $P_{line,loss}$ is the power loss in the line, P_{load} is the load, P_{export} exported energy, $\eta_{gridloss}$ is the losses in the grid and P_{import} imported energy. The i represents the number of generator- or storage system technologies and t is the time unit. As shown in the constraint, the losses could be positive or negative, referring to the direction of the energy in the line.

5.5.2 Line

To determine the required line capacity, a constraint is used. The line's maximum flow should always be less than or equal to the line's capacity. The capacity consists of the already installed capacity and any additional capacity required to increase the line's capacity. Equation 5.16 shows the constraint.

$$P_{flow,line} - P_{installed,line} - P_{inv,line} \leq 0 \tag{5.16}$$

where $P_{flow,line}$ is a variable describing the actual flow through the line, $P_{installed,line}$ is the installed capacity of the line and , $P_{inv,line}$ is the invested capacity of the line. It is the invested capacity that represents the capacity upgrade. Maximum flow is a simulated value for the model, while the installed capacity is a parameter imported to the model which represents the available capacity.

5.5.3 Transformer Station

This constraint is a variable that details the capacity of the transformer station, and is given in equation 5.17. The constraint explains that the capacity of the transformer station cannot exceed the capacity of already installed transformer station capacity plus new investment in transformer station capacity.

$$P_{trans} - P_{intalled,trans} - P_{inv,trans} \leq 0 \tag{5.17}$$

where P_{trans} is a variable describing the capacity of the transformer, $P_{insalled,trans}$ already installed capacity and $P_{inv,trans}$ is the invested capacity. In this constraint, the invested capacity is the variable that the algorithm determined.

The power flow constraint of the transformer is displayed as Equation 5.18. The energy entering the transformer should always be equal to the energy exiting the transformer minus the transformer losses.

$$(1 - \eta_{trans})Flow_{in}[t] - Flow_{out}[t] = 0 \tag{5.18}$$

where η_{trans} is the efficiency of the transformer, $Flow_{in}[t]$ is the power flow into the transformer for each time unit and $Flow_{out}[t]$ is energy exiting the transformer for each time unit. The same constraints are also defined for substations.

5.5.4 Substation

The substation's constraints are similar to the constraints of the transformer. If the power flow through the substation is higher than the already installed capacity, a new capacity of the substation must be invested. This is shown in Equation 5.19.

$$P_{sub} - P_{intsall,sub} - P_{inv,sub} \leq 0 \tag{5.19}$$

where P_{sub} is a variable describing the capacity of the substation, $P_{intsall,sub}$ already installed capacity and $P_{inv,sub}$ is the required capacity of the substation.

Similar to the power balance of the transformer, the energy entering and exiting the substation should always be in balance. To ensure this balance, a constraint is defined that also includes substation losses. This constraint is displayed in Equation 5.20.

$$(1 - \eta_{sub})Flow_{in,sub}[t] - Flow_{out,sub}[t] = 0 \tag{5.20}$$

where η_{sub} is the efficiency of substation, $Flow_{in,sub}$ is the line power flow entering the substation and $Flow_{out,sub}$ is the power flow exiting the transformer.

5.5.5 Generator

Since the model does not generate it is own production profile, the profiles are imported from a PV simulation model. This profile is normalized and will be adjusted according to the selected rated power of the generator. The adjustment is carried out in the constraint shown in Equation 5.21. As shown in the constraint, both the installed and invested capacity are multiplied by the normalized profile. Additionally, the constraint includes the losses in the conversion system to the generator, which are represented by the efficiency.

$$P_G - P_{profile,G}(P_{installed,G} + P_{inv,G})\eta_G \leq 0 \tag{5.21}$$

where P_G is a variable describing how much power the generator produces, $P_{profile,G}$ is the normalized production profile, $P_{installed,G}$ is the already installed capacity and $P_{inv,G}$ is the

invested capacity of generators. The model determined the capacity of the generators that are most economically viable. If this value is higher than the installed capacity, the model will invest in new capacity.

To ensure the model does not generate an unnaturally large amount of capacity for the generators, the limit is included as a constraint. This constraint limits the allowed investment capacity, which is determined as a parameter. This will make the model more realistic, when in some cases where the area is a limited factor. Equation 5.22 displays the constraint, where the installed and invested power can not be larger than the allowed capacity.

$$P_{installed,G} + P_{inv,G} - P_{allowed,G} \leq 0 \tag{5.22}$$

where $P_{allow,G}$ is the input parameter that limits the maximum allowed production.

5.5.6 Energy Storage System (ESS)

The simulation of the (ESS) includes some constraints. The model starts with the smallest SOC for each ESS technology. Thereafter, the model can discharge and charge depending on the system's demand. In the ESS, the power flow must always be balanced. To ensure this, a constraint is introduced to ensure that the power input equals the power output, including losses. The model includes the losses in the energy stored and in the discharge and charging process. The Equation 5.23 shows the power flow as an equation.

$$(1 - \eta_{ss}) E_{stored,ss}[t] + \eta_c P_c[t] - \frac{P_{dis}[t]}{\eta_{dis}} = 0 \tag{5.23}$$

where η_{ss} is the efficiency of the ESS, $E_{stored,ss}$ is the amount of the storage energy at the time unit, P_c and P_{dis} is the charge or discharge power at the time and η_c and η_{dis} are the efficiency of charge and discharge.

To determine the optimal storage capacity, the constraint in Equation 5.24 is used. The model estimates the optimal storage capacity. Is this capacity is higher than the already installed capacity, the model will invest in new storage capacity.

$$E_{installed,ss} + E_{inv,ss} - E_{max,ss} \leq 0 \tag{5.24}$$

where $E_{installed,ss}$ is already installed capacity, $E_{inv,ss}$ is the invested capacity of the storage system and $E_{max,ss}$ is the storage capacity that model requirement.

The model includes constraints to simulate the charge and discharge power. This is carried out by ensuring that the charging and discharging power are lower than or equal to the c-rate multiplied by the storage capacity, as illustrated in Equation 5.25 for charging and Equation 5.26 for discharging.

$$P_{ss,charge} - Crate \ (E_{installed,ss} + E_{inv,ss}) \leq 0 \tag{5.25}$$

$$P_{ss,discharge} - Crate \ (E_{installed,ss} + E_{inv,ss}) \leq 0 \tag{5.26}$$

where $P_{ss,charge}$ and $P_{ss,discharge}$ is the charge and discharge power and $Crate$ is the C-rate.

Since various storage systems technologies have a limited state of charge interval, a constraint is used to ensure the lowest and highest level of the state of storage capacity. If the state is lower than the limit, the storage system can not supply the demand or grid with energy. If the state is higher than the limit, the generator can not supply the storage system. This

is illustrated in Equation 5.27 for the minimum state of charge and Equation 5.28 for the maximum state of charge.

$$SOC_{min} \ (E_{installed,ss} + E_{inv,ss}) - E_{stored,ss} \leq 0 \tag{5.27}$$

$$E_{stored,ss} - SOC_{max} \ (E_{installed,ss} + E_{inv,ss}) \leq 0 \tag{5.28}$$

where SOC_{min} is the lowest level of storage and SOC_{max} is the highest level of storage.

Chapter 6

Model Input Data Collection Approach

6.1 Location Determination

To identify viable locations for this case study, a tool from Glitre Nett's digital toolbox called Infrastructure Management was employed. Firstly, the map was filtered to display only grid connection requests of charging stations. On the map, each request is represented with a point. The size of the point represents the amount of requested capacity. A large point represents a big capacity requirement, while a small point represents a low capacity requirement. Locations with large points or locations with several small points were selected for further evaluation. Thereafter, Data Arena was used as a tool to evaluate the available capacity. For each location, the available capacity was evaluated. To gather information about the estimated cable/line length required between the customer and the primary substation, a tool called Plan Portal was used. This digital tool is also a part of Glitre Nett's toolbox.

6.2 Data Collection of Load Profiles

In 2019, a requirement was established mandating that every customer must have smart meters. These instruments measure and record the production and consumption of electrical energy. In addition, smart meters are placed in substations and transformers to measure and record the power transfer at several points in the grid. The hourly data are sent to the grid company and saved. For Agder County, it is Glitre Nett who is responsible for measuring and saving this data. The data are the foundation for the project and are saved in Glitre Nett's digital toolbox in PowerBI reports.

For each selected location, large-scale charging stations were identified using Glitre Nett's Toolbox. A load profile for each location, within the criterion of about 1 to 10 MW and connected to the High Voltage Level, was selected to represent the specific location. The selected load profiles, which should represent the location, were converted from PowerBI reports to xlsx-files. The exported data consisted of various data, but only the consumption data of electricity was of interest in this project. Some data points were missing, which was replaced by predicted consumption. The prediction of consumption was conducted by Glitre Nett for all periods and all measurement points without measured data. To process the replacement of missing data, Python was used. The xlsx-files were imported and formatted; all data without consumption data was removed. At the end, the load profiles were normalized.

6.3 Data of Economic Key Values

Data on key economic values were collected from various sources. Most of the values were obtained from literature sources (Chapter 4) and evaluated based on unpublished internal estimates conducted by Å Energi. Typically, different sources reported the costs in various currencies. In this project, the Norwegian Krone has been used. Therefore, all economic values were converted to the Norwegian Krone. Table 6.1 shows the currency exchange rates that were used to convert the values to Norwegian Krone. The currencies were converted using the exchange rate from March 11, 2024.

Table 6.1: The currency exchange rate in Norwegian Kroner on March 11, 2024 [57]

Currency	Norwegian krone exchange rate
1 Dollar ($)	10.42 NOK
1 Euro (€)	11.42 NOK

6.3.1 PV

To evaluate the cost of each PV technology which is used in the optimization model, internal estimated cost and previous PV project bids saved in Å Energy's database were used. In addition, these values were compared to the cost found in the literature. The capital cost of land-installed PV systems was determined to be 6000 NOK/kW, 7500 NOK/kW for flat-roof-installed PV systems and VBiPV systems the cost was set to 8000 NOK/kW. The lifetime of the PV applications and the inverter efficiency were selected to be 30 years and 98%, which are typical values for these components. In addition, for land-installed and VBiPV systems, the operative cost was set to 2 %, while for flat-roof-installed systems was this parameter set to 0.5%. Table 6.2 displays the selected cost of each technology.

Table 6.2: Cost for different PV technology

Technology	CAPEX	OPEX
Land	6 000 NOK/kW	120 NOK/kW
Flat-roof	7 500 NOk/kW	38 NOK/KW
VBiPV	8 000 NOK/kW	160 NOK/KW

6.3.2 Battery Energy Storage SYstem(BESS)

The battery cost of the storage system is based on NREL's Technical report [50] about cost projections for utility-scale battery storage. Table 6.3 shows the cost of the battery related to the C-rate. Additionally, the report describes the battery will have a typical round-trip efficiency of around 85 %. A typical lifetime of the battery is 15 years. The price of utility-scale batteries is predicted to fall in the future as shown in table 7.2 in section 6.5.

Table 6.3: Price of BESS related to C-rate

C-rate	CAPEX
1/2	5 600 NOK/kWh
1/4	4 647 NOK/kWh
1/6	4 022 NOK/kWh

6.3.3 Hydrogen Energy Storage System (HESS)

For the cost of HESS, a combination of PNNL's reports [53] [54] and PNNL's cost calculator [58] was used as the foundation of determination. Table 6.4 shows the cost of HESS related to storage capacity. Since neither the reports nor the calculator provided any costs for a 20-hour system, the figure was interpolated between 24 and 10 hours

Table 6.4: Discharge duration

Discharge duration	CAPEX
10 hours	3 303 NOK/kWh
20 hours	1 698 NOK/kWh
100 hours	414 NOK/kWh

In comparison to BESS, the lifetime of the hydrogen storage system was set to 15 years. The roundtrip efficiency is 35%, which is a result of PEM electrolysis (60%) and PEM fuel cell efficiency (58%). These values were selected based on the literature.

6.3.4 Grid Connection

The cost linked to the grid connection is based on the model to Roestad and Alfsvåg [8]. The substation cost was approximated as a linear function due to GLPK's restrictions where it can only solve linear problems. The cost of building grid lines has a linear relationship with the length of the line, while the transformer station has is linearly dependent on the capacity given in kW. Table 6.5 shows the cost value of each component of the grid. The cost of the line only depends on the line length and a fixed investment cost, while the substation and transformer station depend on capacity requirements. Additionally, the lifetime was set to 60 years.

Table 6.5: The cost of the component in the grid system

Component	Variable CAPEX	Fixed CAPEX
Line	783 436 NOK/km	149 625 NOK
Substation	285 NOK/kW	85 220 NOK
Transformer station	5 000 NOK/kW	0 NOK

6.4 PV Production Profiles

An important factor in the model is the electrical production profile of PV installations. The PV simulation model development in the course ENE 503 by Brohaug and Nesse [14] was used to estimate the electrical production profiles for various PV systems. The article is referenced in Chapter 2. The model uses a generated dataset called a typical meteorological year (TMY) to simulate AC PV power production in a given location. A TMY contains hourly data of radiation, wind speed, air temperature, and more in a given location. The PV production profiles are highly dependent on radiation data, which in this thesis is based on a typical meteorological year (TMY). The TMY used in this thesis is generated from 20 years (2000 - 2020) of meteorological data in each location using the ISO 15927-4 procedure. Essentially, a TMY selects data from the "best" months in the chosen years to create a reference year or TMY [59]. Changing the input data for the TMY can drastically change the PV power production profile, and in turn the results of this thesis. For each location, a

independent production profile was generated. The model was written in Python using the library pvlib, which gives easy implementation with the optimization algorithm.

The summarized flow of the python script which simulates the production profiles is firstly to import necessary libraries. Where pvlib is the essential library. Secondly, the coordinates of the location is given to the model. Furthermore, data for inverter and PV module is imported. Pvlibs [16] function *pvlib.iotools.get_pvgis_tmy* imports a TMY from pvgis [60] in the given location and with elevation . When all necessary data is imported the solar irradiance on the module and solar position is calculated. The power losses due to temperature in the PV module is calculated using the irradiance and weather data previously obtained. Lastly, the PV power output is calculated considering shading losses and inverter efficiency, where the output power is normalized and formatted for further use in the linear solver.
To simulate the different PV systems some more information is needed: Surface azimuth, surface tilt and bifaciality. Bifaciality is defined as the efficiency of the backside of a bifacial module. The input parameters for the different PV systems is given in table 6.6.

Table 6.6: PV production profile system parameters

PV system	**Surface azimuth**	**Surface Tilt**	**Bifaciality**
Solar Land	180°	40°	0.902
Solar VBiPV	90°	90°	0.902
Solar Roof	± 90°	10°	0

The numerical degrees presented in the table above is the rotation of the PV module, where 0°surface azimuth is North and 0°surface tilt is parallel to the surface. For roof installed PV systems the east and west facing modules were simulated individually and added together after.

6.5 Price Profiles

The electricity prices that were used in the model are forecast conducted by Volt Power Analytics. The forecast is commercial and exempt from the public. The electricity prices are estimated from 2024 to 2047 for the South-Norway zone (NO2). The forecast is based on 30 estimates for each year, where each estimate represents a specific weather year. The different weather years represent the weather in the time range of 1991 to 2020. An average for each year was used to calculate an overall price prediction. In the simulation, the price was used for a representative year except 2050. Since the range of the data set stops in 2047, the prices of 2047 were used instead of 2050.

Even though the forecast is exempt from the public, it is broadly similar to what The Norwegian Water Resources and Energy Directorate predicted, which is described in Section 3.2.

6.6 Grid Tariff and Tax

Table 6.7 displays the values of the cost rates which was used in the simulation in lifespan simulation (Case E in Section 7.3.5). To simplify the model, only summer cost rates were used. Additionally, in the calculations of grid tariff, the system was set to be a high voltage system.

Table 6.7: The used cost rate for the grid tariff for the simulation

Constants	**Value**
Production tariff (T_P)	0.0149 NOK/kWh
Load tariff (T_L)	0.0660 NOK/kWh
Electricity tax (T_E)	0.0951 NOK/kWh

Chapter 7

Location and Case Description

This chapter provides an overview of the analysed locations. Additionally, it reviews of the cases and the analyses that were conducted to support and discuss the result of the case simulations.

7.1 Location Definition

Four locations within Agder County were analyzed. All of these areas have a high load share stemming from charging stations. Each area is located close to the main highway and serves as a typical stopping point for summer tourists. Additionally, there is an expectation that the requests for new capacity for charging stations will increase for all locations. An overview of the locations' capacity requests and cable length is given in table 7.1 below.

Table 7.1: Total capacity request for the four locations, including cable length to grid.

Location	Capacity request	Cable length
Location I	9.25 MW	1.0 km
Location II	6.75 MW	5.0 km
Location III	3.40 MW	2.5 km
Location IV	4.00 MW	1.0 km

In all four locations, there is no available grid capacity. To meet the capacity request either more grid capacity needs to be built or some alternatives needs to be implemented. A more detailed description of the different locations is given in sections 7.1.1, 7.1.2, 7.1.3 and 7.1.4, where the traffic pattern and load profile are displayed.

7.1.1 Location I

Location I, in addition to serving as a typical stopping point for tourists along the main highway, is a service and commercial centre. There is already a high portion of charging stations, but there exist several requests for grid connection of charging stations. In total, there exist requests for 9.25 MW capacity in charging stations, with no available capacity in the grid. A grid expansion will result in a new 1km cable/line.

Figure 7.1 describes the annual traffic pattern. As shown, there is significantly higher traffic in the summer season. There are also small peaks around the Easter and Christmas holidays, which indicates higher activity during these periods.

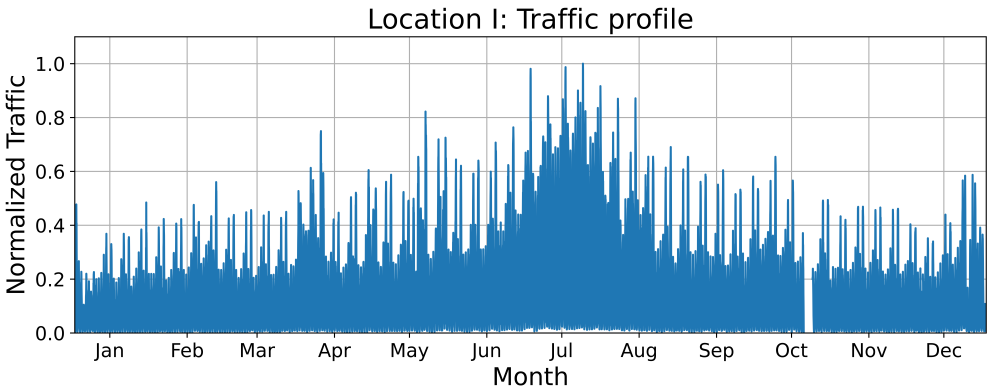

Figure 7.1: The traffic pattern past Location I.

Figure 7.2 illustrates the selected load profile representing the location. The profile is normalized and plotted against the number of hours of the year. As shown in the figure, there is higher activity in the summer season, similar to what the traffic pattern indicated. Additionally, it is a clear peak in Easter and Christmas week.

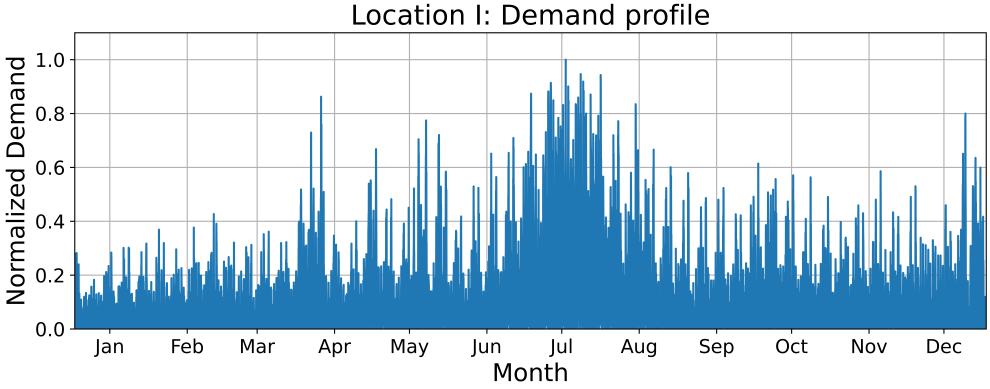

Figure 7.2: Load profile for location I

7.1.2 Location II

Location II is also a typical stopping point for tourists near a main highway. Unlike Location I, Location II has a high portion of industry. There are some charging stations already operational, but there is a need for more. Several actors plan to construct charging stations and the total requested capacity is 6.75 MW. A grid expansion will need 5 km with cable/line.

In contrast to Location I, Location II is situated next to a typical commuter road. Figure 7.3 illustrates the traffic pattern past this location. In contrast to Location I, which has a significantly higher peak during the summer season, the traffic past Location II is more stable, although there is a slight increase in the number of cars that pass the location in the summer.

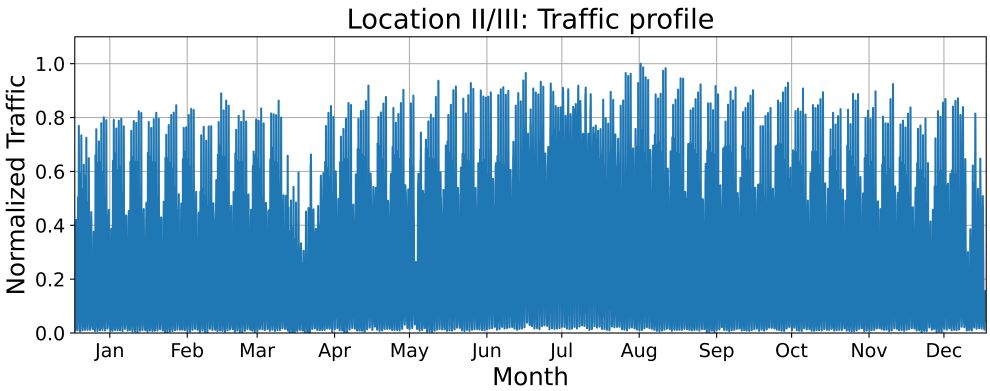

Figure 7.3: The traffic pattern past Location II and Location III

Figure 7.4 displays the load profile that represents Location II. In comparison to the location's traffic pattern, the load profile has not a clear season peak. However, it can be indicated sign of higher activity in the summer season.

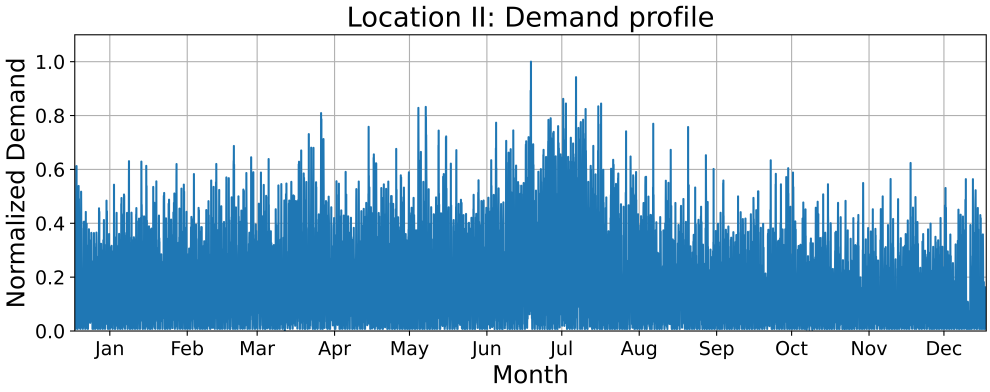

Figure 7.4: Load profile that represents the location II

7.1.3 Location III

Location III is situated close to Location II and the traffic pattern in Location III is approximately equal to the traffic pattern in Location II, which is illustrated in Figure 7.3. The total capacity requests are 3.4 MW, and all of them are charging stations. A grid expansion will involve installing a new cable/line of 2.5 km.

Figure 7.5 illustrate the load profile that represents location III. Notwithstanding that Location II and Location III have the same traffic pattern, the load profiles have variations. Unlike location II, Location III has a more clear summer season peak. Additionally, the Easter peak is more clear than Location II. In contrast to Location I, the Christmas peak is less clear in this load profile.

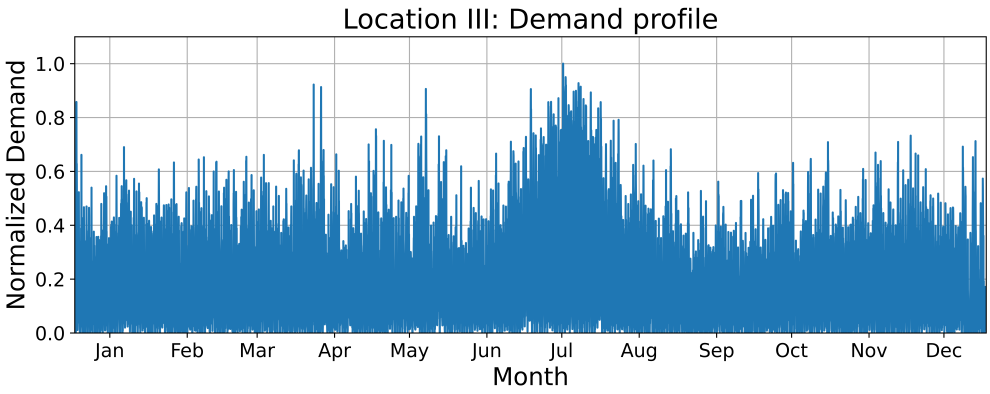

Figure 7.5: Load profile that represents the location III

7.1.4 Location IV

Location IV, unlike the other locations, serves as a tourist stopping point near a main highway. This location is close to a city and hosts both industrial and commercial centers. Charging stations already exist at this location, but there are requests for an additional 4 MW capacity for charging stations. Like the other locations, there is no available capacity, which traditionally results in grid expansion. Due to the geography and its proximity to the city, the location is not suitable for land-installed PV stations. It is estimated that there is an available area for flat-roof PV systems capable of generating 6 MWp. The required grid expansion involves installing a 1 km cable or line.

The traffic pattern in Location IV is a hybrid between Location I and Location II/III. The pattern has a more stable activity than Location I, but a clearer peak in the summer compared to Location II/III. Figure 7.6 illustrates the pattern of traffic past Location IV.

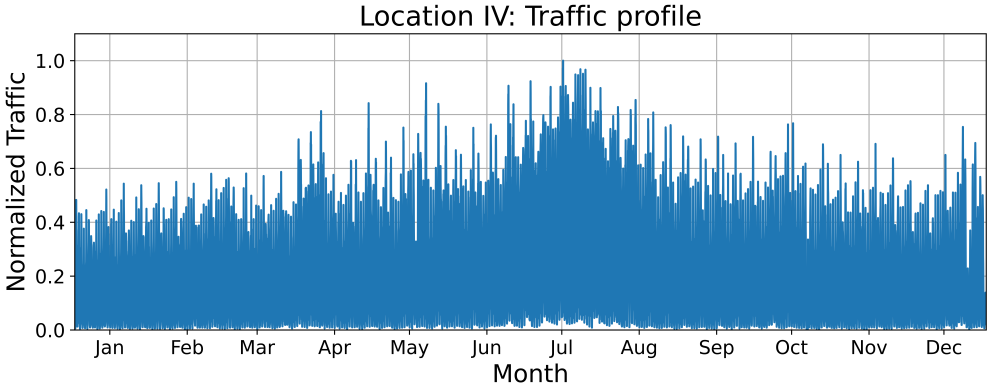

Figure 7.6: The traffic pattern past Location IV

Figure 7.7 displays the load profile that represents Location IV. In the manner of Location I, Location II has a clear summer season peak. Additionally, the profile indicate clearly sign of a Easer and a Christmas Peak.

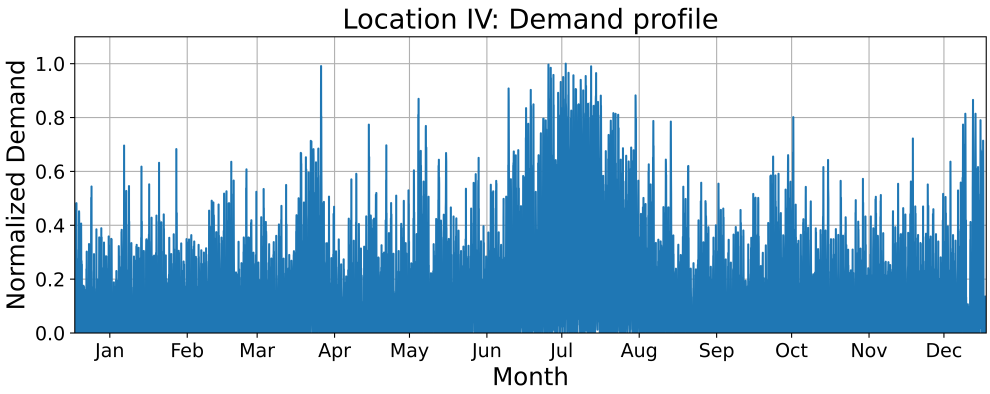

Figure 7.7: Load profile that represents the location IV

7.2 Supporting Analysis

Three sub-analyses were conducted to discuss the simulated cases: analysis of the load profile, traffic pattern analysis and peak matching analysis.

7.2.1 Average Daily Load Profile

An analysis of the load profile for each location was conducted. First, the load profiles (illustrated in Section 7.1) were observed, and two seasons were defined: high activity season (when the load is typically high) and low activity season (when the load is typically low). Thereafter, a daily average profile of the low-activity season (representing typical low load) and the high-activity season (representing typical high load) was calculated and plotted for each location.

7.2.2 Traffic Pattern Analysis

A simple analysis of the traffic pattern was conducted to observe if the traffic pattern of the locations could be used as a future indicator of load behaviour. For each location, historical traffic data was imported from The Norwegian Public Roads Administration data bank [61]. The closest registration point was used. The charging stations were assumed to only handle passenger sized cars, not heavy-duty vehicles, such that only the traffic pattern for passenger cars was Thereafter, Python was used to calculate Person and Spearman correlation to check how load behaviour relates to the traffic pattern.

7.2.3 Peak Matching

As mentioned in section 8.3, the PV production profiles are heavily dependent on the input radiation data. Therefore, it is necessary with an analysis of the PV production profile compared to the load profile. The normalized load profile and normalized PV production profile were compressed in the same data frame and plotted against each other to analyse how they match.

7.3 Case Study

The cases are related to the research questions defined in Section 1.2. For Case A to D, the objective function of investment cost was used (described in Subsection 5.3.1), while for Case E the objective function of lifespan (described in 5.3.2) was conducted.

7.3.1 Case A: Current Cost Scenario Simulations

To simulate the most cost-effective investment cost of grid connection in the current cost situation, the original cost given earlier in Chapter 6 was used as input in the model. Only the investment costs are considered, meaning buying and selling electricity does not influence these costs of the grid expansion. The objective function of investment cost was used in this case. The simulation was conducted over a year for each location, giving the total cost of grid expansion as well as technology capacity.

7.3.2 Case B: Future Cost Scenario Simulations

To investigate when the alternatives could more realistically compete with traditional grid expansion in investment costs, a cost scenario analysis was conducted. Predictions of the cost development from the literature is displayed in Table 7.2. The table shows the reduction for 2030 and 2050 in percent and for a low-, base- and high-cost scenario. Each Location, all selected cost scenario was simulated and plotted.

Table 7.2: The cost development of technologies

Technology	**Year**	**Low**	**Base**	**High**
PV (flat-roof)	2024	-	0%	-
	2030	45%	27%	7%
	2050	60%	45%	31%
PV (land)	2024	-	0%	-
	2030	54%	40%	20%
	2050	62%	54%	40%
BESS	2024	-	0%	-
	2030	40%	32%	16%
	2050	67%	53%	28%
HESS	2024	-	0%	-
	2030	54%	48%	42%
	2050	- %	- %	-%

In the literature review, the authors does not have a price prediction for P2P hydrogen in 2050. Additionally, the authors does not have predictions of cost development for VBiPV systems. For the purpose of this thesis, the VBiPV system cost is assumed to follow the development of land PV as a simplification. This simplification is made because its reasonable to assume that VBiPV systems becomes cheaper, following the cost development of the other PV technologies. Additionally, the authors did not manage to find any good sources on price predictions on VBiPV.

7.3.3 Case C: Cost Sensitivity of Technologies

A sensitivity analysis was performed to investigate how the cost of PV and storage technologies influences the models investment decisions. This analysis was made to observe how much the different technologies have to drop in cost before they can compete with traditional grid expansion in cost-effectiveness. Each of the technologies had its cost reduced, separately, from 0 % to 99 %. The result of this analysis gives an invested technology capacity plotted against technology price reduction and grid expansion reduction plotted against technology price reduction. Grid expansion reduction meaning how much less grid expansion is needed when the price of a technology falls.

7.3.4 Case D: Grid Capacity Limitation

Initially, the model allowed unlimited grid capacity expansion, therefore an analysis in grid capacity limitation was conducted. This analysis was performed to investigate the investment cost of a grid connection when forcing the model to use alternatives. The current cost of technologies, found in chapter 6, was used for this analysis. Simplifications of the technology input data were necessary due to the sheer time requirement of running this analysis. The simplifications made was to include only some of the technology types, where the technologies included are 2h BESS, 6h BESS, 100h HESS and land PV. The storage systems that was dropped was due to its likeness to the other storage systems. Two PV technologies, VBiPV and roof PV, was dropped because of the cost of the technologies. The cost of the dropped PV technologies was higher than land PV and the model only wanted to invest in land PV. The grid capacity limitation ranged from no limitation to 90% limitation. The results of this analysis gives a bar plot of the capacity of the invested technology compared to the total investment cost when the grid capacity is limited.

7.3.5 Case E: Grid Capacity Limitation over Life Time

An analysis was conducted to estimate which option would result in the cheapest grid connection when economic income is included. The result was simulated over 30 years and the objective function for lifespan simulation was used (Section 5.3.2). To avoid the model investing in the unlimited capacity of PV systems, the permitted production capacity was limited to match the load peak capacity. Additionally, the model also includes calculations for economic income from selling electrical energy, as well as expenses from buying electrical energy and grid tariffs. Due to limitations in the model's solver, the grid tariff was simplified to only include the energy term and electrical tax for load and only the fixed term for production. This was added to the objective function of the model. The results of this analysis are the same as in section 7.3.4.

Chapter 8

Results and Discussion

This chapter presents all the results and discussions which are analyzed and simulated in this project. The chapter starts with an analysis of the load and continues with presenting the results of the PV power production profile simulation. Further, the result of the simulated current and future cost scenario is illustrated. Following cost scenarios comes technology cost sensitivity analysis. In the end, the simulation of the cheapest grid connection related to the reduction of allowed grid capacity expansion for installation cost over 30 years lifetime.

8.1 Average Daily Load Profile

The daily average load profiles for low- and high-activity seasons at each location are displayed in Figure 8.1. The high-activity period is defined as the times of the year with the highest load, specifically weeks 28, 29, and 30 (summer holiday), as well as week 52 (Christmas week) and week 15 (Easter week). Where the high-activity season is plotted in red and an average of these five weeks. While the low-activity season is plotted in blue and an average of the rest of the year.

As illustrated in Figure 8.1, there is a difference in the load at the low-activity and the high-activity season. The difference is largest in Location I and II. Additionally, the load during high-activity season is highest at these two locations. For the low-activity season, Location II and III have the highest load. The result can be compared to the location descriptions, where it is claimed that Location II and III are located close to typical commuter routes, while Location I and IV are more reliant on summer tourists. Additionally, the result describes the load is most active during the day and until around 21.00. For an average high-activity day, the load peaks around midday, while for a low-activity day, the peak becomes later. A potential explanation is during the low-activity season, the user prefers to charge the EV after work. In high activity, the user group of charging stations has changed, in this time of the year, a larger part of the customers is tourists, which perform to drive and charge at midday.

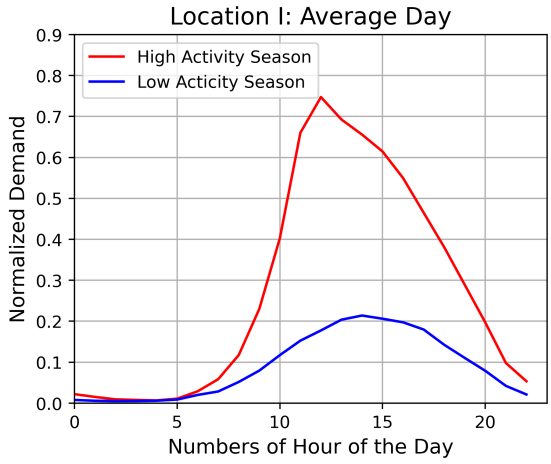

(a) Location I

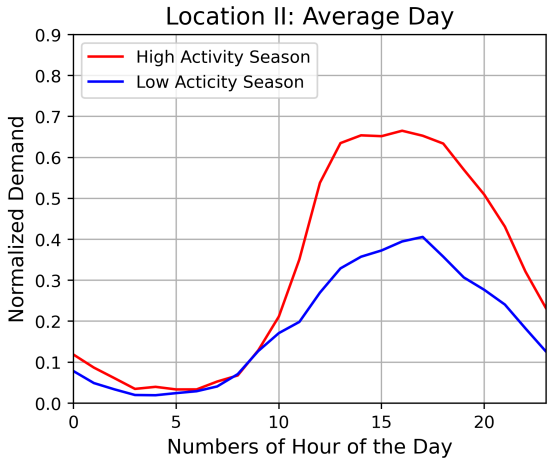

(b) Location II

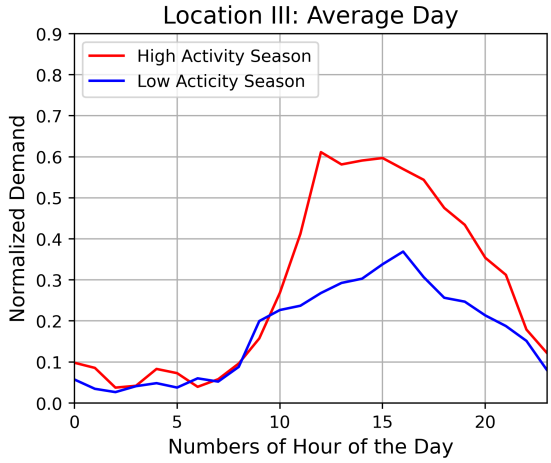

(c) Location III

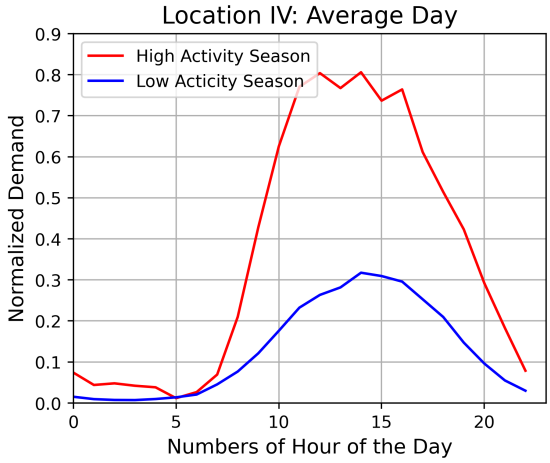

(d) Location IV

Figure 8.1: The average day for high and low season

As depicted in the figure above, the peaks of each location peaks around midday with low load activity during the hours of night. Where the hours of night can be defined as the hours between 18:00 - 06:00. These averaged load profiles coincides well with PV power production profiles, in particular land and roof PV applications. Clear sky PV profiles are shown in figure 8.3 in section 8.3. This is a indicator that profile matching these specific type of load profiles with PV production could potentially reduce stress on the power grid.

8.2 Traffic Pattern Analysis

The result of the correlation analysis shows a positive correlation between traffic and load demand from charging stations. Table 8.1 displays the Pearson and Spearman correlation factors for each location. As illustrated, Location I has the strongest correlation, followed by Location IV. For both Location I and IV, which are typical typical tourists, the linear correlation is stronger than the rank-based correlation. The factor indicates a moderate to strong linear relationship between traffic patterns and load in these two locations. For Location II and III, the linear correlation is weak to moderate. In contrast, for these two locations, the rank-based correlation has a higher factor than the linear correlation, but these factors represent a moderate correlation. The plotted correlation is illustrated in Appendix C.

Table 8.1: Correlation between load and traffic for each location

Location	Pearson	Spearman
Location I	0.7318	0.6770
Location II	0.5380	0.5604
Location III	0.4740	0.5000
Location IV	0.6600	0.6098

One of the reasons for the difference between the locations related to correlation is the intention of the road users. Location II and III, have a higher proportion of commuters, deducted from figure 7.3, where the traffic profile is relatively flat comparing to location I (figure 7.1 and location IV (figure 7.6. For shorter distances, road users have the option of using a home charger. Location I, which a more a typical stopping point for tourists and fewer commuters, has a higher correlation, which can help strengthen the hypothesis. However, the result can indicate the traffic pattern cannot be used to determine charging patterns to an exact degree, but can indicate how the charging profile may look in a rough outline. There are some uncertainty in the matching of the two profiles due to lack of data, and is subject to change in the future. Where the load data for the EV charging stations only goes back a few of years, while the traffic data goes back over 10 years. With more data, a correlation between traffic and load could potentially predict a load profile for a given location. A factor in the correlation is fraction of EV in the Norwegian traffic fleet, where a bigger fraction of EV's may improve the correlation between traffic and EV charging station load profiles. However, as of May 2024, traffic cannot be used to predict load and would need further study.

8.3 Production Profiles

Figure 8.2 displays the simulated production profiles from the PV applications in a TMY on location II. The production profiles for the other locations is in the appendix. The blue curve represents the production profile for a land-installed bifacial PV system with a 40-degree tilt, the red curve is a vertical bifacial PV system facing east-west direction and the green curve is a typical roof installed application with a 10-degree tilt and faced east-west direction. As indicated in the figure, the land installation has the highest annual production, followed by vertical PV application, and lastly roof installed PV.

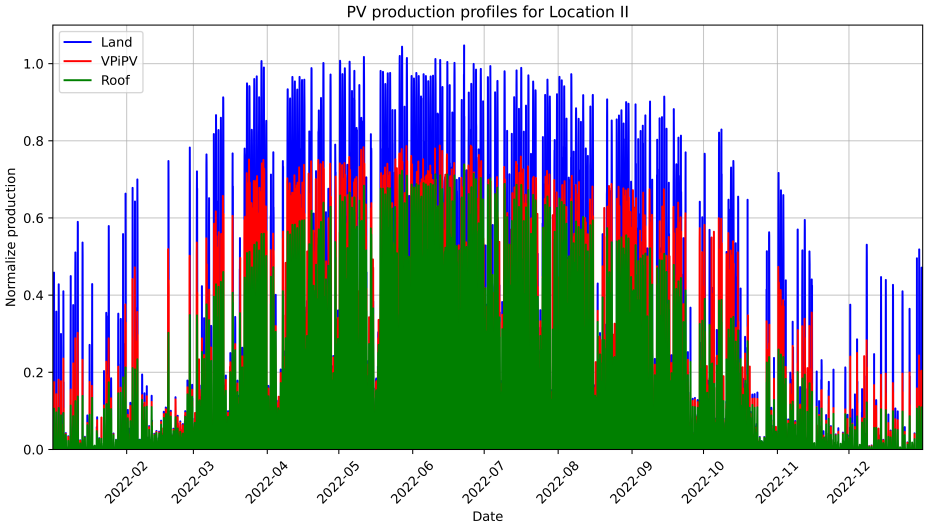

Figure 8.2: The simulated production profiles of land-installed, vertical-installed and roof-installed PV applications

Unsurprisingly, the PV yield is highest during the summer months and lowest during the winter months. These yearly deviations loosely compares to the nature of the demand profiles seasonal swings, further indicating a good match between PV production EV charging station demand.

In table 8.2 the specific yearly yield is summarized for the different locations and PV technologies. For the first three locations the specific yearly yield varies little. Where the biggest difference is around 5.5 % between location I and II for roof installed PV. In contrast, location IV's specific yield differs between 15-30 %, depending on the technology type. The reasons for this difference is most likely local geography and weather, where location IV is located closer to mountains/hills and is subjected to more cloudy days. These large differences shows that having place specific PV power production profile can be an important factor when evaluating whether PV applications can be an alternate solution than grid expansion.

PV technology	**Location I**	**Location II**	**Location III**	**Location IV**
Roof	855.65	881.89	907.56	773.24
Land	1258.39	1273.85	1303.02	1062.50
VBiPV	1173.64	1135.20	1177.76	996.19

Table 8.2: Specific yearly yield (kWh/kw/year) for the different locations.

Figure 8.3 illustrates the daily production profile for a clear sky summer day in Juni. The blue curve, which represents the land-installed application, will reach rated production at 12:00. The VBiPV application, which is the red curve, has a different pattern than the two other systems. Unlike a typical system, with a peak at noon, the VBiPV has two peaks: one in the morning and one in the evening. Additionally, in this case, the largest peak is in the morning. This is due to the efficiency of the bifacial modules called bifaciality, which is a factor of the power production of the back compared to the front. The bifaciality used in this thesis is 90 %. Bifaciality ranges between 70% to 95 %, where 85 % is mostly common in commercial bifacial modules. The green curve, which is the curve that represents the roof-installed PV system has a similar pattern as land-installed PV, but the peak production is lower. In this case, the peak is around 0.6 of rated power, and same time as land-installed applications. All of the technologies will start production at 04:00 and the production at 20:00

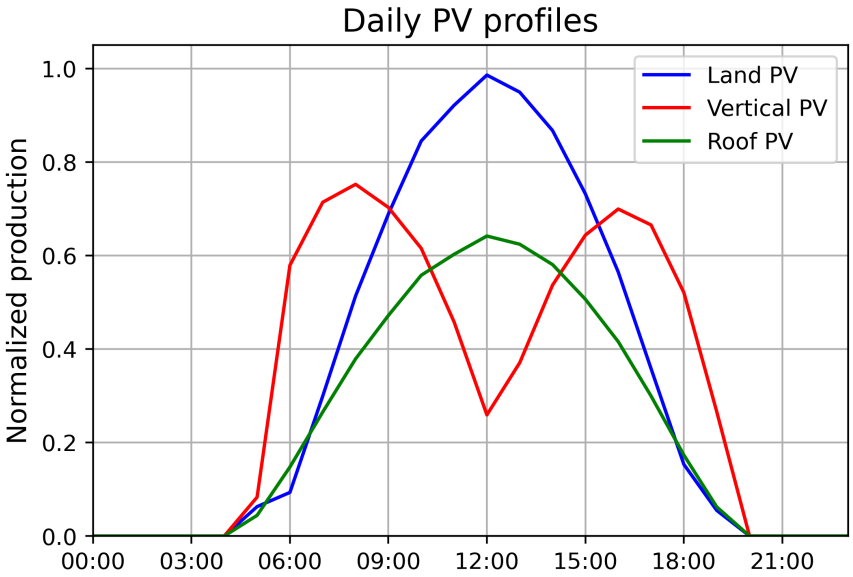

Figure 8.3: Production profiles for a perfect summer day

8.4 Peak Matching

In contrast to BESS and HESS, the PV technologies have different breaking points for when the technology becomes an economical alternative to grid expansion. While BESS and HESS are flexible systems which can be controlled, the PV system is non-regulative and is controlled by irradiation. This results in peak mismatching or peak matching by coincidence, where the peak of the load is hit or miss with the peak of the PV production profile. This matching greatly influences the result on whether PV applications can reduce grid connection capacity or not. Figure 8.4 illustrates two examples of cloudy days and peak mismatching. Figure 8.4a displays day number 98, which starts with a clear day in the morning and the sky becomes covered throughout the day. When the load reach the peak at 16.00, the PV production is low and it is the day that limited the reduction in grid capacity requirement for Location II. As shown in the figure, the load peaking around 0.9, which is approximately the grid expansion reduction for the breaking point illustrated in Figure 8.21, 8.22 and 8.23. Figure 8.4b displays day number 184 for Location III. This day is completely cloudy, at the same time as the demand reaches the peak of the load. That is the reason why the breaking points for PV technologies were linked to a high-cost reduction.

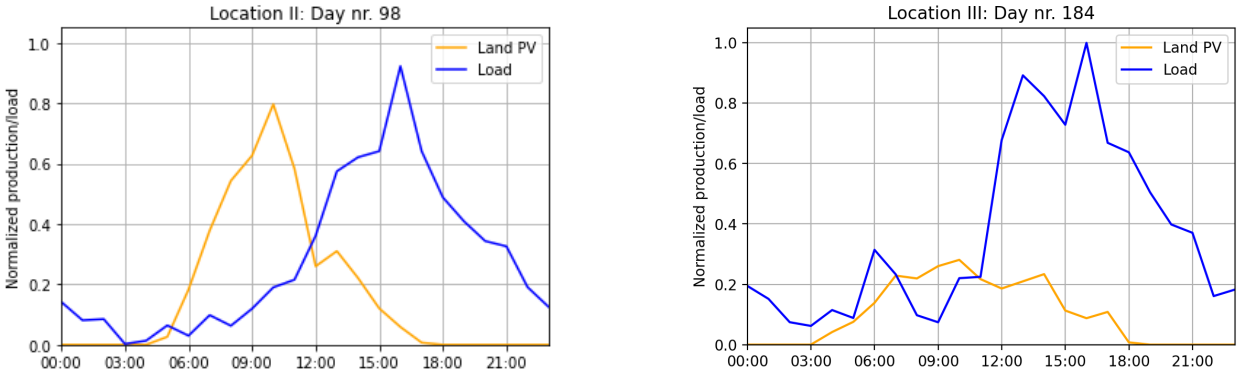

(a) Location I

(b) Location III

Figure 8.4: A portion of the days in the high-activity season have low production of energy from the PV application, where day number 98 and 184 are two of them

If PV systems should be used to supply all peaks, the system must be extremely oversized.

A portion of the days in high-activity season will be cloudy days. Additionally, there is a probability that the load can reach its peak after sunset. In such situations, a PV system will not reduce the grid capacity requirement. However, if restrictions of the allowed load is an option, PV applications without ESS can supply the load and reduce the requirement of grid capacity. Relying solely on PV systems for grid capacity reduction results in a reduction in security of supply, and in reality is not a feasible solution. PV applications are dependent on a ESS.

8.5 Case A: Current Cost Scenario Simulations

In the current cost situation (found in Table 6.2, 6.3 and 6.4), none of the locations are suitable for the development of integrated energy system (IES). According to the result of the model, the traditional grid expansion is the most economical choice related to the installation cost. This result matches the conclusion in Brubæk's master thesis [19] and Spjotvolf et al. master thesis [20], which concluded the battery system is a good technical alternative, but not an economically sustainable solution. Table 8.3 shows the result of the simulation for each location.

Table 8.3: Cost of grid connection in current cost scenario for the four locations.

Location	Generator	Storage	Line	Transformer	Substation	Total cost
Location I	-	-	1 km	9.25 MW	9.25 MW	49.90 MNOK
Location II	-	-	5 km	6.75 MW	6.75 MW	39.90 MNOK
Location III	-	-	2.5 km	3.4 MW	3.4 MW	24.34 MNOK
Location IV	-	-	1 km	4 MW	4 MW	22.62 MNOK

8.6 Case B: Future Cost Scenarios Simulations

This section presents the simulation of the future cost scenarios. According to the literature, the cost of PV, BESS and HESS will drop. The cost-efficient combinations of IES are displayed in a plot for each location, where each cost scenario is represented by a bar. Additionally, a plot of the investment cost is included for each location.

8.6.1 Location I

Figure 8.5 displays the optimal IES combination for the minimum installation cost. The result shows that land-based PV systems are more cost-effective than the other simulated PV technologies, and can be used as a cheaper alternative to grid connection. For base and low-cost scenario in 2030, the model claims that 1.58 MWp of PV system will reduce the regional grid expansion requirement of 1.18 MW, which is 12.8 % of the original capacity. Here the total capacity is higher than in the base case, indicating an over sizing of the PV system to cover the peaks shown more clearly in figure 8.7.In a high-cost scenario in 2030, the cost of PV applications is still too high. The cheapest alternative will still be traditional grid expansion. In 2050, for all cost scenarios, the cost of land-based PV systems will become cheaper than traditional grid connection. Additionally, for the low-cost scenario in 2050, 2h BESS will be an economical alternative to reduce the installations cost. Where the 2h BESS capacity invested in is 2.47 MWh For base and high-cost scenarios in 2050, land-based PV are still the best option to reduce the installation cost.

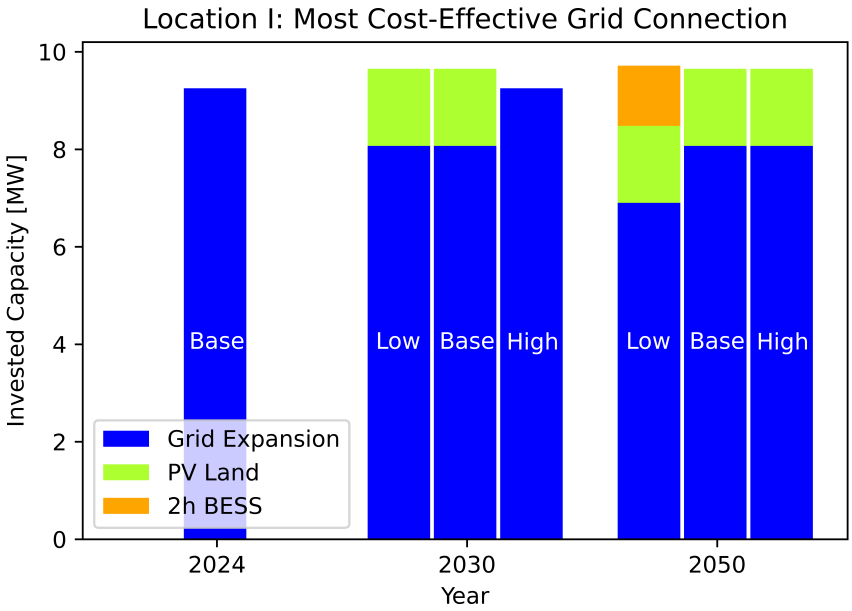

Figure 8.5: The most economically advantageous strategy for minimizing grid connection installation costs at Location I

Figure 8.6 illustrates the reduction in percent for Location I. In 2030, the cost reduction will be between 100% and 97% of the current cost. The base-cost scenario will result in a cost reduction to 99.7% of the current cost. In 2050, in a high cost scenario, the cost of grid connection will be approximately constant. For a base-cost scenario, the total cost will be reduced to 97% of the original price, while in a low-cost scenario, the total cost will decrease to 93% of the current cost.

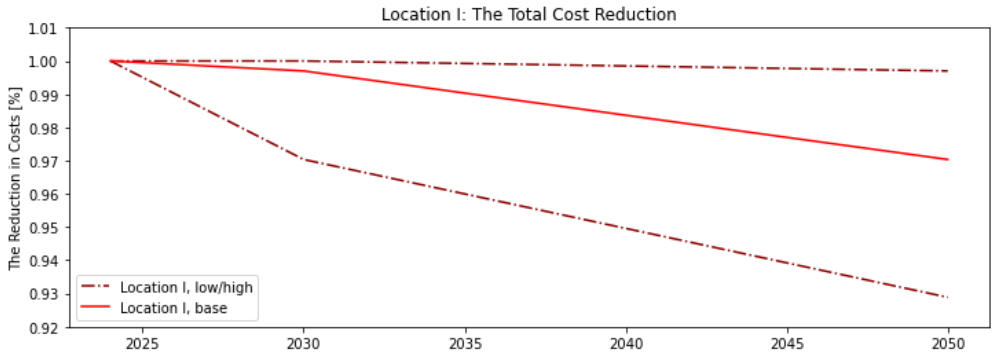

Figure 8.6: Cost reduction, in percentage, for Location I from 2024 to 2050

Figure 8.7 illustrates the power flow in Location I on its peak load day. All power flow related to consumption in the location is negative and all power flow related to import or production is positive. Where the grey stippled line is equal to the negative demand, indicated by the red line. The inverted demand illustrates that the peak demand is not saturated by the grid import, where the PV production and BESS works as peak load support. Another point to note is that the BESS also sells power during low demand, seen at 06:00 in the figure below.

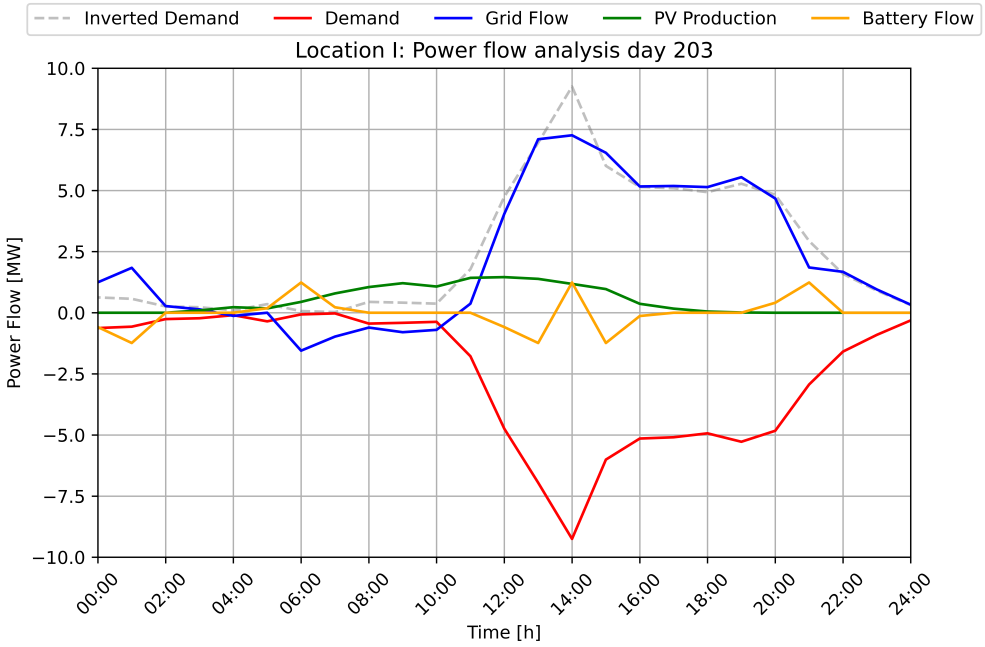

Figure 8.7: Power flow of location I on its peak load day.

8.6.2 Location II

In comparison to Location I, for low- and base-cost scenarios, the land-installation PV system will be an economically beneficial option to reduce the grid expansion capacity requirement for cost. The model claims 650 kW land-installed PV application will reduce the capacity requirement of the grid connection of 530 kW. That is a reduction of 7.8% of the capacity requirement. For the high-cost scenario, the cheapest grid connection solution is the traditional grid connection. In 2050, correlated to Location I, for a low-cost scenario, 2h BESS can be used to reduce the installation cost of the grid connection. The model will invest in 620 MW BESS with a storage capacity of 1.23 MWh. The combination of the BESS and the PV system will reduce the grid capacity of 980 kW, which is a reduction of 14.5%. For the base- and the high-cost scenario in 2050, the cheapest installation still be a combination of a PV system and traditional grid expansion. Figure 8.8 displays the most economically beneficial IES combination in the future for Location II.

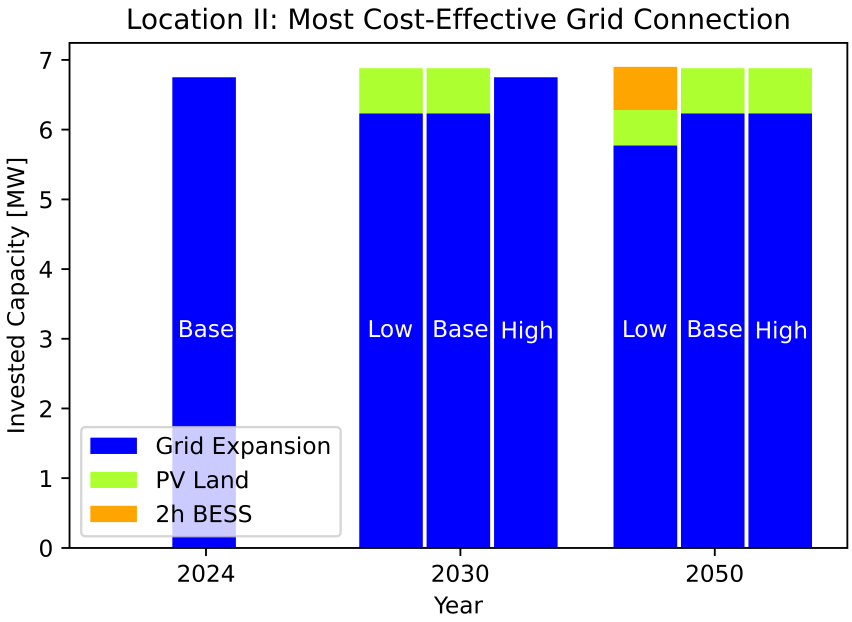

Figure 8.8: The most economically advantageous strategy for minimizing grid connection installation costs at Location II

In comparing Location I, the cost of the high-cost scenario is approximately constant for all years. In 2030, for a base-cost scenario, the total cost will decrease to 99.4% of the current cost, while in 2050, the cost will decrease to 98% of the current cost. For the low-cost scenarios, the cost decreases more. in 2030, the cost will decrease to 98%, while in 2050 will the cost be reduced to 96% of the current price. Figure 8.9 illustrates the changing in the cost of the cheapest installation alternative to grid connection for location II.

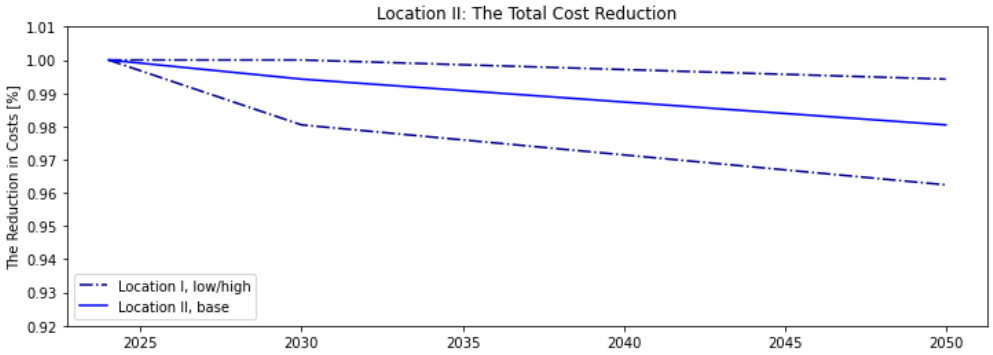

Figure 8.9: Cost reduction, in percentage, for Location II from 2024 to 2050

8.6.3 Location III

In contrast to Location I and Location II, a PV system will not reduce the investment cost of grid connection in any of the cost scenarios. In 2030, the traditional grid expansion is the most economically beneficial for grid connection. It is a similar situation in 2050, where the cheapest solution of base- and high-cost scenario is traditional grid expansion. However, the low-cost scenario in 2050, The cost of a 2h BESS becomes cheap enough to reduce the installation cost of the grid connection. A 740 kW BESS with a capacity of 1.47 MWh will reduce the capacity requirement of the grid expansion of 700 kW, which results in a reduction of 20.6 %. The result of the optimal IES combination is shown in Figure 8.10.

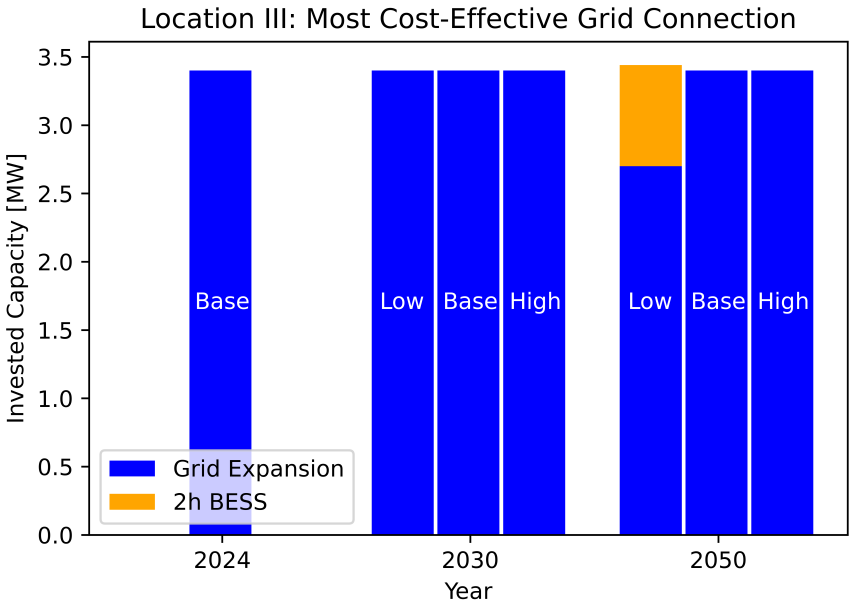

Figure 8.10: The most economically advantageous strategy for minimizing grid connection installation costs at Location III

Figure 8.11 illustrates graphically the total cost development of the most economic grid connection in Location III. As illustrated, the base- and high-cost scenario is equal, and the cost will not be reduced. It is similar to the low-cost scenario in 2030, where the cost reduction is equal to zero. However, for the low-cost scenario 2050, the total cost of the grid connection is 96%.

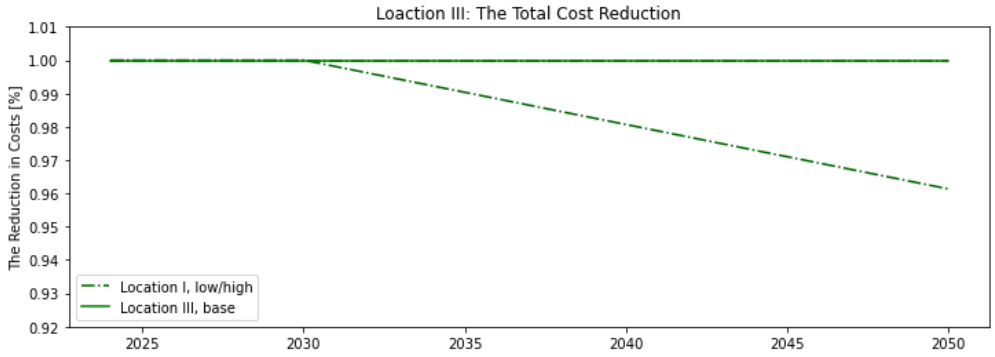

Figure 8.11: Cost reduction, in percentage, for Location III from 2024 to 2050

8.6.4 Location IV

As described earlier in Chapter 7.1.4, Location IV is not suitable for land-installed PV application. In comparison to location III, the result claims the best alternative in 2030 for all cost scenarios is traditional grid expansion. The model gave a similar result for the base- and the high-cost scenario in 2050. However, in the low-cost scenario for 2050, a combination of flat-roof PV system and 2h BESS, in addition to traditional grid expansion, can be used to reduce the installation cost of grid connection. The model claims the cheapest alternative is 250 kW PV system and 620 kW BESS with a capacity of 1.24 MWh. That will result in a reduction of 600 kW of capacity requirement, which constitutes a reduction on 15%. Figure 8.12 shows the simulated cost scenarios for location IV.

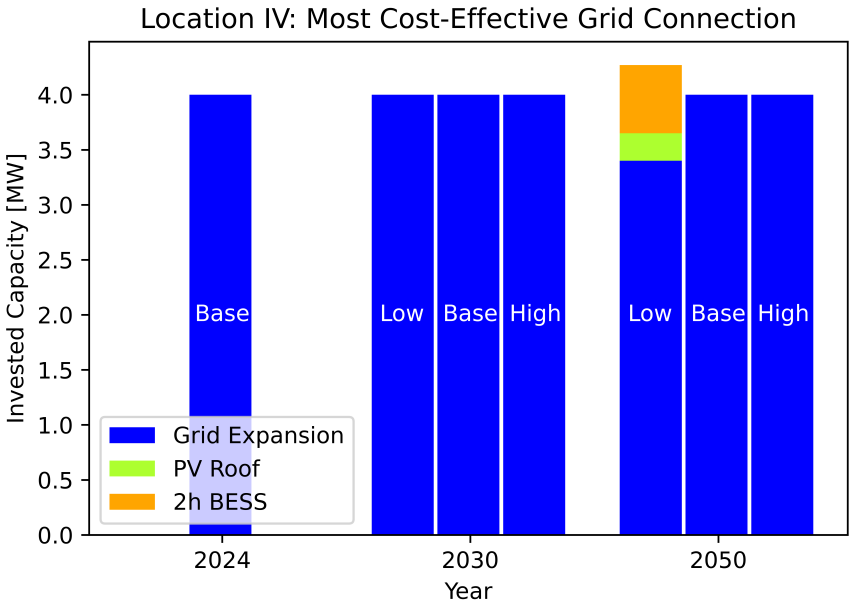

Figure 8.12: The most economically advantageous strategy for minimizing grid connection installation costs at Location IV

In comparison to Location III, the cost is constant for all years in base- and high-cost scenarios. The same applies to the low-cost scenario, without 2050. In low-cost scenario in 2050, the total cost of the grid connection will be reduced to 97% of the current price. Figure 8.13 shows the three cost scenarios for Location VI.

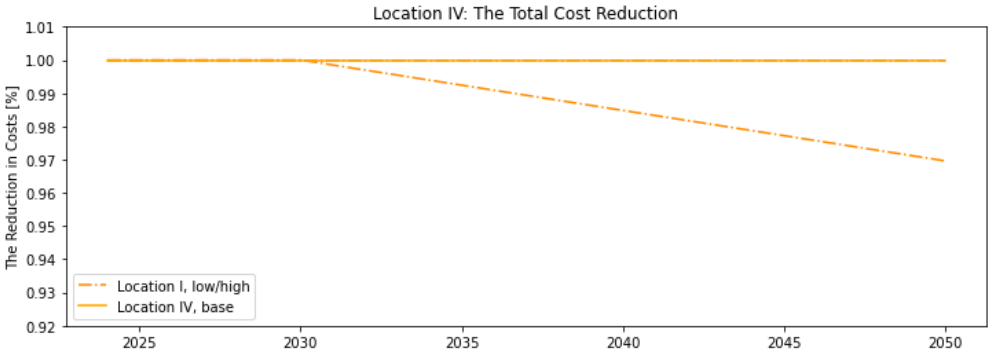

Figure 8.13: Cost reduction, in percentage, for Location IV from 2024 to 2050

8.6.5 Total Cost Development of Integrated Energy System

As concluded in the master thesis by Roestad and Alfsvåg [8], the influential parameter of the total cost is the grid capacity requirement. The reason is the cost of regional grid expansion, which is dependent on the capacity of the grid. Figure 8.14 shows the total investment cost of the grid connection for each location, including a low-, base- and high-cost scenario. Location I, which has the highest capacity requirement, has the highest installation cost, followed by Location II, which has the next highest capacity requirement. At the bottom are Location III and Location IV.

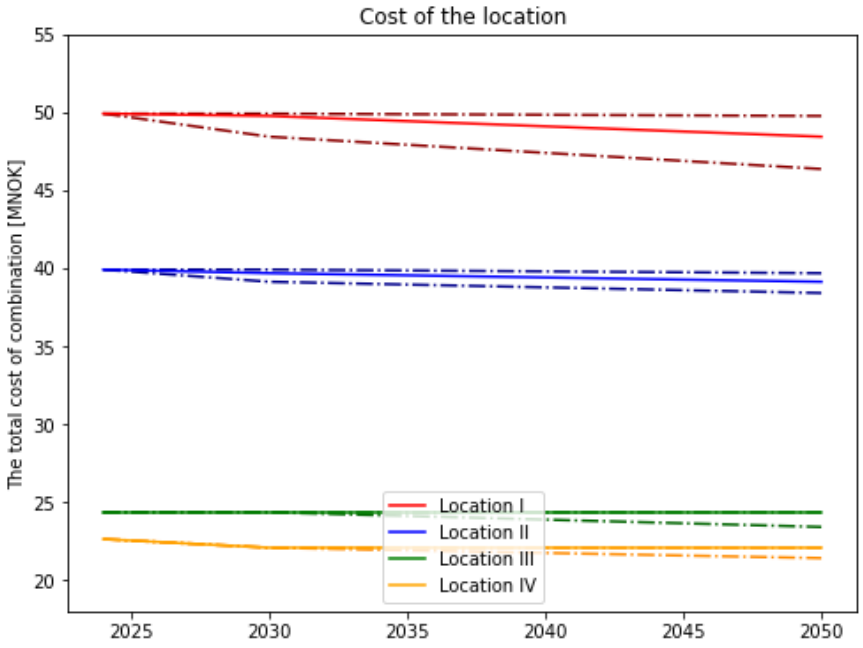

Figure 8.14: The development of the total cost of the most cost-effective grid connection from 2024 to 2050

8.6.6 Discussion of the Total Cost Development

As the figures above indicate, the total cost of grid connection can be reduced with the help of IES. The largest reduction in percentage is at Location I, where the total cost will be reduced to 7% of the total cost in a low-cost scenario in 2050. For the other location, the reduction is only a few percentage points. The reason for the reduction is the cost of alternative technologies will drop, ensuring a reduction in the total cost. In Location III and IV, the base- and high-cost scenarios is constant for the whole time range. The model suggests investing in the entire capacity as grid expansion and claims this is the most economically efficient installation cost. For grid expansion, the cost remains constant, and the development of grid expansion cost is neglected. In the reality, the cost of the grid expansion will increase, due to increasing material costs. This cost increment will benefit the cost-effectiveness of IES.

Although there is a reduction in the total cost of grid connection, the cost difference is small. A reduction of a few percentage cost is minimal. Additionally, IES is a new solution, which can result in uncertainty and unforeseen expenses. There are higher risks linked to IES, due to it being an untested system compared to traditionally grid expansion. Additionally, the installation cost simulation does not include the operating time or lifespan of the different technologies. BESS and HESS require a reinvestment every 15 years, while traditional grid expansion has a determined lifetime of 60 year.

8.7 Case C: Cost Sensitivity of Technologies

This section displays the result of cost sensitivity analyses for each single technology. The result is displayed in two plots for each technology, where the left plot displays the amount of capacity that gives the most cost-effective grid connection for each location in relation to the cost reduction of the technology. The right plot illustrates the reduction in grid capacity requirement related to the cost drop of the technology. The breaking point is defined as the technology price reduction that leads to a more cost-effective investment cost than traditional grid expansion.

8.7.1 Battery Energy Storage System (BESS)

As shown in Figure 8.15, for all locations, the breaking point is at 59% reduction in cost of BESS. Thereafter, the 2h BESS invested capacity remains constant from the initial breaking point till around 85% reduction in BESS cost. This invested capacity will result in a grid expansion reduction between 10 and 25 %, depending on the location. After this point, the results indicate that continuous new investments in BESS are becoming a more affordable alternative to grid expansion, and this will also lead to a corresponding reduction in grid capacity requirements for the same cost reduction. After 95% reduction of cost, the model will not invest in new storage capacity. At this point, the gird requirement reduction ranges from 40% to 50%.

For a 2h rated BESS, Location I and Location II have the highest invested storage capacity, while Location III and Location IV have the lowest. This is due to the load requirements of the locations; Location I and II have higher load than location III and IV. This also applies to the reduction in grid requirement, where Location I and Location II have a higher reduction than Location III and Location IV. In essence 2h BESS reduce grid expansion more, percentage wise, the higher the load demands when the cost of 2h BESS falls.

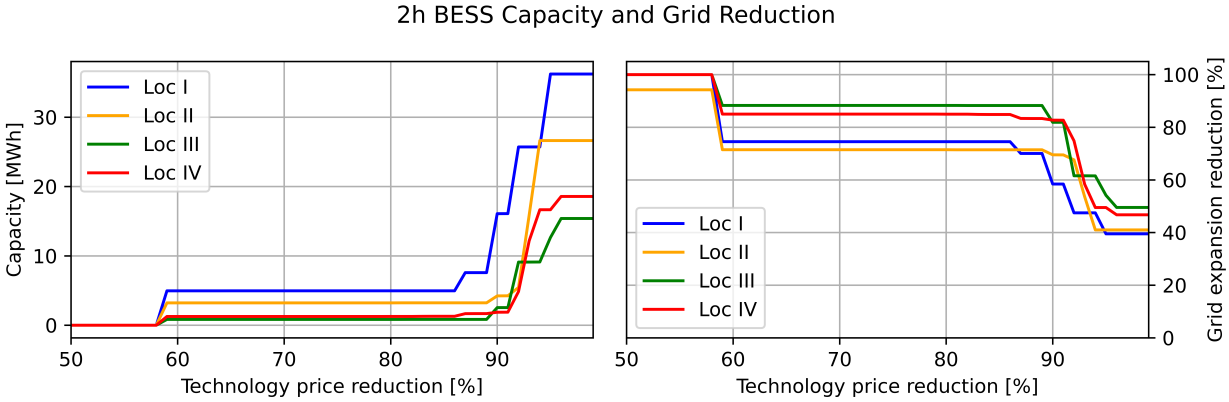

Figure 8.15: A 2-hour BESS storage capacity that provides the most cost-effective grid connection (on the left), and the reduction in grid capacity requirement that will result from it (on the right)

For a 4h BESS, as shown in Figure 8.16, the breaking point is 75% for Location II, III and IV, while for Location I, the breaking point is 74 %. At this cost reduction, the installed BESS will reduce the grid capacity requirement between 20 to 40% depending on location. After the breaking point, the model will not recommend investment in new BESS installations before the cost is reduced to 90% of the original cost. After a 95% reduction of cost, the optimal storage capacity is constant. At this cost reduction, the grid requirement can be reduced to between 40% and 50%.

When comparing to 2h BESS, Location I and II have the highest invested 4h BESS and which results in the highest grid capacity reduction, while Location III and IV have the lowest invested storage capacity and lowest grid requirement reduction.

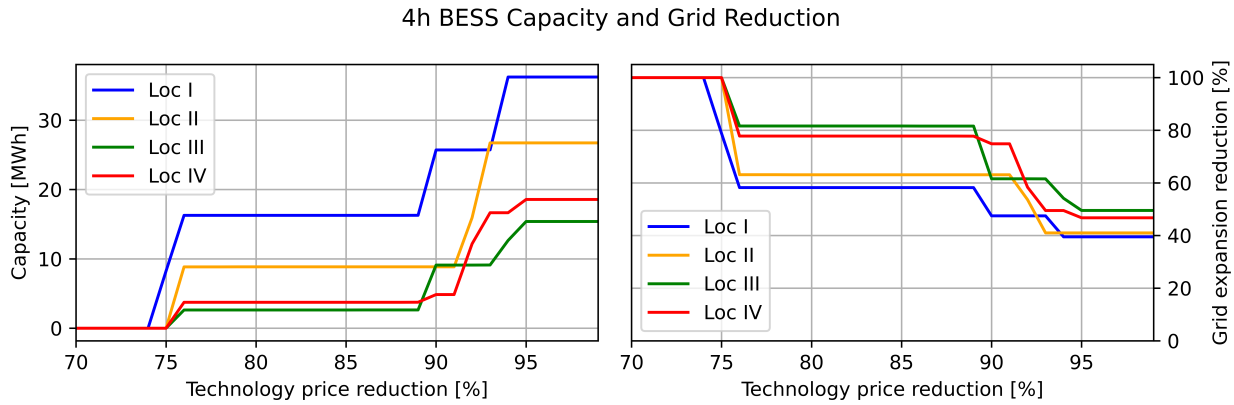

Figure 8.16: A 4-hour BESS storage capacity that provides the most cost-effective grid connection (on the left), and the reduction in grid capacity requirement that will result from it (on the right)

The breaking point, as shown in Figure 8.17, for 6h BESS is 80% for all locations without Location IV. In Location IV the breaking point is 81%. In Location I, the model recommends investing in a significantly large energy storage capacity, which results in a great grid capacity reduction. at 83% reduction of cost, the grid capacity requirement is decreased to 40 % in location I. For the rest of the location, the determined storage capacity will reduce the grid capacity requirement to 75% and 55% of the original capacity requirement. After the initial breaking point, the invested storage capacity will be constant up to 86% reduction of cost. In this case, new small steps invested will result in a reduction in the grid capacity requirement. At 94%, the invested storage capacity becomes constant. At this reduction, the reduction of grid capacity requirement is between 50% and 40% of the total capacity requirement.

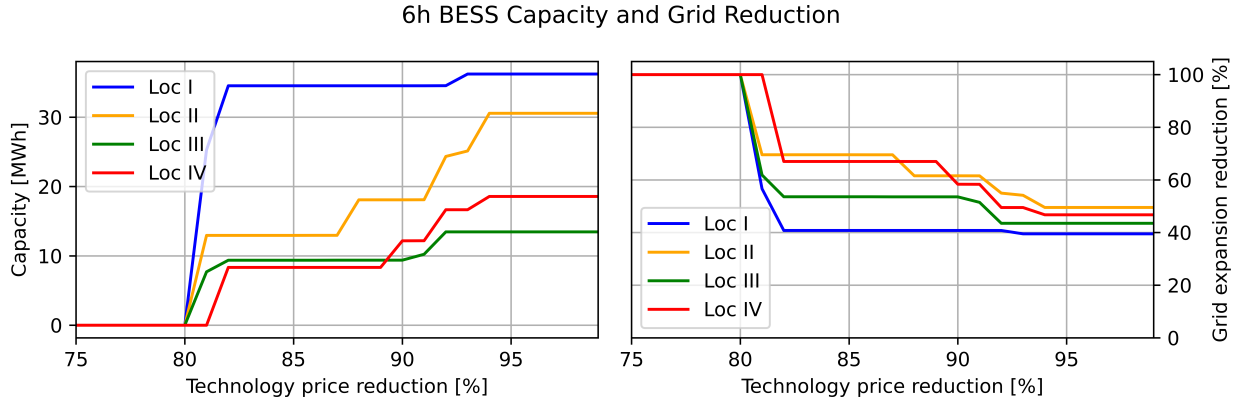

Figure 8.17: A 6-hour BESS storage capacity that provides the most cost-effective grid connection (on the left), and the reduction in grid capacity requirement that will result from it (on the right)

As shown in the figures, the same technology has the approximately same breaking points for each location. There are some locations with a small variation. Variations are due to primary scaling steps in the simulation. In the simulation, it was used 1% steps in the reduction of cost. For locations with the breaking point between two integer percentage numbers, small variations can give different results. In summary, with the price reduction for BESS needs to be large (between 59 % and 81 %) for BESS to be a cheaper alternative for grid expansion. Realistically, with the price reduction expected from BESS, only 2h BESS can compete with traditional grid expansion. Notably, this result does not include reinvestment due to the shorter lifespan of BESS (15 years) compared to grid expansion (60 years). If lifespan was included the price reduction would need to be drastically larger.

As illustrated in this section, for 2h and 4h BESS, Location I and II will have a greater

reduction in grid capacity requirement than Locations III and IV. A potential reason is the various load profiles. In profiles with high variations, special with high and short-lived peaks, the BESS is suitable to reduce the grid capacity requirement. This is because the system can not supply the load with max capacity longer than the BESS's time rate.

8.7.2 Hydrogen Energy Storage System (HESS)

As shown in Figure 8.18, the breaking point is around 92% and Location I will invest in the largest storage capacity, followed by Location III, II and IV. Location I and III will have the largest reduction in the grid capacity requirement of 40% of the total capacity requirement, while Location II and IV will be around 55%. After the breaking point, the invested capacity is constant, with a slight increase in invested 10h HESS capacity for location II when the technology cost reduction is at 99%. This slight increase may come from rounding errors and does not impact grid expansion reduction, and is therefore ignored.

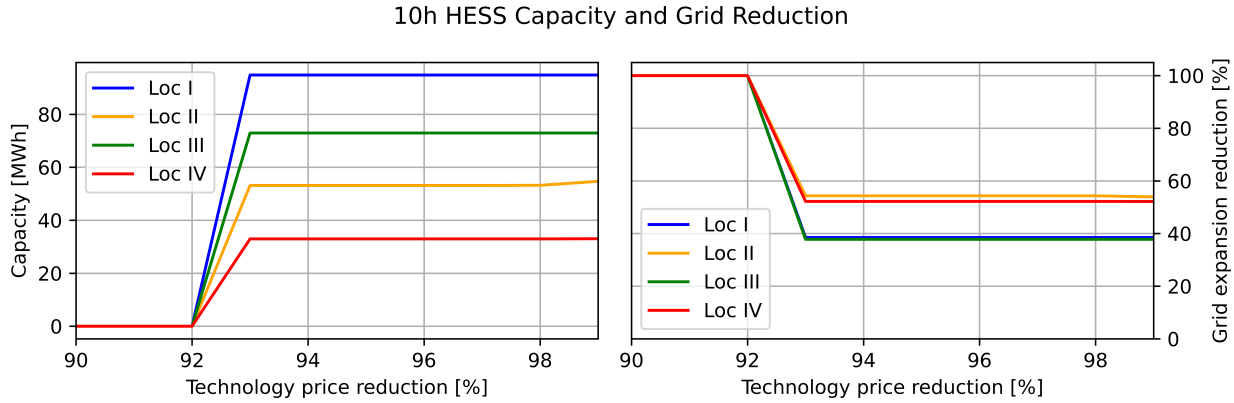

Figure 8.18: A 10-hour HESS storage capacity that provides the most cost-effective grid connection (on the left), and the reduction in grid capacity requirement that will result from it (on the right)

As shown in Figure 8.19, 20h HESS has a similar pattern as 10h. It is at the breaking point as the same cost-reduction value and after this point the installed storage capacity is constant. In comparison to 10h HESS, the result indicates a 20h HESS system can reduce the grid connection to 35% of total capacity for Location I and III and 40% for Location II and IV.

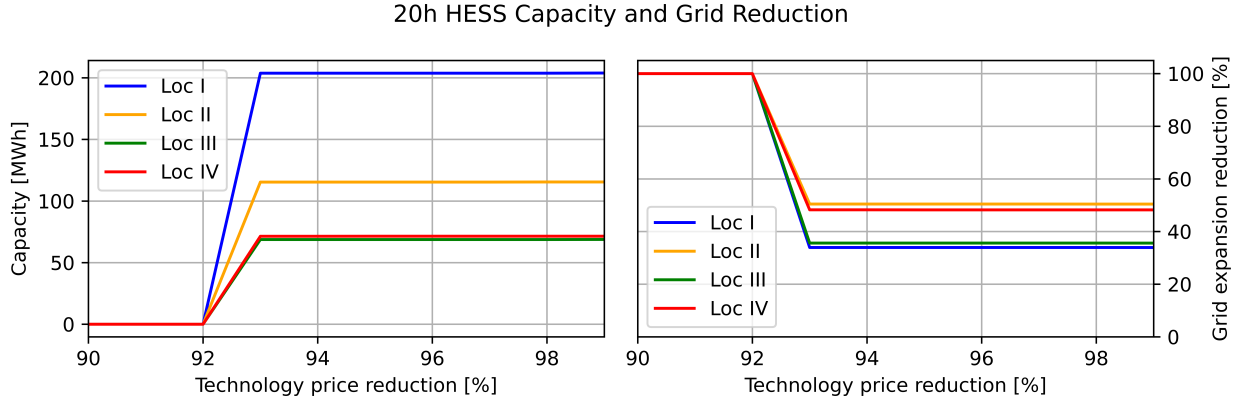

Figure 8.19: A 20-hour HESS storage capacity that provides the most cost-effective grid connection (on the left), and the reduction in grid capacity requirement that will result from it (on the right)

In comparison to the 10h HESS and 20h HESS, 100h HESS is constant after the breaking point. The breaking point is a 93% reduction of the investment cost of HESS. The model claims Location I has the highest reduction in grid capacity requirement by 20% of the total capacity requirement, followed by Location IV, III and II.

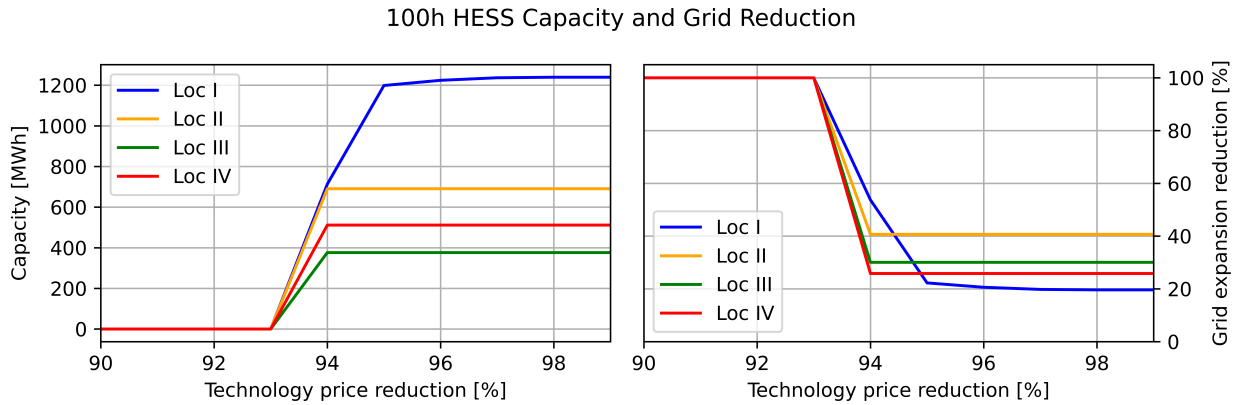

Figure 8.20: A 100-hour HESS storage capacity that provides the most cost-effective grid connection (on the left), and the reduction in grid capacity requirement that will result from it (on the right)

This technology is too expensive to single-handedly compete with traditional grid expansion, where a over 90% cost reduction is needed. Looking at the cost predictions mentioned in Section 7.3.2, HESS is unlikely to make a grid connection more cost-effective. Additionally, when the capacity of HESS reaches magnitudes this large, the preventative security measures needed becomes significant.

For 10h and 20h HESS, locations I and III have the highest reduction in grid capacity requirement. That can indicate these two locations are more suitable for HESS than Location II and IV. However, the reduction is great in comparison to BESS. In contrast to BESS, the breaking point for the various time-rated HESS was similar. The reason is the cost of the elements of HESS. As described in Chapter 4, the electrolyzer and fuel cell consists of the greatest part of the HESS's total cost. The cost of these elements depends on the installed capacity (kW), while a small part of the cost linked to hydrogen storage depends on storage capacity (kWh). That results in the cost difference related to installed capacity (kW) being more similar between the various time-rated HESS.

8.7.3 PV System

According to Figure 8.21, the land-installed PV application has different breaking points depending on the location. The different breaking points are due to the PV power production profile and the load profile of the location, which are discussed more thoroughly in section 8.4. For Location I, the breaking point is around 37% reduction of cost and results in the largest installed capacity of the location. Additionally, at the initial breaking point, the grid capacity requirement will be reduced to 88% of the total capacity requirement. Location II has a breaking point of around 53% and will result in a reduction to 92% of the total grid capacity requirement. For location III, the breaking point is approximately 81% reduction of cost. At this point, land-installed PV will result in a reduction to 85% of the total grid requirement. Location IV has a small investment at 39% reduction of cost, which will result in a reduction to 98% of the total capacity requirement. For all locations, after 80% cost reduction, the model claims a new investment can reduce the grid capacity requirement. Additionally, at 98% cost reduction, the model will invest in new production capacity, but this invest will not reduce the grid capacity requirement.

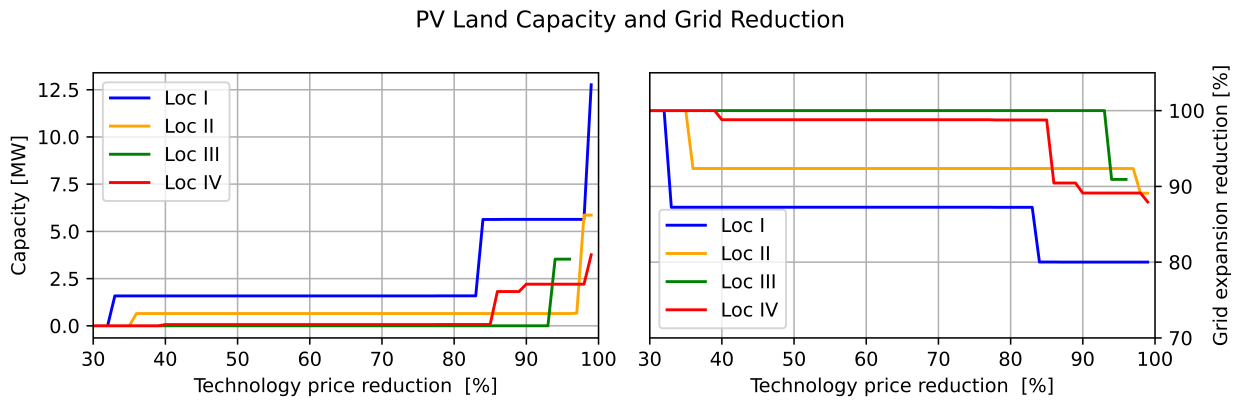

Figure 8.21: Invested capacity of land PV at the different locations with technology price reduction (left), with corresponding grid expansion reduction (right).

For VBiPV systems, as displayed in Figure 8.22, Location I has the breaking point at 50% and will reduce the grid capacity requirement to 88% of the total capacity requirement. Location II has the breaking point at 67% reduction of cost and that will result in a reduction of grid requirement to 92% of the total capacity requirement. Compared to land-installed PV systems, the VBiPV system has a small investment in Location IV at a 62% reduction of cost, which results in the grid capacity requirement decreasing to 98% of the capacity requirement. With around 90% reduction of the cost, the model invest new production capacity for all locations which will reduce the grid capacity requirement. For Location I and II, a new investment at around 98% reduction. However, at this cost-reduction level, it is not a new capacity of production that will not reduce the grid capacity requirement.

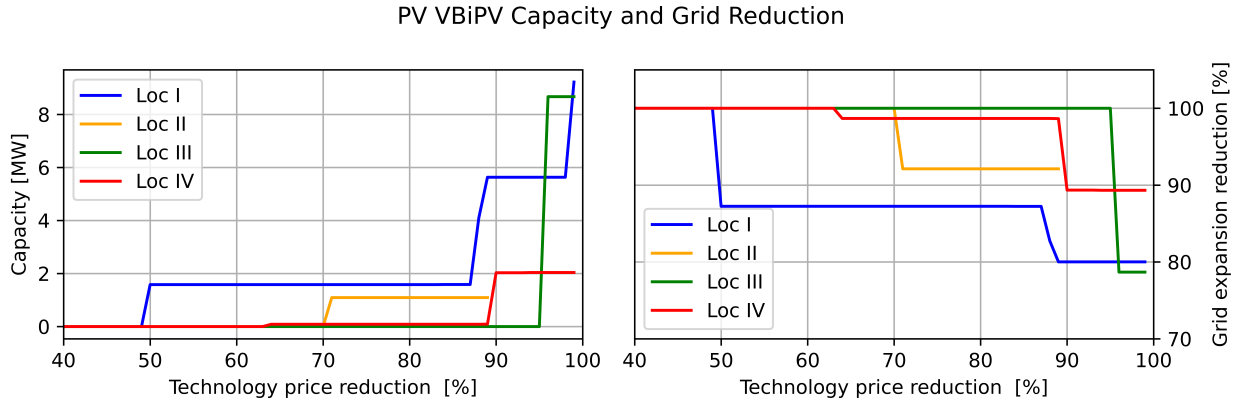

Figure 8.22: Invested capacity of VBiPV PV at the different locations with technology price reduction (left), with corresponding grid expansion reduction (right).

Figure 8.23 shows the cost sensitivity for a Roof installed PV. The simulated result of Roof-installations has similarities with the two other technologies. Location I, which needs the lowest reduction of cost, has the breaking point at 55%, and will reduce the grid capacity requirement to 88% of the total capacity requirement. Location II has a breaking point at 58% and will reduce the grid capacity requirement to 91%. Location III has the breaking point at 74% reduction of cost and will reduce the result to 79% of the original. In comparing the two other PV technologies, Location IV has the highest cost reduction need to reduce the requirement of grid capacity. At the breaking point at 86%, the requirement of grid capacity will be reduced to 92% of total capacity.

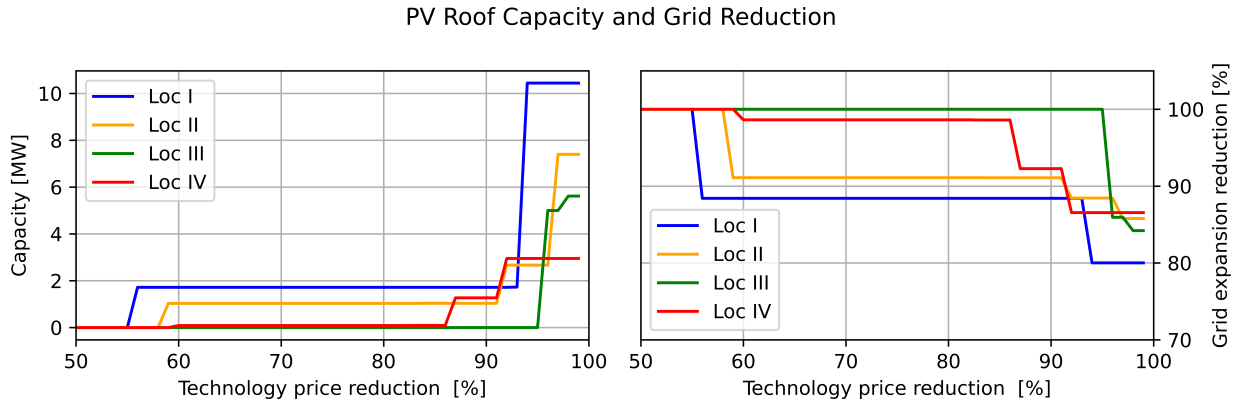

Figure 8.23: Invested capacity of roof PV at the different locations with technology price reduction (left), with corresponding grid expansion reduction (right).

These breaking points seem feasible with the cost development and cost predictions of PV applications, but the model suffers from some issues discussed below, in section 8.4.

The different PV technologies' ability to reduce the grid capacity requirement is similar. The largest difference is the breaking point. That is because the technology has different investment costs. This is also the reason why the model always wants investment in land-installed PV. Additionally, roof-installed and VBiPV will never reach their own rated production, which is the production level the cost referred to.

8.7.4 Evaluation of the Suitability of Locations for Alternatives to Grid Expansion

As illustrated in Section 8.7, the Location I has is the most suitable location for an alternative. It is at this location the reduction in grid capacity requirement is largest. For 2h and 4h BESS, it is Location II that follows Location I as a great area for reduction. That can indicate the location's load profile has high and short-lived peaks. For HESS, location III has a similar reduction of grid capacity requirement as Location I, which may be due to a narrower load profile.

8.8 Case D: Grid Capacity Limitation

This section displays the result of analysis of the limitation in permitted grid capacity expansion. All plots in the sub-chapter illustrates which combination of technologies has the cheapest installation cost for each location when forcing the model to accept a reduced grid connection. Additionally, the cost is also depicted in the figure, indicated red dashed lines. Figure 8.24 displays an overview of the alternatives to grid expansion when restricting the grid capacity and its monetary cost for all four locations. The grid limitation is capped, due

to the exponential nature of the cost, shown in the in the appendix in figure B.1, B.2, B.3 and B.4. Furthermore, the figure below illustrates that peak-load support is implemented to reduce the grid capacity when the limitation in grid expansion is around 0 and 30 %. Peak-load support meaning that the alternative technologies provide assistance to the grid during periods of high demand. Where the invested technologies are BESS 2h, and PV. When the limitation becomes bigger than around 30 %, depending on location, long-term storage is required and the model prioritizes investment into PV and BESS 6h. HESS 100h is not prioritized until around 55-65 % limitation. Interestingly, in three out of the four locations, PV is the first technology to replace grid expansion. In real world application this would not hold true due to peak matching discussed in section 8.4.

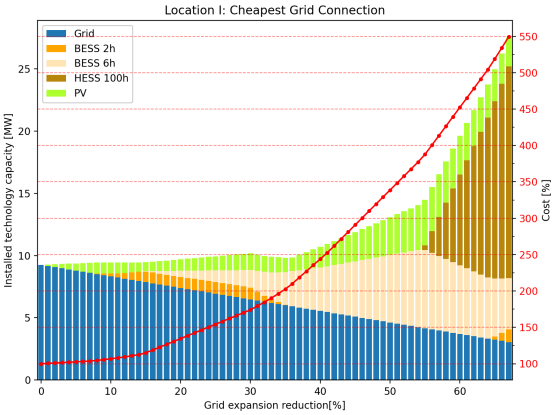

(a) Location I

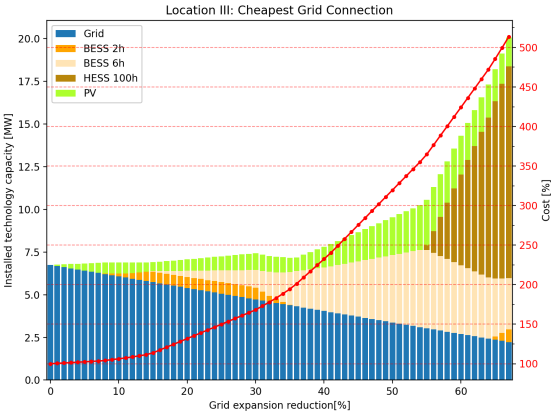

(b) Location II

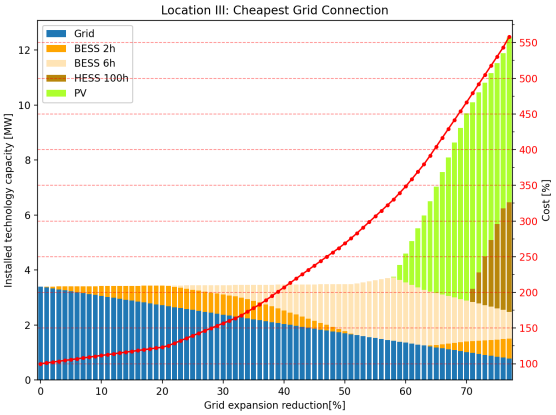

(c) Location III

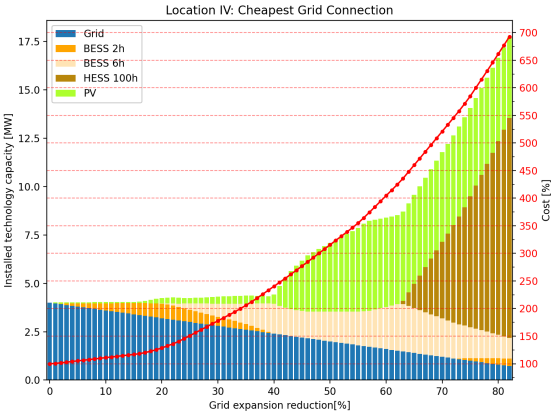

(d) Location IV

Figure 8.24: Technology investment mix with limited grid expansion for all four locations.

Some simplifications were made to the model technology input due to the long simulation runtime. The technologies cut was either due to cost or overlap in functionality. As seen in the figures below PV applications is indicated solely as "PV", but only land based PV applications was used in the simulations. Previous testing showed that the price of roof based PV applications and VBiPV applications are too expensive to be considered by the model, described in section 8.6. Ultimately, the and observation when halving the grid connection capacity, the cost increases between 200 - 350 % depending on location. Each location scenario is more closely described in the sections below.

8.8.1 Location I

As shown in Figure 8.25, the cheapest method of establishing a reliable electrical power supply in location I is traditional grid expansion. However, if the grid access becomes limited, alternatives are required. When reducing the grid accessibility by 8 %, the model invests in PV to compensate for the grid accessibility loss. Between 9-17% limitation in grid capacity, the model indicates the PV system fails to deliver sufficient energy to meet the demand. In addition to PV, the model invests in 2h BESS capacity. After 17% limitation, according to the model, a 6h BESS will reduce the installation cost in combination with PV and 2h BESS. Additionally, the 6h BESS will take a larger part of the capacity mix up to 55% limitation. At this point, all of the storage capacity is 6h BESS. In 70% limitation of grid capacity access, the model recommends an investment in 20h HESS.

In relation to the limitation of available grid expansion, there is an increase in the installation costs. This growth can be characterized as exponential growth. After a limitation of 40% in grid capacity, the total cost is more than doubled and after a 70% limitation, it is 5.5 times higher than traditional grid connection. Location I, II and IV follow similar trends, where in all locations the model invests solely in PV for the first steps. This phenomena is due to "luck" in peak matching between the demand and PV production. If the model was run again with a PV production profile from the last ten years, in most cases PV would not be able to replace the grid alone.

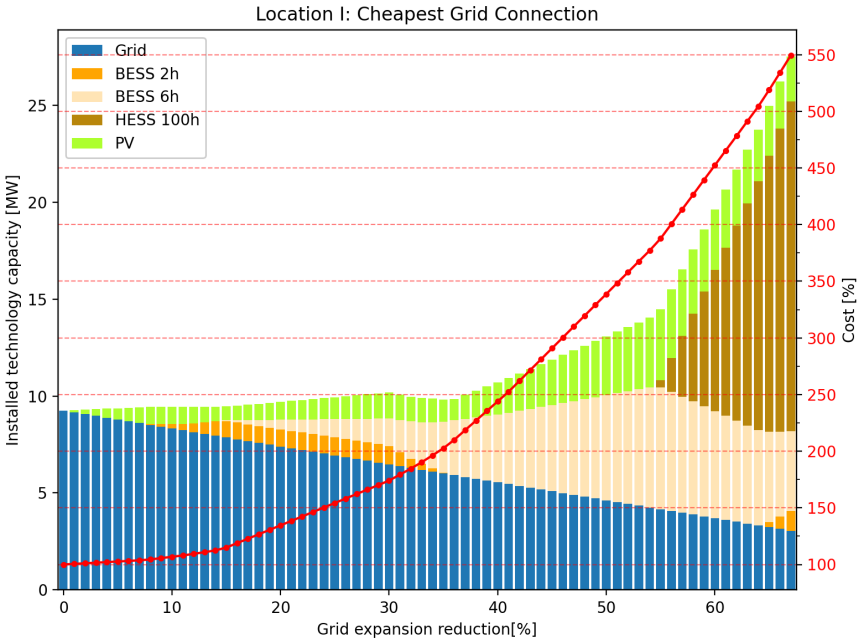

Figure 8.25: Technology investment mix with limited grid expansion for Location I

8.8.2 Location II

Comparatively to location I, in location II PV is the most cost-effective alternative in the early stages of grid capacity limitation. Meanwhile, the preferred storage technology between 1 - 20 % grid capacity limitation is 2h BESS. The sole difference between the locations is the total cost increment, where in location II the total cost is somewhat less when reducing grid connection.

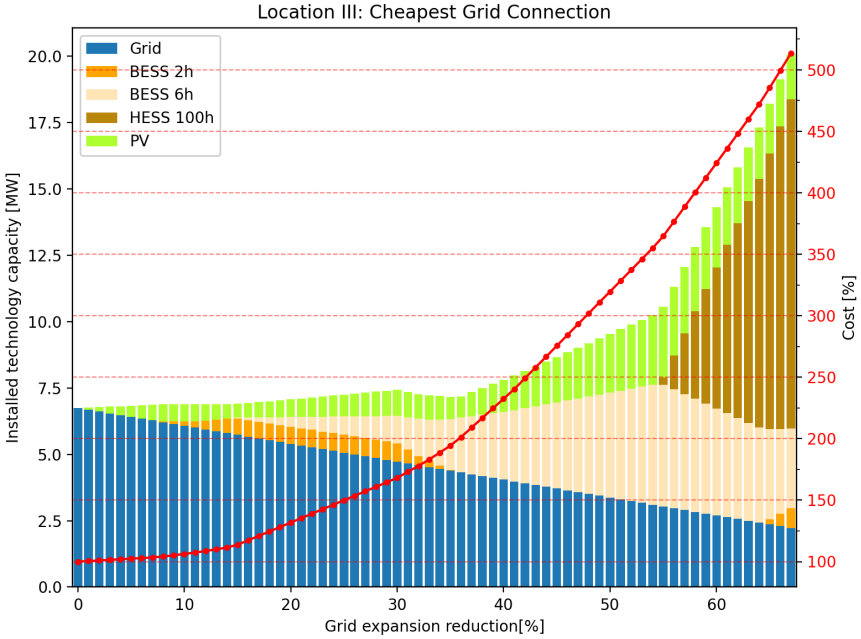

Figure 8.26: Technology investment mix with limited grid expansion for Location II

8.8.3 Location III

Figure 8.27 below is a good example of poor peak matching. Due to this, the model does not invest in PV until 60% grid connection limitation. Instead the model invests solely in 2h BESS and 6h BESS, before the 60% mark. Afterwards, the model invests into HESS and PV. Contrary to technology investment, the cost increment is similar to the other locations.

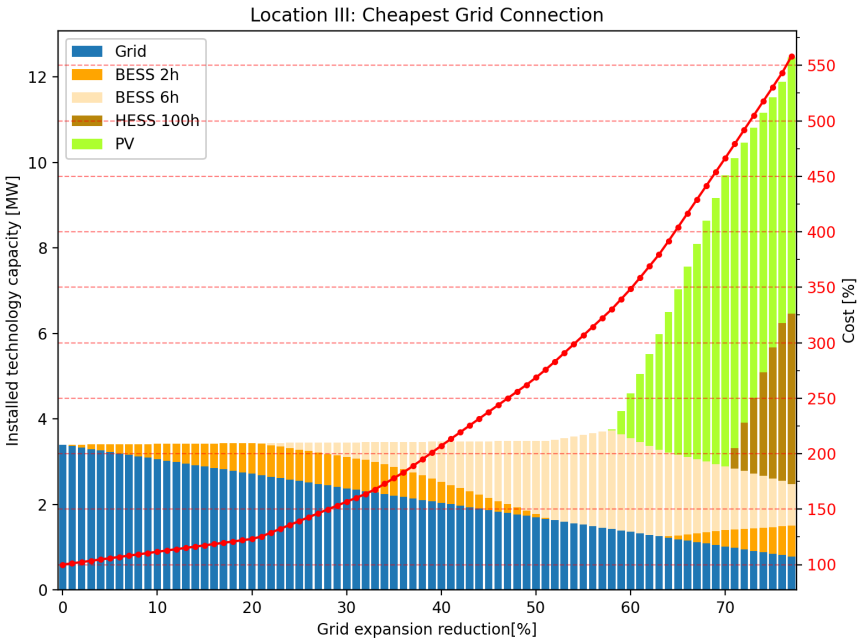

Figure 8.27: Technology investment mix with limited grid expansion for Location III

8.8.4 Location IV

The only big difference in location IV, compared to the other locations, is how the model tolerates a larger limitation in grid connection capacity before the cost turn exponential. As seen in figure B.3 the cost is exponentially higher after 83% limitation.

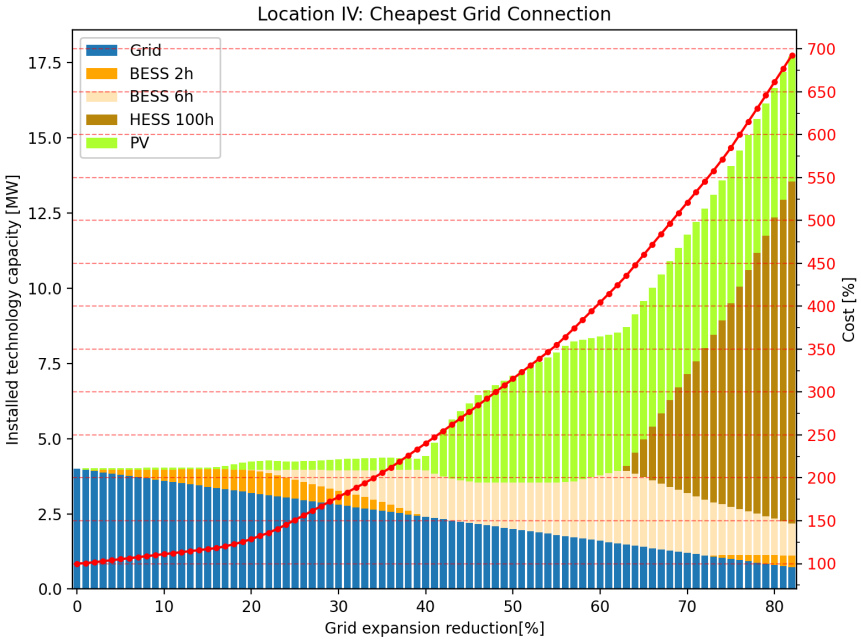

Figure 8.28: Technology investment mix with limited grid expansion for Location IV

To summarize, alternatives to traditional grid expansion is feasible but at a increased cost. The costs of IES rises exponentially and ends up costing over 1000 times more than grid connection, making it an unrealistic target. These high costs might be due to load peaks in the winter when PV produces a significantly lower power output.

8.9 Case E: Grid Capacity Limitation Over Life Time

This section presents the results of cost simulation spanning 30 years, where electricity sales are included. The results are plotted in a figure for each location, illustrating the cheapest grid connection over 30 years in relation to the limitation in allowed grid capacity expansion. Additionally, the increase in the compared to traditional costs is included.

8.9.1 Location I

Figure 8.29 displays the cheapest grid connection for Location I simulated over 30 years. The model wants to maximize the capacity of the PV system. According to the model, that is the most economical solution. In the simulation of Location I, the PV system can supply the load down to a 20% limitation of the allowed grid capacity expansion. After this limitation, ESS, as 2h BESS, 4h BESS and 100h HESS will have the responsibility to supply the load and balance the internal grid relative to the surplus energy from the PV system. Between 20% and 40% limitation in grid capacity expansion, the model suggests only 2h BESS as the ESS. After that point, the model claims 6h BESS is a better solution, and 6h BESS gradually taking a larger part of the energy storage capacity mix. Around 60% limitation of allowed grid capacity expansion, the model starts investing in 100h HESS. Before this point, almost of energy storage capacity consisted of 6h BESS. After investing 100h HESS, the model suggests investing in more 2h BESS.

As shown in the figure, the total cost of the integrated energy system increases in a pattern that resembles exponential growth. With around 65% limitation in allowed grid capacity expansion, the total cost will double. Around 80%, the total cost is around four times higher than in traditional grid connection.

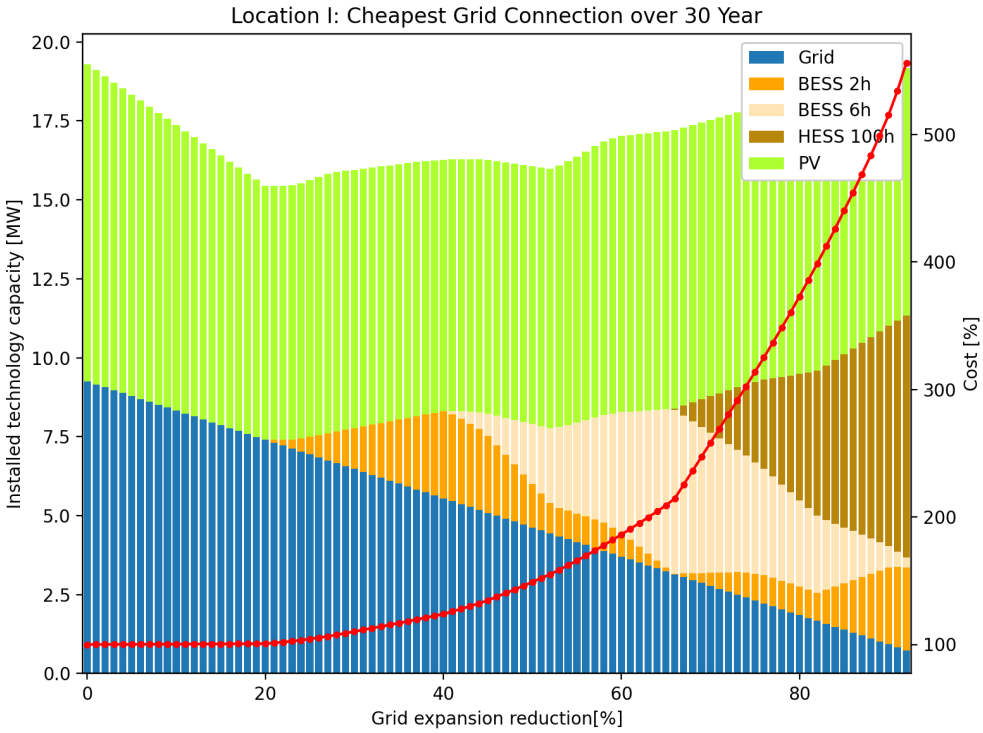

Figure 8.29: The simulated grid connection for Location I over 30 years in relation to the limitation in permitted grid expansion, including electricity sales

8.9.2 Location II

Compared with Location I, the model claims that maximising the capacity of PV is the most economical investment for all levels of allowed grid expansion limitation. That is shown in Figure 8.30, which illustrates the cheapest grid connection for Location I simulated over 30 years. Up to 13% limitation of grid expansion, the model indicates that the most economical grid connection is to invest in a combination of PV applications and grid. Beyond this limitation level, the model suggests investing in 2h BESS. Before around 30% limitation of grid capacity expansion, the model recommends to start investing in 6h BESS. The 6h BESS gradually takes on a larger part of energy storage capacity until around 55%. In this limitation level, the model suggests investing in 100h HESS. At the same time, the model recommends a gradual limitation in 6h BESS, and rather more in 100h HESS and 2h BESS.

The increase in the total cost can be described as an exponential growth pattern, similar to that observed in Location I. At a 45 % limitation, the total cost of the grid connection has been increased to 25% higher than the traditional grid. Around 65%, the total cost has doubled.

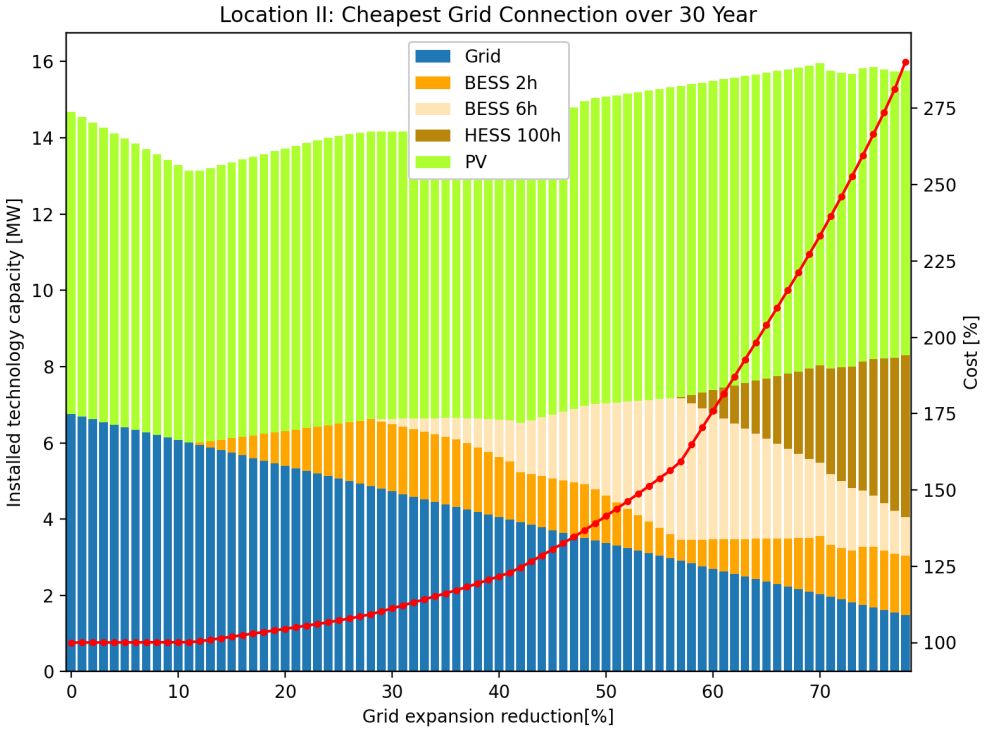

Figure 8.30: The simulated grid connection for Location II over 30 years in relation to the limitation in permitted grid expansion, including electricity sales

8.9.3 Location III

Figure 8.31 displays the cheapest grid connection for Location III simulated over 30 years. In comparison to other locations, the model recommends to maximum the capacity of PV application. Up to 23% limitation, the model claims the most economical combination is PV applications and grid expansion. After this point, the model starts investing in 2h BESS until around 45% limitation. At this limitation level, the model suggests investing 6h BESS. Thereafter, the 6h BESS start gradually takes a larger part of the energy storage capacity. Behind 70%, the model suggests gradual investment in a combination of 100h HESS and 2h BESS.

Compared to the other locations, total cost can be described as an exponential growth pattern. With around 50% limitation in allowed grid capacity expansion, the cost is 20% more expansive than traditional grid expansion. At around 75% limitation, the cost has doubled.

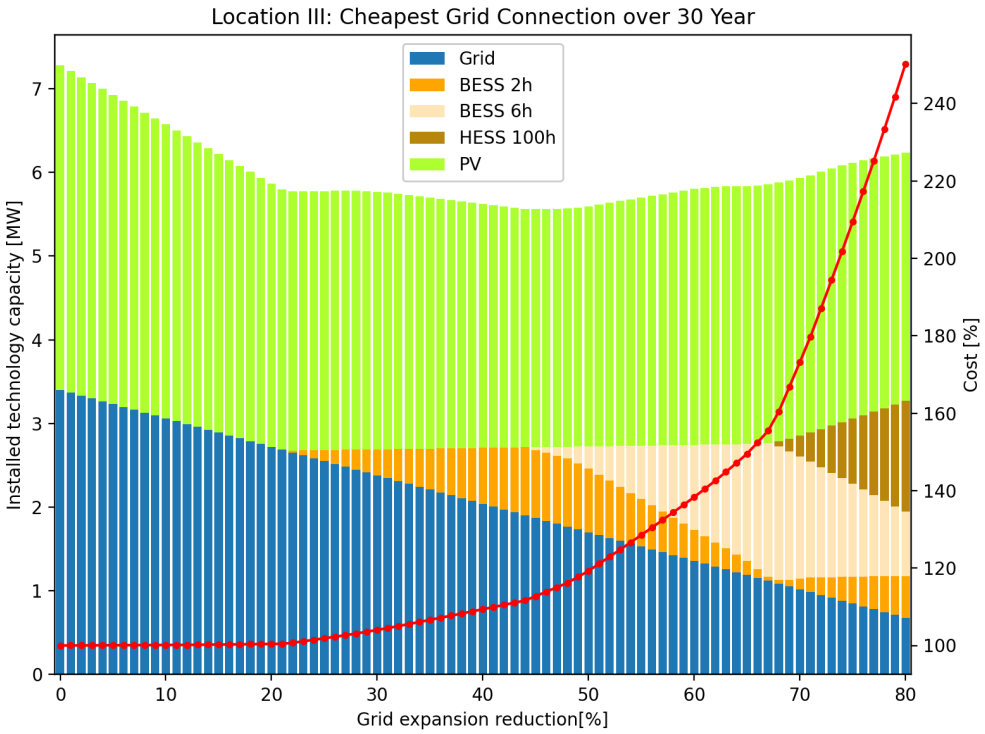

Figure 8.31: The simulated grid connection for Location III over 30 years in relation to the limitation in permitted grid expansion, including electricity sales

8.9.4 Location IV

Compared to the other locations, the model indicates that most economical investment is to maximize the PV capacity. Additionally, the most economical grid connection solution prior to 15% limitation is a combination of PV application and traditional grid connection. After reaching this limitation level, the model suggests investing in 2h BESS, which is the recommended ESS until around 25% limitation. At this limitation level, the model suggests investing in 6h BESS in addition to the capacity level of the 2h BESS system. After a 45% limitation in allowed grid expansion, the model recommends a gradual limitation until reaching a 55% limitation of allowed grid capacity expansion. Between 55% and 60% limitation, the model suggests investing in 6h BESS as the sole ESS. After this point, the model suggests gradual investment in 100h HESS, which will reduce the demand for 6h BESS. Around 70% limitation, the model recommends an investment in 2h BESS will be economically beneficial.

Similar to the other locations, total cost can be described as an exponential growth pattern. With approximately a 35% limitation, the total cost is 25% higher than that of traditional grid expansion. At around 55% limitation, the total cost is 50% higher, and by approximately 65% limitation, the cost has doubled.

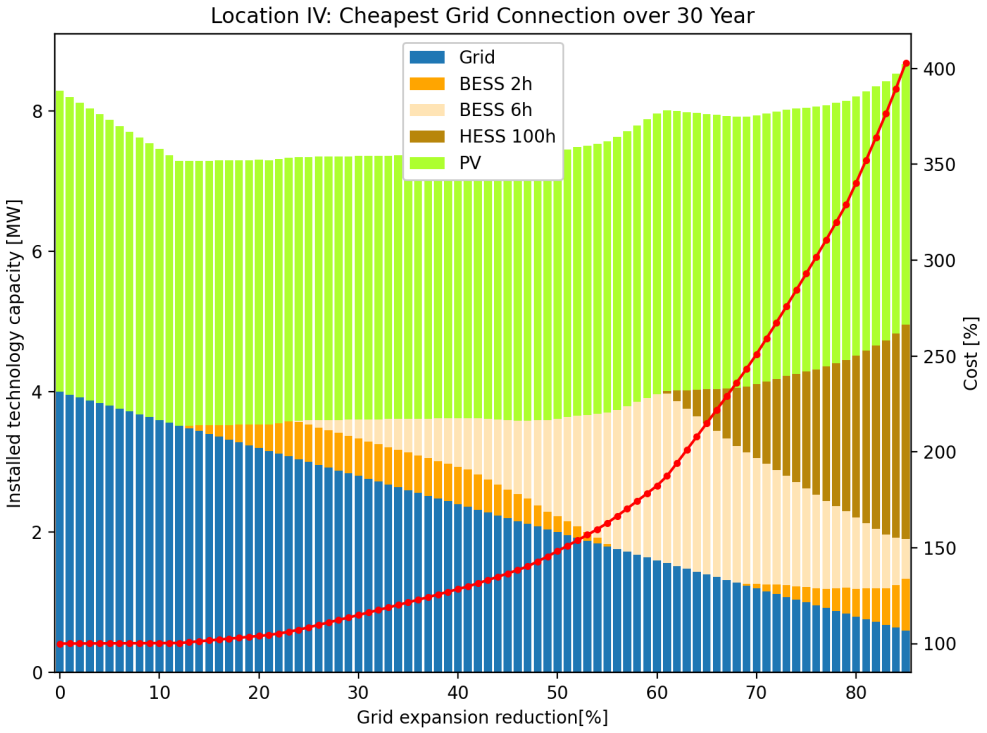

Figure 8.32: The simulated grid connection for Location IV over 30 years in relation to the limitation in permitted grid expansion, including electricity sales

8.9.5 Full Picture

Figure 8.33 displays the result of the cheapest grid connection spanning 30 years. As shown, after around 80% limitation of allowed grid capacity expansion, the total cost will increase multiple times higher than that of traditional grid connection. Around 400 times the cost of traditional grid expansion, the model stops and becomes constant for all limitations thereafter. There is probably an error/weakness in the simulation. However, the model illustrates the point that systems approaching off-grid have a significantly high cost compared to the traditional grid expansion.

The reason for the high cost associated with the limited allowed grid capacity expansion is the demand of the HESS. As indicated in Section 8.7, the cost of HESS is significantly higher than traditional grid expansion. When such severe restrictions are placed on expansion, there is a need for long-time storage with a longer storage capacity than BESS has. Additionally, when the time rate demand of ESS increases to a such level, according to the literature, the BESS become more expensive than HESS

Furthermore, the result indicates an increase in production capacity when the HESS capacity increases significantly. That possibly be a sign of seasonal storage. The model designed a system to produce surplus energy in the summer season and supply that in the winter season, when the production from PV is lower.

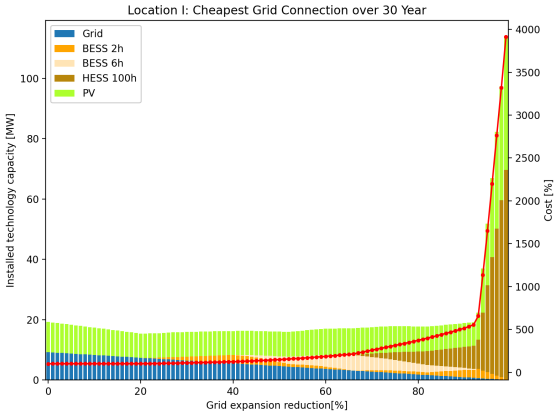

(a) Location I

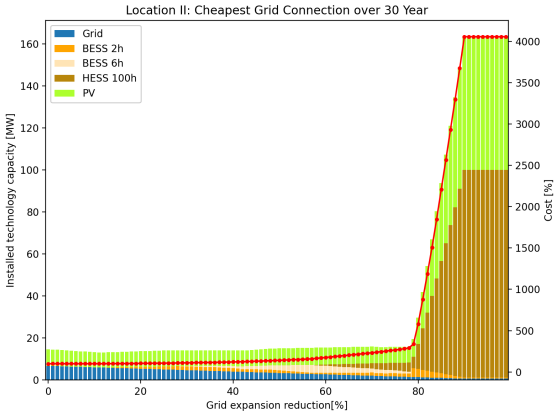

(b) Location II

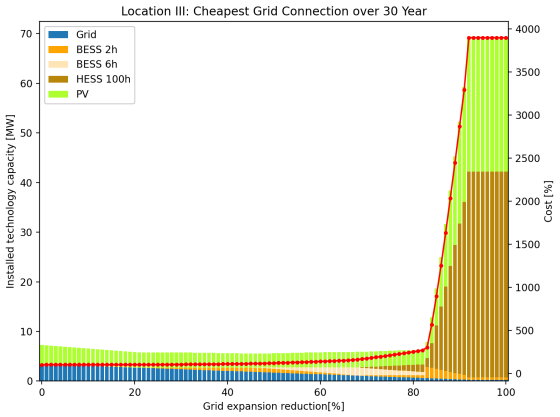

(c) Location III

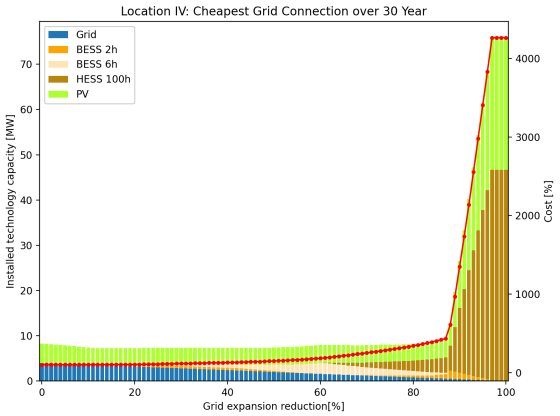

(d) Location IV

Figure 8.33: The simulated grid connection for all locations over 30 years in relation to the limitation in permitted grid expansion between 0 and 100, including electricity sales

8.9.6 Discussion of Grid Tariff

As described in Chapter 7.3.5, the grid tariff of the load was simplified. To neglect the power term of the grid tariff, an important part of the grid tariff is ignored. That will impair the importance of the reduction of the load peaks from the public grid. On the other hand, the power terms of grid expansion constitute the largest part of grid connection cost. Although the importance becomes weakened, the model will try to reduce peaks.

Another weakness of the 30-year simulation is the economic expense linked to the PV system. The simulations include only the installation cost of the PV application, grid cost and energy terms of production grid tariff. Tax, the cost linked to buying the production area and the energy term of production grid tariff are some of which were excluded. It is a large part of the total cost and will result in a greater economic income than the actual. That will probably significantly influence the simulation cost.

The sum of simplifying the grid tariff will also weaken ESS. The cost linked to the export and import of electrical energy from the grid will benefit the local ESS. When the grid tariff is simplified, the simulation does not take into account the economic benefits of storing energy locally instead of relying on the grid. On the other hand, the cost of the ESS are high, and probably, given the current cost situation, the economic benefit related to grid tariff is too low that an ESS could be economically beneficial.

Due to the sum of the simplification in the tariff the cost reduction have some uncertainty, displayed as the right axis in the figures Section 8.9 . Regardless, the cost indicates the investment cost will increase when the reduction of allowed grid expansion increases.

8.9.7 The Influence of Lifetime

This simulation has been conducted for 30 years, but the simulation ignores lifespan longer than the simulation time. For simulated ESS the system requires a reinvestment after 15 years, while a grid system will have a reinvestment after 60 years. Although BESS has a considerably more expensive installation cost than a grid connection, a grid connection will be even cheaper over 60 years because of its lifespan. A more realistic simulation should be over a duration of 60 years. Another alternative way to consider the lifespan in the simulation is using annual investment cost. That will ensure the technology with a high lifespan will have more years to spread their costs over.

8.9.8 PV Investment

A significant difference in the result of the simulation of 30 years and installation cost, the result of 30 years indicates for all locations the most economical investment is to maximize the production capacity. The reason is the economic income. The lifetime simulation includes the selling and buying of electricity, which results in repayment and profit on the investment. When it is economically advantageous, the model recommends investing more. There was no limitation of Production capacity, without location IV, where the production capacity was limited to the roof area. What makes the investment in PV production more profitable is the grid connection. In this situation, the production becomes connected next to the load, which will result in a cheaper grid connection. When the grid is being expanded anyway, and production is directly connected to the same grid connection, this will result in a cheaper grid connection than if two separate connections had to be expanded.

Chapter 9

Conclusion

The thesis investigated the use of integrated energy system (IES) to reduce the investment cost for grid connection to EV charging stations. The research questions for thesis were as follows:

- Are PV applications, battery energy storage systems (BESS) and/or hydrogen energy storage systems (HESS) economically competitive alternatives to traditional grid expansion for large scale EV charging stations?
- How will technology cost development affect the competitiveness of alternatives to traditional grid expansion for large scale EV charging stations?
- If traditional grid expansion is the most cost-effective solution for new grid connections in large scale EV charging stations, how much of a cost reduction does PV applications, BESS and HESS need to be economically competitive? And what are the effects on the grid structure?
- Can PV applications and energy storage systems (ESS) increase the capacity of EV charging stations without building additional grid capacity? How will this influence the total investment cost?
- Is there a correlation between traffic patterns and the load of EV charging stations?

With the current cost of PV and ESS, the alternative technologies are too expensive to competitive alternatives to traditional grid expansion for large scale EV charging stations. However, according to the literature, the cost will decrease, which allows the Integrated Energy System to help reduce the requirement for grid capacity. In 2030, the cost of land-based PV will be low enough to be an alternative. Due to PV technology being a non-regulate energy source, the results are more coincidental than facts. In situations with cloudy days and peak loads, PV production cannot reduce the grid capacity, which will reduce the security of supply. In a low-cost scenario in 2050, the 2h BESS can reduce the requirement of grid capacity expansion. The amount of reduction in grid expansion requirement depends on location and scenario, ranging from 0-25.4% in 2050. Although the cost of technologies will be reduced, the total cost of the grid connection is low. The highest reduction of the simulated locations was 7% percentage points, but a typical reduction in 2050 is a few percentage points.

According to the cost estimate used in this thesis, the 4h and 6h BESS will not be economically competitive. The cost of BESS must be reduced by 75% and 80% before it becomes economically competitive. HESS must decrease by 93-94% before it becomes an economically competitive alternative. However, if the cost of HESS drops by 93-94%, it could reduce the grid capacity alone by up to 80%. Due to the unpredictable nature of PV power production the authors cannot conclude that its a lone replacement for grid expansion, regardless of

price development. PV is dependent on ESS when discussing grid replacement.

If one chooses to invest in an IES with a limited grid connection, the costs will increase exponentially. For a combination of IES with a 20% grid capacity limitation, the installation cost is typically 20-30% higher. However, for a system with 90% grid capacity limitation, increases the cost by a factor of around 1000. This can make it possible for already installed customers to expand their charging stations without requesting additional capacity. On a total investment overview over 30 years, it is in all locations economically beneficial to invest in PV production.

The analysis of the load profile to large-scale EV charging stations located close to the main road through Agder displayed the load was higher in the summer, Christmas and Easter holidays than the rest of the year. Typically, the load is active between 06.00 and 24.00. The correlation analysis between the traffic pattern and load profile at these locations gave inconclusive answers, as to if traffic patterns can be used as an indicator for load in future locations. The analyses show that the linear correlation was highest in locations where the proportion of commuters was the lowest. Nevertheless, a more thorough analysis needs to be conducted to predict load profiles for EV charging stations.

Chapter 10

Further Work

This work used GLPK to estimate the most cost-efficient grid connection by including a limited selection of various PV applications and ESS. The solver limited the complexity of the model. A replacement of the solver can reduce the running time, which makes the possible to include a more complex model. The computer running the model used a 2.3 GHz two core Intel i5 from 2017 CPU, which impacted the runtime of the model. Other than replacing the solver or running the original solver on a more powerful computer, the authors recommends the following:

- **Multiple production and ESS technologies:** This thesis included only PV technologies, HESS and BESS. To increase a larger range of various power production and ESS technologies can open up more cost-efficient alternatives and different combinations of integrated energy systems (IES).
- **Grid tariff:** As discussed in this thesis, the simulation included only a simplification of the grid tariff. Including a more complex model for grid tariff yields more realistic results.
- **Cost flow analyses:** The issue of the current optimization model is that it only considers investment costs. A modification is needed to add a cash flow analysis, which can reduce the life cycle costs of the alternative technologies but increase initial investment costs. I.e. the profits of the electricity sale is incorporated into the investment cost of PV and ESS. Incorporating a cash flow analysis over the lifetime of various grid components and alternative technologies, can ultimately reduce the total cost of grid connection. Additionally, the cash flow analysis includes risk analysis and required rate of return.
- **Traffic pattern:** In areas where there are no existing EV charging stations, it is challenging to assess whether alternative technologies would be more cost-effective than expanding the grid, primarily because there is no existing demand profile to use in the model. As shown in the thesis the demand profiles of EV charging stations can vary from location to location. Therefore, a more thorough analysis into traffic patterns can be viable option to determine a demand profile for new locations not discussed in this thesis.
- **Stochastic analysis:** The results are heavily dependent on the radiation data input. Therefore a stochastic analysis should be conducted to see how the results of the optimization model varies with different data input. Additionally, more load profiles should be included to observe if the model makes the same decisions.

Bibliography

[1] University of Agder, *AI in Assignment Writing*, Accessed: 18 Apr. 2024, Last modified: 14 May 2024, 2024. [Online]. Available: https://www.uia.no/english/studies/for-students/examinations/ai-in-assignment-writing.html.

[2] Energi Fakta Norge, *Norwegian power grid*, Accessed on January 18, 2024, 2024. [Online]. Available: https://energifaktanorge.no/en/norsk-energiforsyning/kraftnett/.

[3] Energi Fakta Norge, *Development of energy supply in norway*, Accessed on January 18, 2024, 2024. [Online]. Available: https://energifaktanorge.no/om-energisektoren/energiforsyningens-utvikling-i-norge/.

[4] Energi Fakta Norge, *Supply security in norwegian energy supply*, Accessed on January 18, 2024, 2024. [Online]. Available: https://energifaktanorge.no/norsk-energiforsyning/forsyningssikkerhet/.

[5] Norges vassdrags- og energidirektorat (NVE), "Rapport 2017/77," Norges vassdrags- og energidirektorat (NVE), Tech. Rep., 2017, Accessed on January 18, 2024.

[6] Norges vassdrags- og energidirektorat (NVE), *Reserving capacity for regular electricity customers*, Accessed on January 18, 2024, 2024. [Online]. Available: https://www.nve.no/reguleringsmyndigheten/regulering/nettvirksomhet/nettilknytning/dette-er-leveringsplikten/reservere-kapasitet-til-vanlige-stroemkunder/.

[7] J. Gustavrud, M. Buvik, I. Holm, *et al.*, "Langsiktig kraftmarkedsanalyse 2023: Energiomstillingen – en balansegang," Norwegian Water Resources and Energy Directorate (NVE), NVE Report 25/2023, Nov. 2023.

[8] Ø. H. Alsvåg and S. Å. Roestad, "Modell for grovkalkyle for anleggskostnader ved tidligfase veiledning," 2023. [Online]. Available: https://hdl.handle.net/11250/3074511.

[9] T. N. Government. "Norway is electric." Article last updated on June 10, 2021. Available in English. (2021), [Online]. Available: https://www.regjeringen.no/no/tema/transport-og-kommunikasjon/veg_og_vegtrafikk/faktaartikler-vei-og-ts/norge-er-elektrisk/id2677481/ (visited on 04/15/2024).

[10] Glitre Nett. "Dataarena." Accessed: 2024-05-25. (2024), [Online]. Available: https://www.glitrenett.no/om-Glitre-Nett/teknologi-utvikling-og-prosjekter/dataarena.

[11] S. Myhre, "Modell for estimating av alternativer til nettutbygging," 2024, unpublish: internal work to Glitre Nett.

[12] G. Inc., *Grammarly*, Accessed: 20 May 2024, 2024. [Online]. Available: https://www.grammarly.com/.

[13] OpenAI, *Chatgpt-4.o*, Accessed: 20 May 2024, 2024. [Online]. Available: https://openai.com/index/gpt-4/.

[14] K. Brohaug and J. E. Nesse, "Python simulation of vertical bifacial pv application," 2024, UiA-course ENE504: Energy Research Project 1.

[15] S. Jouttijärvi, J. Thorning, M. Manni, *et al.*, "A comprehensive methodological workflow to maximize solar energy in low-voltage grids: A case study of vertical bifacial panels in nordic conditions," *Solar Energy*, vol. 262, p. 111 819, 2023, ISSN: 0038-092X. DOI: https://doi.org/10.1016/j.solener.2023.111819. [Online]. Available: https://www.sciencedirect.com/science/article/pii/S0038092X23004449.

[16] W. F. Holmgren, C. W. Hansen, and M. A. Mikofski, "Pvlib python: A python package for modeling solar energy systems," *Journal of Open Source Software*, vol. 3, no. 29, p. 884, 2018. DOI: 10.21105/joss.00884. [Online]. Available: https://doi.org/10.21105/joss.00884.

[17] H. Gabrielsen, "Kapasitetsutnyttelse og stabilitet ved nettilknytning av vindkraftverk," 2013. [Online]. Available: https://ntnuopen.ntnu.no/ntnu-xmlui/handle/11250/257480.

[18] O. S. Johansson, *Hva skjer når man kobler solkraft til det norske nettet?* presentation, 2021. [Online]. Available: https://www.nve.no/media/12973/sesjon-5-hvilken-rolle-kan-solkraften-spille-i-norge.pdf.

[19] M. R. Brubæk, "Battery storage as alternative to grid reinforcement in the low voltage network," 2020. [Online]. Available: https://hdl.handle.net/11250/2778199.

[20] J. Spjotvold, R. Berg, and E. S. Tekseth, *Batteri som potensiell losning til kostbar nettutbygging*, https://ntnuopen.ntnu.no/ntnu-xmlui/handle/11250/3075907, Accessed on January 18, 2024, 2023.

[21] H. Rasoulinezhad, M. Abapour, O. Sadeghian, and K. Zare, "The role of risk-based demand response in resource management of a grid-connected renewable-based large-scale microgrid with stationary and mobile energy storage systems and emission tax," *Computers and Industrial Engineering*, vol. 183, p. 109 555, 2023, ISSN: 0360-8352. DOI: https://doi.org/10.1016/j.cie.2023.109555. [Online]. Available: https://www.sciencedirect.com/science/article/pii/S036083522300579X.

[22] H. Ramadan, A. Ali, M. Nour, and C. Farkas, "Smart charging and discharging of plug-in electric vehicles for peak shaving and valley filling of the grid power," pp. 735–739, 2018. DOI: 10.1109/MEPCON.2018.8635173.

[23] L. Henden, T. Ericson, A. Fidje, *et al.*, "Batterier i bygg kan få betydning for det norske kraftsystemet," Norges vassdrags- og energidirektorat, Rapport 66, 2017. [Online]. Available: https://publikasjoner.nve.no/rapport/2017/rapport2017_66.pdf.

[24] T. O. Hellesø, "Metodikk for identifisering av potensielle nettområder for mikronett i distribusjonsnett," 2017. [Online]. Available: https://ntnuopen.ntnu.no/ntnu-xmlui/handle/11250/2456596.

[25] Ø. Ulleberg, T. Nakken, and A. Eté, "The wind/hydrogen demonstration system at utsira in norway: Evaluation of system performance using operational data and updated hydrogen energy system modeling tools," *International Journal of Hydrogen Energy*, vol. 35, no. 5, pp. 1841–1852, 2010, ISSN: 0360-3199. DOI: https://doi.org/10.1016/j.ijhydene.2009.10.077. [Online]. Available: https://www.sciencedirect.com/science/article/pii/S0360319909016759.

[26] K. Utvik, "Systematikk for planlegging av mikronett: Eksempel på bruk ved reelt casestudie: Utsira mikronett," 2023.

[27] R. H. Berge, F. R. Haugland, and I. E. W. Langseth, "Optimization of microgrids: Feasibility study and economic analysis of rye microgrid," May 2019.

[28] P. Živković, M. Tomić, D. Petković, *et al.*, "Possibilities of wind energy usage in the ski center kopaonik," *ANNALS of Faculty Engineering Hunedoara – International Journal of Engineering*, vol. 14, no. 2, pp. 233–236, 2016, ISSN: 1584-2665. [Online]. Available: https://annals.fih.upt.ro/pdf-full/2016/ANNALS-2016-2-37.pdf.

[29] R. Fachrizal, M. Shepero, M. Åberg, and J. Munkhammar, "Optimal pv-ev sizing at solar powered workplace charging stations with smart charging schemes considering self-consumption and self-sufficiency balance," *Applied Energy*, vol. 307, p. 118 139, 2022, ISSN: 0306-2619. DOI: https://doi.org/10.1016/j.apenergy.2021.118139. [Online]. Available: https://www.sciencedirect.com/science/article/pii/S030626192101415X.

[30] G. Chandra Mouli, P. Bauer, and M. Zeman, "System design for a solar powered electric vehicle charging station for workplaces," *Applied Energy*, vol. 168, pp. 434–443, 2016, ISSN: 0306-2619. DOI: https://doi.org/10.1016/j.apenergy.2016.01.110. [Online]. Available: https://www.sciencedirect.com/science/article/pii/S0306261916300988.

[31] H. Nes, "Load match study of photovoltaic production and charging demand of electric vehicles in a zero emission neighbourhood – case campus evenstad," p. 30, 2017, Environmental Physics and Renewable Energy.

[32] E. Omdal, "Kraftflytanalyse i distribusjonsnettet for å identifiserer etterspørselsstyring-scenario og integrasjon av solceller," 2022, M.Sc. Thesis.

[33] J. Johansson, "Optimization of section points locations in electric power distribution systems: Development of a method for improving the reliability," 2023, Course: Degree project, Course code: ERA400, Subject: Energy Technology, Points: 30 hp, Program: M.Sc. Energy Systems Engineering.

[34] K. Mertens, *Photovoltaics: Fundamentals, Technology, and Pracatices*. Wiley, 2019.

[35] R. Younas, H. Imran, M. H. Riaz, and N. Z. Butt, "Agrivoltaic farm design: Vertical bifacial vs. tilted monofacial photovoltaic panels," *arXiv: Applied Physics*, 2019. [Online]. Available: https://api.semanticscholar.org/CorpusID:203626570.

[36] Y. Yang, S. Bremner, C. Menictas, and M. Kay, "Battery energy storage system size determination in renewable energy systems: A review," *Renewable and Sustainable Energy Reviews*, vol. 91, pp. 109–125, 2018, ISSN: 1364-0321. DOI: https://doi.org/10.1016/j.rser.2018.03.047. [Online]. Available: https://www.sciencedirect.com/science/article/pii/S1364032118301436.

[37] R. Borah, F. Hughson, J. Johnston, and T. Nann, "On battery materials and methods," *Materials Today Advances*, vol. 6, p. 100 046, 2020, ISSN: 2590-0498. DOI: https://doi.org/10.1016/j.mtadv.2019.100046. [Online]. Available: https://www.sciencedirect.com/science/article/pii/S2590049819301201.

[38] I. Hassan, H. S. Ramadan, M. A. Saleh, and D. Hissel, "Hydrogen storage technologies for stationary and mobile applications: Review, analysis and perspectives," *Renewable and Sustainable Energy Reviews*, vol. 149, p. 111 311, 2021, ISSN: 1364-0321. DOI: https://doi.org/10.1016/j.rser.2021.111311. [Online]. Available: https://www.sciencedirect.com/science/article/pii/S1364032121005980.

[39] S. Grigoriev, V. Fateev, D. Bessarabov, and P. Millet, "Current status, research trends, and challenges in water electrolysis science and technology," *International Journal of Hydrogen Energy*, vol. 45, no. 49, pp. 26 036–26 058, 2020, Progress in Hydrogen Production and Utilization, ISSN: 0360-3199. DOI: https://doi.org/10.1016/j.ijhydene.2020.03.109. [Online]. Available: https://www.sciencedirect.com/science/article/pii/S0360319920310715.

[40] S. Mekhilef, R. Saidur, and A. Safari, "Comparative study of different fuel cell technologies," *Renewable and Sustainable Energy Reviews*, vol. 16, no. 1, pp. 981–989, 2012, ISSN: 1364-0321. DOI: https://doi.org/10.1016/j.rser.2011.09.020. [Online]. Available: https://www.sciencedirect.com/science/article/pii/S1364032111004709.

[41] M. Schulze, "Linear programming for optimization," Sep. 2000. [Online]. Available: https://markschulze.net/LinearProgramming.pdf.

[42] D. R. Morrison, S. H. Jacobson, J. J. Sauppe, and E. C. Sewell, "Branch-and-bound algorithms: A survey of recent advances in searching, branching, and pruning," *Discrete Optimization*, vol. 19, pp. 79–102, 2016, ISSN: 1572-5286. DOI: https://doi.org/10.1016/j.disopt.2016.01.005. [Online]. Available: https://www.sciencedirect.com/science/article/pii/S1572528616000062.

[43] A. Makhorin, "Gnu linear programming kit: Reference manual for glpk version 4.64," GNU, Tech. Rep., 2017. [Online]. Available: https://hpc.nih.gov/apps/glpk/latest/glpk.pdf.

[44] *Pearson and spearman correlations: A guide to understanding and applying correlation methods*, https://datascientest.com/en/pearson-and-spearman-correlations-a-guide-to-understanding-and-applying-correlation-methods, Accesed: 19.05.24, Datascientest, Jan. 2024.

[45] Norwegian Water Resources and Energy Directorate (NVE), "Forutsetninger for estimering av kostnader for kraftproduksjon," Norwegian Water Resources and Energy Directorate, Tech. Rep., Oct. 2023, Report.

[46] Norwegian Water Resources and Energy Directorate (NVE), *Costs of power production*, Accessed: 2024-03-16, 2023. [Online]. Available: https://www.nve.no/energi/analyser-og-statistikk/kostnader-for-kraftproduksjon/.

[47] K. Haaskjold, E. Rosenberg, and P. M. S. Seljom, "Documentation of ife-times-norway v3," Institute for Energy Technology (IFE), Technical Report, Feb. 20, 2023, p. 86.

[48] National Renewable Energy Laboratory, *Utility-scale pv*, https://atb.nrel.gov/electricity/2023/utility-scale_pv, Accessed: 2024-04-22, 2023.

[49] J. Scharf, M. Grieb, and M. Fritz, "Agri-photovoltaik: Stand und offene fragen," Technologie- und Förderzentrum (TFZ), Straubing, TFZ Bericht 73, May 2021. [Online]. Available: https://www.tfz.bayern.de/mam/cms08/rohstoffpflanzen/dateien/tfz_bericht_73_agri-pv.pdf.

[50] W. Cole and A. Karmakar, "Cost projections for utility-scale battery storage: 2023 update," National Renewable Energy Laboratory, Tech. Rep. NREL/TP-6A40-85332, 2023.

[51] *Utility-scale battery storage*, Webside, Accessed: 2024-04-10. [Online]. Available: https://atb.nrel.gov/electricity/2023/utility-scale_battery_storage.

[52] C. Martínez de León, C. Ríos, P. Molina, and J. Brey, "Levelized cost of storage (lcos) for a hydrogen system," *International Journal of Hydrogen Energy*, vol. 52, pp. 1274–1284, 2024, ISSN: 0360-3199. DOI: https://doi.org/10.1016/j.ijhydene.2023.07.239. [Online]. Available: https://www.sciencedirect.com/science/article/pii/S0360319923037485.

[53] K. Mongird, V. Viswanathan, J. Alam, C. Vartanian, V. Sprenkle, and R. Baxter, "2020 grid energy storage technology cost and performance assessment," Pacific Northwest National Laboratory, Tech. Rep., Dec. 2020, Technical Report Publication No. DOE/PA-0204. [Online]. Available: https://www.pnnl.gov/sites/default/files/media/file/Hydrogen_Methodology.pdf.

[54] V. Viswanathan, K. Mongird, R. Franks, X. Li, V. Sprenkle, and R. Baxter, "2022 grid energy storage technology cost and performance assessment," Pacific Northwest National Laboratory, Tech. Rep., Aug. 2022, Technical Report Publication No. PNNL-33283. [Online]. Available: https://www.pnnl.gov/sites/default/files/media/file/ESGC%20Cost%20Performance%20Report%202022%20PNNL-33283.pdf.

[55] Glitre Energi Nett, *Grid fee prices for larger business customers*, Online, Accessed on 2023-04-26, 2023. [Online]. Available: https://www.glitrenett.no/kunde/nettleie-og-priser/nettleiepriser-storre-bedriftskunder.

[56] Glitre Energi Nett, *Prices for electricity production*, Online, Accessed on 2023-04-26, 2023. [Online]. Available: https://www.glitrenett.no/kunde/nettleie-og-priser/priser-produksjon-av-strom.

[57] N. Bank, *Exchange rates*, Accessed: [11.mars 2024], 2024. [Online]. Available: https://www.norges-bank.no/tema/Statistikk/Valutakurser/?tab=currency&id=USD.

[58] *Energy storage cost and performance database: Hydrogen (bi-directional)*, https://www.pnnl.gov/hydrogen-bi-directional?fbclid=IwZXh0bgNhZW0CMTAAARoTafnsX4xUos3TzsKs6kt57MYqcUYYZIH7impmt27R7Oy_vsaqp0CN2ok_aem_AcTS6R83urHWPQ8Q3DgK4t3ffR_-W7XjQYxN4PZhivQLXLxoRCxfzk-eiyEIh5Os9o_6MKQxfHtVFRT2mGwY8gtl, Accessed: [11.mars 2024].

[59] International Organization for Standardization, *ISO 15927-4:2005 – hygrothermal performance of buildings – calculation and presentation of climatic data – part 4: Hourly data for assessing the annual energy use for heating and cooling*, https://cdn.standards.iteh.ai/samples/41371/c806f5d5f0f04d92a9da28f85bbfb5bd/ISO-15927-4-2005.pdf, Accessed: 2024-05-16, 2005.

[60] *European Commission, Joint Research Centre (JRC)*, https://re.jrc.ec.europa.eu/pvg_tools/en/#TMY, Accessed: [2024-04-21].

[61] *Traikkdata atlas*, A map solution for collection of trafficdata in Norway, The Norwegian Public Roads Administration, 2024. [Online]. Available: https://trafikkdata.atlas.vegvesen.no/#/kart?lat=58.47049165974684&lon=8.73269348055719&trafficType=vehicle&zoom=8.

Appendix A

Datasheet A: Cost Scenario

A.1 Cost Scenario in 2030

Table A.1: Base case

Location	Generator	Storage	Line	Transformer	Substation	Total cost
Location I	1.58 MW	-	1 km	8.07 MW	9.25 MW	49.75 MNOK
Location II	0.65 MW	-	5 km	6.23 MW	6.75 MW	39.67 MNOK
Location III	-	-	2.5 km	3.4 MW	3.4 MW	24.34 MNOK
Location IV	-	-	1 km	4 MW	4 MW	22.07 MNOK

Table A.2: low-cost scenario in 2030

Location	Generator	Storage	Line	Transformer	Substation	Total cost
Location I	1.58 MW	-	1 km	8.07 MW	9.25 MW	48.42 MNOK
Location II	0.65 MW	-	5 km	6.23 MW	6.75 MW	39.12 MNOK
Location III	-	-	2.5 km	3.4 MW	3.4 MW	24.34 MNOK
Location IV	-	-	1 km	4 MW	4 MW	22.07 MNOK

Table A.3: high-cost scenario in 2030

Location	Generator	Storage	Line	Transformer	Substation	Total cost
Location I	-	-	1 km	9.25 MW	9.25 MW	49.90 MNOK
Location II	-	-	5 km	6.75 MW	6.75 MW	39.90 MNOK
Location III	-	-	2.5 km	3.4 MW	3.4 MW	24.34 MNOK
Location IV	-	-	1 km	4 MW	4 MW	22.07 MNOK

A.2 Cost Scenario in 2050

Table A.4: low-cost scenario in 2050

Location	Generator	Storage	Line	Transformer	Substation	Total cost
Location I	1.58 MW	2.47 MWh	1 km	6.90 MW	9.25 MW	46.35 MNOK
Location II	0.51 MW	1.23 MWh	5 km	5.77 MW	6.75 MW	38.40 MNOK
Location III	-	1.47 MWh	2.5 km	2.7 MW	3.40 MW	23.40 MNOK
Location IV	0.25 MW	1.24 MWh	1 km	3.40 MW	4 MW	21.40 MNOK

Table A.5: base-cost scenario in 2050

Location	Generator	Storage	Line	Transformer	Substation	Total cost
Location I	1.58 MW	-	1 km	8.07 MW	9.25 MW	48.42 MNOK
Location II	0.65 MW	-	5 km	6.23 MW	6.75 MW	39.12 MNOK
Location III	-	-	2.5 km	3.4 MW	3.4 MW	24.34 MNOK
Location IV	-	-	1 km	4 MW	4 MW	22.07 MNOK

Table A.6: high-cost scenario in 2050

Location	Generator	Storage	Line	Transformer	Substation	Total cost
Location I	1.58 MW	-	1 km	8.07 MW	9.25 MW	49.75 MNOK
Location II	0.65 MW	-	5 km	6.23 MW	6.75 MW	39.67 MNOK
Location III	-	-	2.5 km	3.4 MW	3.4 MW	24.34 MNOK
Location IV	-	-	1 km	4 MW	4 MW	22.07 MNOK

Appendix B

Datasheet C: Grid Capacity Reduction Full Picture

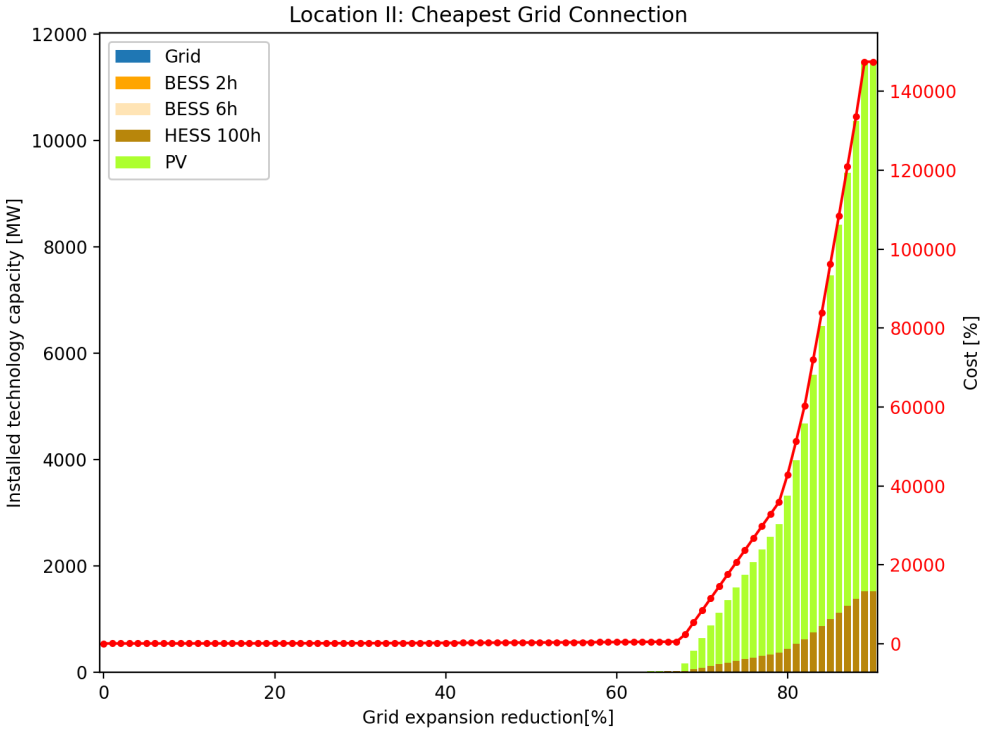

Figure B.1: Full picture of technology investment mix with limited grid expansion for Location I

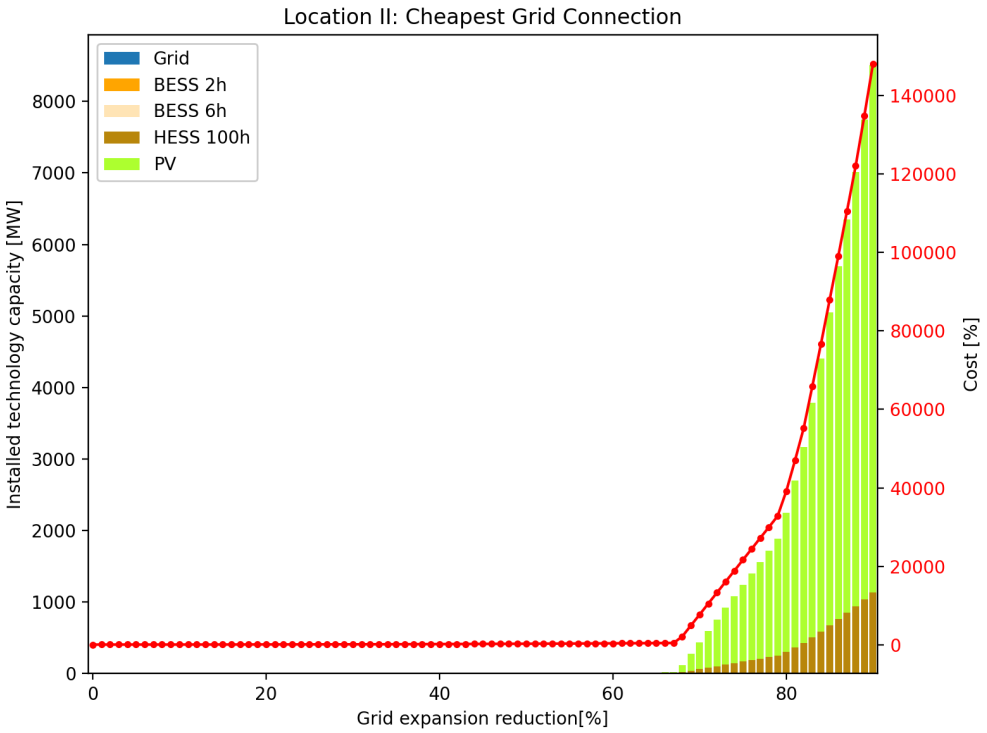

Figure B.2: Full picture of technology investment mix with limited grid expansion for Location II

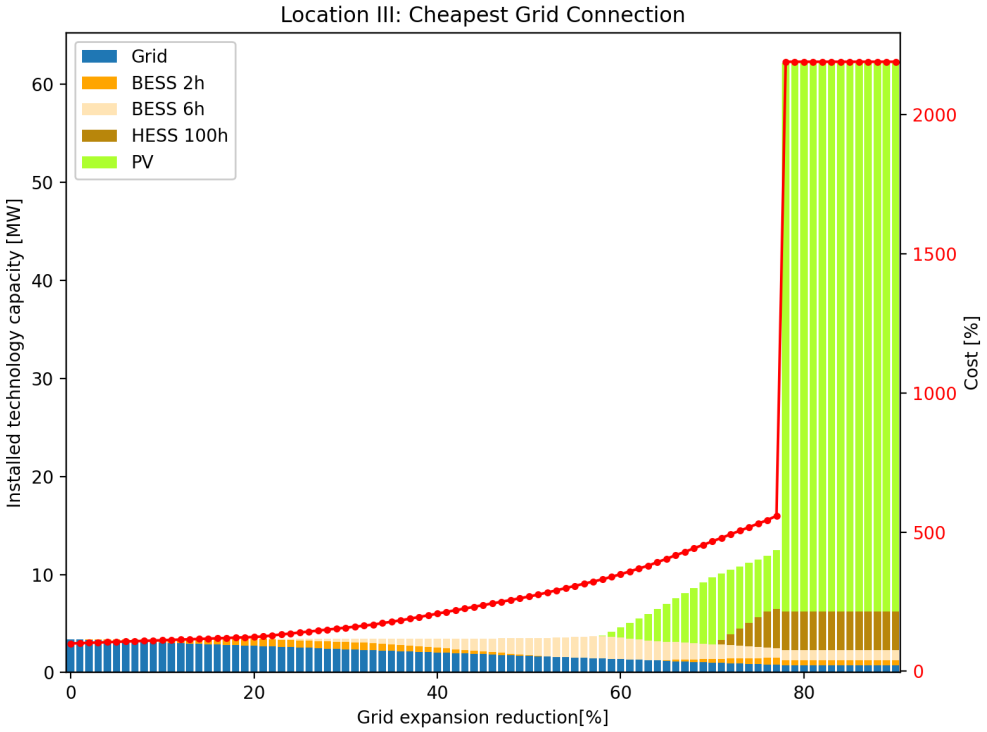

Figure B.3: Full picture of technology investment mix with limited grid expansion for Location III

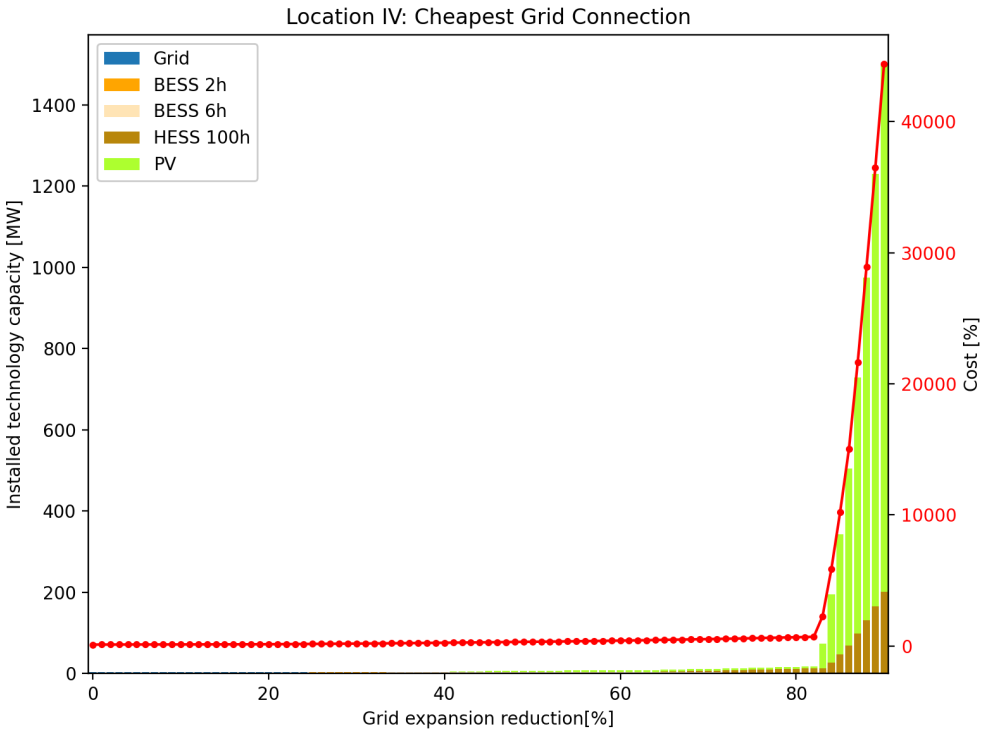

Figure B.4: Full picture of technology investment mix with limited grid expansion for Location IV

Appendix C

Datasheet D: Correlation

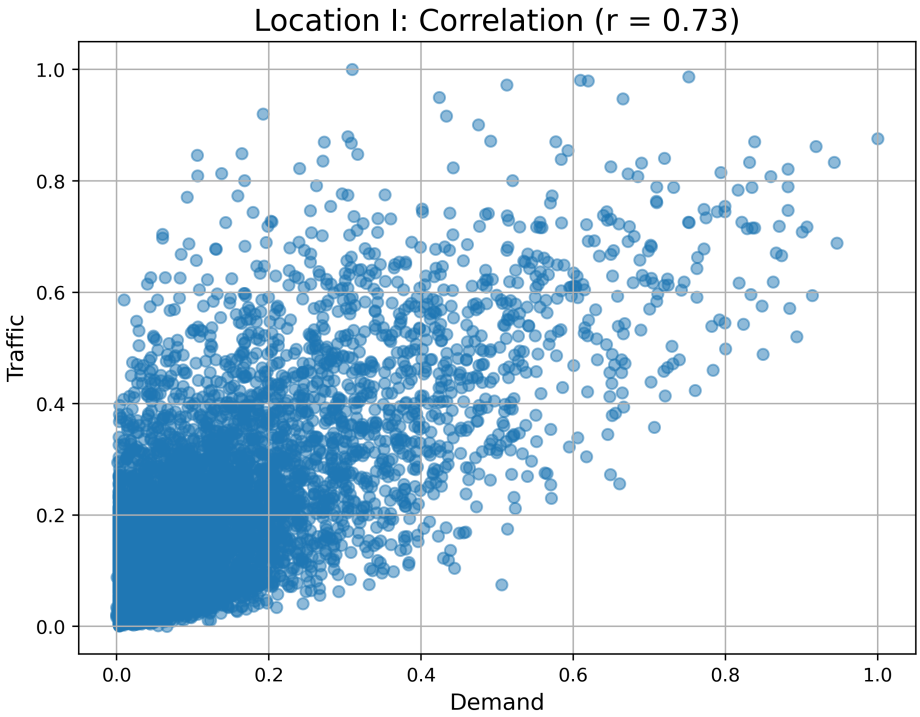

Figure C.1: Location I

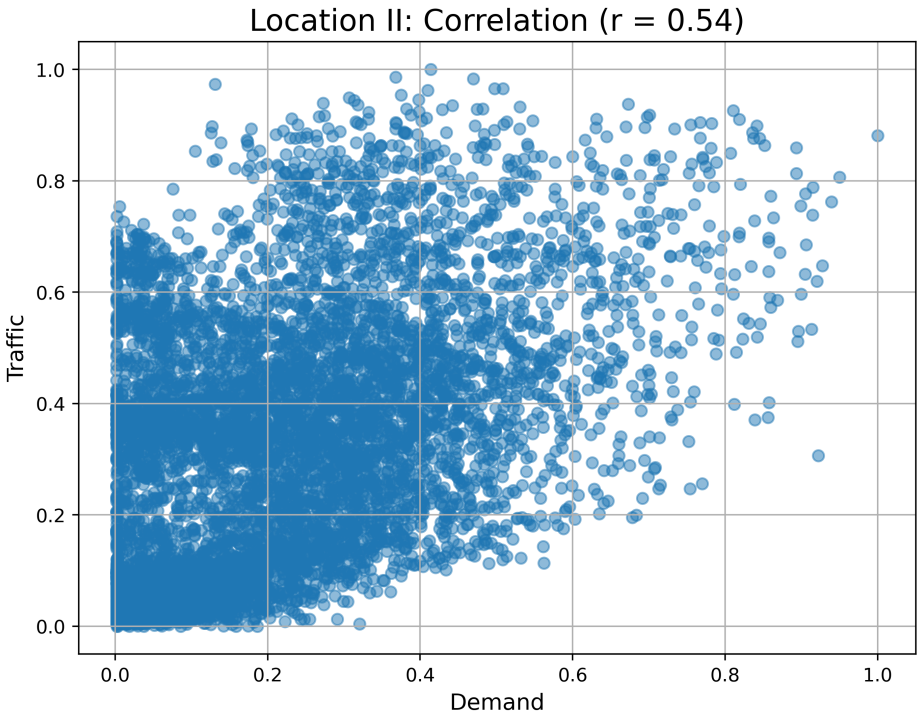

Figure C.2: Location II

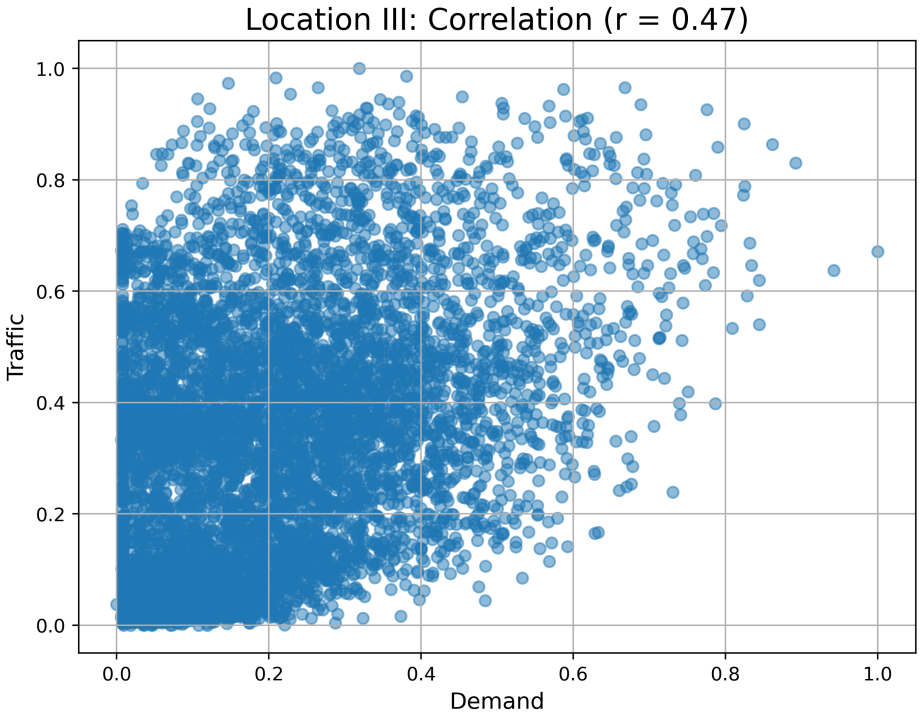

Figure C.3: Location III

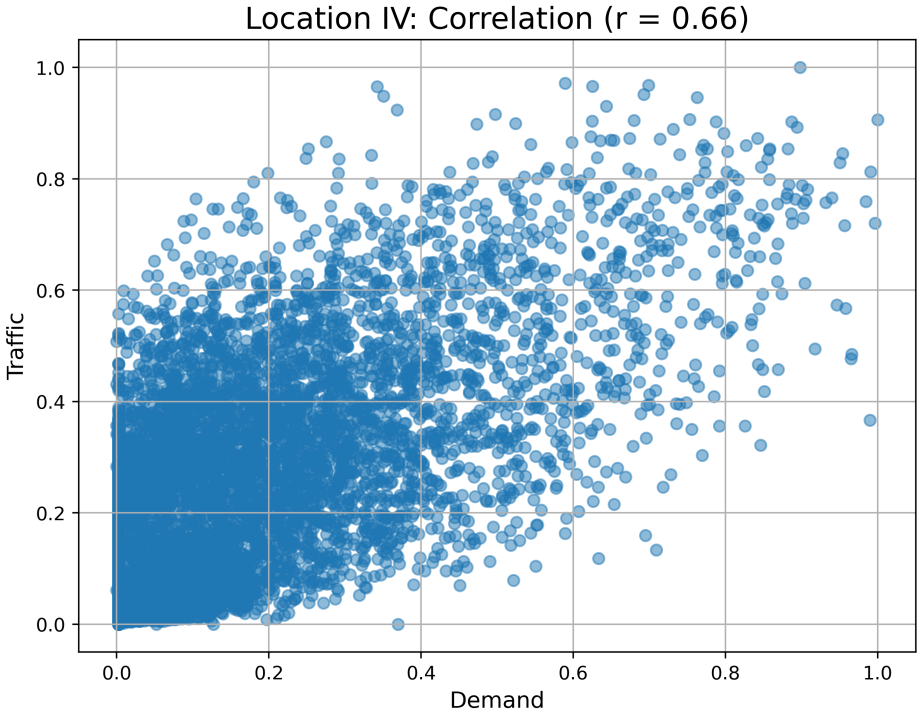

Figure C.4: Location IV